

ANALYSIS OF STRESS IN A SOLID CYLINDER WITH PERIODIC HEAT
GENERATION

A THESIS SUBMITTED TO
THE GRADUATE SCHOOL OF NATURAL AND APPLIED SCIENCES
OF
MIDDLE EAST TECHNICAL UNIVERSITY

BY

EKIN VARLI

IN PARTIAL FULFILLMENT OF THE REQUIREMENTS
FOR
THE DEGREE OF MASTER OF SCIENCE
IN
ENGINEERING SCIENCES

SEPTEMBER 2015

Approval of the thesis:

ANALYSIS OF STRESS IN A SOLID CYLINDER WITH PERIODIC HEAT GENERATION

submitted by **EKIN VARLI** in partial fulfillment of the requirements for the degree of **Master of Science in Engineering Sciences Department, Middle East Technical University** by,

Prof. Dr. M. Gülbin Dural Ünver
Dean, Graduate School of **Natural and Applied Sciences**

Prof. Dr. Murat Dicleli
Head of Department, **Engineering Sciences**

Prof. Dr. Ahmet N. Eraslan
Supervisor, **Engineering Sciences Department, METU**

Examining Committee Members:

Assoc. Prof. Dr. Ferhat Akgül
Engineering Sciences Department, METU

Prof. Dr. Ahmet N. Eraslan
Engineering Sciences Department, METU

Assoc. Prof. Dr. M. Tolga Yılmaz
Engineering Sciences Department, METU

Assoc. Prof. Dr. Hakan Argeşo
Manufacturing Engineering Department, Atılım University

Assoc. Prof. Dr. Tolga Akış
Civil Engineering Department, Atılım University

Date:

I hereby declare that all information in this document has been obtained and presented in accordance with academic rules and ethical conduct. I also declare that, as required by these rules and conduct, I have fully cited and referenced all material and results that are not original to this work.

Name, Last Name: EKin VARLI

Signature :

ABSTRACT

ANALYSIS OF STRESS IN A SOLID CYLINDER WITH PERIODIC HEAT GENERATION

Varlı, Ekin

M.S., Department of Engineering Sciences

Supervisor : Prof. Dr. Ahmet N. Eraslan

September 2015, 100 pages

Thermoelastic stress response of a periodic heat generating solid cylinder is investigated by analytical means. The cylinder is initially at zero temperature. For times greater than zero, heat is generated internally and slowly at a time dependent rate. Two periodic heat generation rates are used. The temperature distribution in the solid cylinder corresponding to each generation rate is obtained by making use of Duhamel's theorem. An uncoupled thermoelastic solution of the solid cylinder is then obtained under generalized plane strain condition. The effects of various parameters on the stress and deformation behavior of the cylinder are studied and presented in graphical forms.

Keywords: Solid cylinder, Transient heat conduction, Periodic heat generation, Duhamel's theorem, Thermoelasticity

ÖZ

PERİYODİK OLARAK İÇ ISI ÜRETEMİ ETKİSİNDEKİ SİLİNDİRİN GERİLİM ANALİZİ

Varlı, Ekin

Yüksek Lisans, Mühendislik Bilimleri Bölümü

Tez Yöneticisi : Prof. Dr. Ahmet N. Eraslan

Eylül 2015 , 100 sayfa

Bu çalışmada periyodik olarak ısı üreten içi dolu silindirin mekanik davranışı analitik olarak incelenmiştir. Silindirin sıcaklığı başlangıçta sıfır olduğu varsayılmaktadır. Daha sonra silindirin içerisinde yavaşça ısı üretimi başlamaktadır. Silindir içerisindeki ısı üretimini tanımlamak için iki değişik periyodik fonksiyon kullanılmaktadır. Bu koşullar altında silindir içerisindeki sıcaklık dağılımının zaman ile değişimi Duhamel teoremi kullanılarak elde edilmektedir. Genelleştirilmiş düzlemsel gerinim varsayımı ile silindirin dekapte termoelastik çözümü elde edilmiştir. Çeşitli parametrelerin silindirin gerilim ve yer değiştirme davranışı üzerindeki etkileri araştırılmış ve grafikler halinde sunulmuştur.

Anahtar Kelimeler: İçi dolu silindir, Geçici ısı iletimi, Periyodik ısı üretimi, Duhamel teoremi, Termoelastisite

To my family

Abdullah Varlı, Hülya Varlı, Dilge Varlı

ACKNOWLEDGMENTS

First and foremost I offer my sincerest gratitude to my supervisor, Prof. Dr. Ahmet Eraslan, whose expertise, understanding, and patience, added considerably to my graduate experience. I appreciate his vast knowledge and skill in many areas, and his assistance in writing reports. I attribute the level of my Masters degree to his encouragement and effort and without him this thesis, too, would not have been completed or written. One simply could not wish for a better or friendlier supervisor. I hope that one day I would become as good an advisor to my students as Professor Eraslan has been to me.

I am thankful to Büşra Yedekçi for her support, smiling face and trust in me for the last three years. Her positive attitude and made hard situations easier to handle. She stood by my side all the time and helped in every possible way. Although I had the chance to know her for a brief period of time, I would also like to thank Nurten Şişman Dersan. She motivated me not to give up with her positive attitude and sincere heart and made me feel safe. I am thankful to her for supporting me all the way she can. It was a great chance for me to have Deniz Atila as a colleague and roommate who always made me smile. I would also like to thank Hande Güneş and Burak Çağrı Duran who never let me feel lonely and stood by me in both good and bad days. I am grateful to Yasemin Öztemur for her valuable friendship, never ending support and trust for the last 15 years.

Most importantly, none of this would have been possible without the love, caring and patience of my family. I feel blessed to have you by my side. I am grateful to my beloved sister and best friend Dilge, who is always by my side no matter what. This thesis could not have been written without her.

TABLE OF CONTENTS

ABSTRACT	v
ÖZ	vi
ACKNOWLEDGMENTS	viii
TABLE OF CONTENTS	ix
LIST OF FIGURES	xi
CHAPTERS	
1 INTRODUCTION	1
2 PROBLEM DEFINITION AND SOLUTION	7
2.1 Temperature Distribution	8
2.2 Elastic Solution	19
3 RESULTS AND DISCUSSION	27
4 CONCLUSION	65
REFERENCES	67
APPENDICES	
A FORTRAN CODES	69
A.1 MAIN PRAGRAMS OF ASINT CASE	69

A.2	MAIN PRAGRAMS OF ATCOST CASE	86
B	MATERIAL PROPERTIES	99
B.1	MATERIAL PROPERTIES OF STRUCTURAL STEEL . . .	99
B.2	MATERIAL PROPERTIES OF YELLOW BRASS	100

LIST OF FIGURES

FIGURES

Figure 2.1	Infinitely long, solid cylinder of radius b	8
Figure 2.2	Temperature distribution verification of structural steel for A_{Sint} case.	15
Figure 2.3	Temperature gradient verification of structural steel for A_{Sint} case. .	16
Figure 2.4	Temperature distribution verification of structural steel for A_{tCost} case.	17
Figure 2.5	Temperature gradient verification of structural steel for A_{tCost} case.	18
Figure 2.6	Elastic solution verification of structural steel for A_{Sint} case. . . .	24
Figure 2.7	Elastic solution verification of structural steel for A_{tCost} case. . . .	25
Figure 3.1	The variation of heat generation rate A_{Sint} with time for $A=1$	28
Figure 3.2	The variation of heat generation rate A_{tCost} with time for $A=1$. . .	29
Figure 3.3	The temperature distribution in the steel cylinder at different times for the heat generation rate A_{Sint}	34
Figure 3.4	The temperature gradient in the steel cylinder at different times for the heat generation rate A_{Sint}	35
Figure 3.5	The radial stress in the steel cylinder at different times for the heat generation rate A_{Sint}	36
Figure 3.6	The circumferential stress in the steel cylinder at different times for the heat generation rate A_{Sint}	37
Figure 3.7	The axial stress in the steel cylinder at different times for the heat generation rate A_{Sint}	38
Figure 3.8	The von Mises stress in the steel cylinder at different times for the heat generation rate A_{Sint}	39

Figure 3.9 The evolution of displacement of the steel cylinder at different times for the heat generation rate AS_{int}	40
Figure 3.10 The evolution of stresses and displacement of the steel cylinder at $t=2.65$ hour for the heat generation rate AS_{int}	41
Figure 3.11 The evolution of axial strain of the steel cylinder at different times for the heat generation rate AS_{int}	42
Figure 3.12 The temperature distribution in the steel cylinder at different times for the heat generation rate At_{Cost}	43
Figure 3.13 The temperature gradient in the steel cylinder at different times for the heat generation rate At_{Cost}	44
Figure 3.14 The radial stress in the steel cylinder at different times for the heat generation rate At_{Cost}	45
Figure 3.15 The circumferential stress in the steel cylinder at different times for the heat generation rate At_{Cost}	46
Figure 3.16 The axial stress in the steel cylinder at different times for the heat generation rate At_{Cost}	47
Figure 3.17 The von Mises stress in the steel cylinder at different times for the heat generation rate At_{Cost}	48
Figure 3.18 The evolution of displacement of the steel cylinder at different times for the heat generation rate At_{Cost}	49
Figure 3.19 The evolution of stresses and displacement of the steel cylinder at $t=4.35$ hour for the heat generation rate At_{Cost}	50
Figure 3.20 The evolution of axial strain of the steel cylinder at different times for the heat generation rate At_{Cost}	51
Figure 3.21 The evolution of stresses and displacement of the brass cylinder at $t=2.35$ hour for the heat generation rate AS_{int}	54
Figure 3.22 The evolution of axial strain of the brass cylinder at different times for the heat generation rate AS_{int}	55
Figure 3.23 The temperature distribution in the brass cylinder at different times for the heat generation rate AS_{int}	56
Figure 3.24 The temperature gradient in the brass cylinder at different times for the heat generation rate AS_{int}	57

Figure 3.25 The evolution of stresses and displacement of the brass cylinder at $t=4.11$ hour for the heat generation rate At_{Cost}	58
Figure 3.26 The evolution of axial strain of the brass cylinder at different times for the heat generation rate At_{Cost}	59
Figure 3.27 The temperature distribution in the brass cylinder at different times for the heat generation rate At_{cost}	60
Figure 3.28 The temperature gradient in the brass cylinder at different times for the heat generation rate At_{cost}	61
Figure 3.29 The verification of the temperature distribution between the materials steel and brass at different times for the heat generation rate AS_{int} . . .	62
Figure 3.30 The verification of the temperature gradient between the materials steel and brass at different times for the heat generation rate AS_{int}	63

CHAPTER 1

INTRODUCTION

The aim of this work is to investigate the stress and deformation behavior of a solid cylinder in which heat is generated periodically. The temperature distribution in this long cylinder is achieved by the analytical solution of one dimensional time dependent heat conduction equation and the solution of the heat conduction equation is handled by the use of Duhamel's theorem. Using the equations of generalized Hooke's law under the assumption of generalized plane strain the governing equation is obtained. The governing equation is eliminated in total strain expressions and then the results are substituted into the strain-displacement relations to find the stress response and after manipulation of this equation, the radial displacement equation is found and solved analytically.

Discs, solid cylinders, tubes, spheres, spherical shells and plates are the basic structures of engineering. It is very significant to study the deformation behavior of these structures under mechanic and thermal loads because of their widespread usage in our daily life and industry. Solid cylinders are one of the most important structures in these areas and due to this reason; a solid cylinder was selected in this work.

Heat is an important factor in some daily issues. For example, in the present work, an analytical model is developed to determine elastic stresses in thick-walled cylindrical panels. These panels are subjected to a radial temperature gradient under the assumption of generalized plane strain [2]. The ends of this thick-walled shell are pre-supposed to be guided in such a way that a displacement in circumferential direction may occur and that the radius of the initial middle surface remains unchanged [3]. In relation to our topic, "Thermo" is studied under the term of thermoelasticity. Ther-

moelastic stresses are investigated in curved beams of constant cross section under temperatures varying in the radial direction only [6]. Thermoelasticity is the change in the size and shape of a solid object as the temperature of that object fluctuates. Materials that are more elastic will expand and contract more than those materials that are more inelastic. Scientists use their understanding of thermoelasticity to design materials and objects that can withstand fluctuations in temperature without breaking.

Scientists have studied the equations that describe thermoelasticity for more than 100 years. However, they have recently focused on the rate of elasticity. Through this method, engineers are able to predict how much these materials will expand at different temperatures. This knowledge is important when building machines or weight bearing structures with pieces that need to fit closely together. Understanding the principles of thermoelasticity helps engineers design things that maintain their structural integrity for a range of temperatures.

The principles of thermoelasticity have affected the way engineers design a number of different objects. Knowing that concrete expands when it is heated, for instance, is the reason that sidewalks are designed with small spaces between the slabs. All materials that are elastic expand when heated and contract when cooled. The expansion that is described by thermoelasticity formulas is caused by an increase in the movement of the atoms in the material [16]. As a solid is heated, these atoms remain linked to each other, but the molecular bonds become larger. With this action, they allow atoms to move away from each other causing the material to grow. Conversely, when a material is cooled, the atoms move less and so the atoms come together.

The principles of thermoelasticity reveal that the expansion which is caused by an increase in temperature will cause an object to expand on all directions. Slabs of concrete expand out towards one another when they are subjected to heat [4]. Specific formulas are used in the study of thermoelasticity to describe how objects change in shape with changes in temperature [22].

In conjunction with heat, some changes are seen. Thermal expansion can be given as an example to these. Thermal expansion is the change in size or volume of a given mass with changing temperature. An increase in temperature implies an increase

in the kinetic energy of the individual atoms. Thermal stress is created by thermal expansion or contraction and occurs under heat or cold [24]. Structures susceptible to it, such as roads, buildings, and railroad tracks, have beams or slabs of materials that are affixed into positions that are rigid [18].

Thermal stresses can be both useful and dangerous. Thermal stress can explain many phenomena, such as the weathering of rocks and pavements by the expansion of ice when it freezes. These examples can be given as the useful ones.

When we talk about the negative impacts of thermal stresses, they can be destructive, such as when expanding gasoline ruptures a tank. Nuclear reactor pressure vessels are threatened by rapid cooling, but none of them are affected. Biological cells are ruptured when foods are frozen and the taste of food is diminished.

Repeated thawing and freezing accentuates the damage. Even the oceans can be affected. A change in the sea level is due to the thermal expansion of sea water, which leads to global warming. Apart from the negative and positive impacts of thermal stresses, another important element is the occurrence of it. Thermal stress occurs under heat or cold. Structures susceptible to it, such as roads, buildings, and railroad tracks, have beams that are rigid [23]. This positioning may make it difficult for the materials to expand or contract. Long structures may have localized effects, in that it is not unusual for one section to be buckled or warped while the others remain relatively intact. And finally thermal stresses are created when thermal expansion is constrained.

When we talk about thermal load, it is important to mention that thermal load is defined as the temperature which causes applied load the effect's on buildings. Air temperature, solar radiation, underground temperature, indoor air temperature and the heat source equipment inside the building can be given as examples. The change of the temperature in the structural and non-structural member causes thermal stress. This is also defined as the effect of thermal load.

One important element in thermal load is the change of temperature. The initial temperature is defined as the temperature which causes no thermal effect on a structure.

The stationary and quasi static problems of the theory of thermal stresses have already

been treated in numerous scientific papers [12]. Important methods of solution and important papers have been removed in various monographs (for instance H. Parkus *Instationare Warmespannungen* [21], B. A. Boley and J. H. Weiner *Theory of thermal stresses* [20], W. Nowacki *Thermoelasticity* [5]).

We know how important the variational theorems play a part in the elasticity theory with variation of deformation state or stress state [24]. They not only make it possible to derive the differential equations describing the bending of plates, shells, tubes, discs, membranes, etc., but also to construct approximate solutions [7].

In this work, we pointed out the concept of thermoelasticity with its formation and then we moved on to thermal stresses with its usage and formation. As pointed out in the reference list, we express the most recent studies from important articles and books that belong to Eraslan, Orcan and others. Scientists have been studying this subject for more than 100 years. For example in the 2000s, the topic being talked about was studied by Y. Orcan, M. Gulgec, A. Eraslan, H. Argeso and by their colleagues.

A. Eraslan has many articles about this study. In 2003, an analytical solution is developed for thermally induced axisymmetric elastic and elastic-plastic deformations in nonuniform heat-generating composite fixed ends tubes [8]. In this study four different boundary condition is used to handle the thermoelastic solution. Another work related to this subject is “A class of nonisothermal variable thickness rotating disk problems solved by hypergeometric functions ” written in 2005 [9]. In this paper nonisothermal variable thickness rotating disks’ solutions are handled under the plane stress condition and Tresca yield criteria is used. In 2007 FGM pressure tubes are searched [10]. A. Eraslan and H. Argeşo have also many articles related to this topic such as “On the Application of von Mises’ Yield Criterion to a Class of Plane Strain Thermal Stress Problems” In this study they developed a computational model in order to find the thermal stresses in nonlinearly hardening elastic-plastic axisymmetric systems in cylindrical polar coordinates. In this study von Mises criteria is used and the results is compared with the Tresca yield criteria [13]. Another study is “Computer Solutions of Plane Strain Axisymmetric Thermomechanical Problems” In this work, to obtain the thermoplastic behavior of structure, the von Mises yield crite-

rion, total deformation theory and a Swift-type nonlinear hardening law is used [12]. In 2003 under Tresca and von Mises criteria elastic-plastic behavior of nonisothermal rotating annular disk is examined by A. Eraslan and T. Akış [11]. A. Eraslan and M.E. Kartal have an article about this study [14]. In order to estimate elastic and elastic-plastic stress behavior in a nonlinearly hardening cooling fin a computational model is developed. In 2014 A. Eraslan and Y. Kaya wrote an article which is “Thermoelastic response of a long tube subjected to periodic heating ” [19]. In this article an analytical model is developed to find the thermoelastic stress behavior of a long tube and to solve the heat conduction equation Duhamel’s theorem is used. Y.Orcan has also some studies in this field such as “The influence of temperature dependence of the yield stress on the stress distribution in a heat generating tube with free ends ” [17] and “Thermal stresses in a heat generating cylinder ” [23] respectively written in 2000 and in 1994. Before 2000s, some studies were also made. One of the most influential example to this is “Thermoelasticity and irreversible thermodynamics” written by H. Parkus and M.A Biot [4]. This article both emphasized the issue of thermoelasticity. Arslan has also important studies related to thermoelasticity and heat. For example in 2010, his article with his colleagues was published in *Acta Mechanica* [1]. In 2014, Arslan pointed out the elastic plastic model in an article [2]. All of these contributions to the topic have been analyzed in this work and a reference list has been provided

CHAPTER 2

PROBLEM DEFINITION AND SOLUTION

A periodic heat generating, infinitely long, solid cylinder of radius b is considered in this study which is presented in Fig.(2.1). The cylinder is initially at zero temperature and for times greater than zero, heat is generated internally and slowly at a time dependent rate. The temperature distribution in the cylinder is governed by the nonhomogeneous heat conduction equation

$$\frac{1}{\alpha_T} \frac{\partial T}{\partial t} = \frac{1}{r} \frac{\partial T}{\partial r} + \frac{\partial^2 T}{\partial r^2} + Q(t) \quad ; \quad 0 < r < b, \quad t > 0, \quad (2.1)$$

subjected to the following boundary and initial conditions:

$$\begin{aligned} T(0, t) &= \text{finite}, \quad t > 0, \\ T(b, t) &= 0, \quad t > 0, \\ T(r, 0) &= 0, \quad 0 \leq r \leq b. \end{aligned} \quad (2.2)$$

In these equations t denotes the time, r the radial coordinate, α_T the thermal diffusivity, $T(r, t)$ is the temperature in the cylinder at radial position r at time t and $Q(t)$ the time dependent heat generation rate.

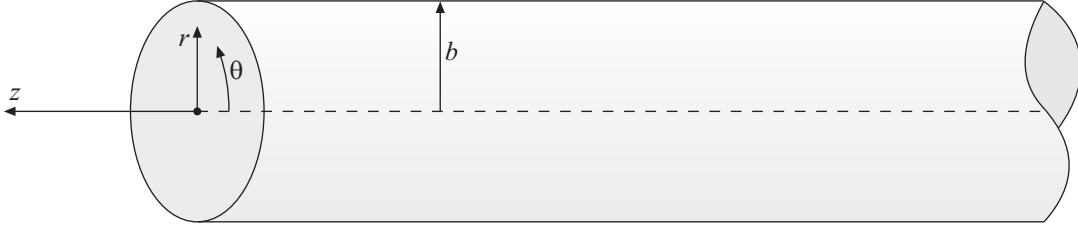


Figure 2.1: Infinitely long, solid cylinder of radius b .

2.1 Temperature Distribution

The solution of the heat conduction equation, Eqn. (2.1), with the conditions indicated by Eqns. (2.2) is obtained by using Duhamel's theorem

$$T(r, t) = \int_0^t Q(\beta) \frac{\partial}{\partial t} \Phi(r, t - \beta) d\beta, \quad (2.3)$$

where $\Phi(r, t)$ is the solution of the auxiliary problem given by

$$\frac{1}{\alpha_T} \frac{\partial \Phi}{\partial t} = \frac{1}{r} \frac{\partial \Phi}{\partial r} + \frac{\partial^2 \Phi}{\partial r^2} + C ; \quad 0 < r < b, \quad t > 0, \quad (2.4)$$

where C is a constant. It is a common practice to select $C = 1$. Boundary and initial conditions are

$$\begin{aligned} \Phi(0, t) &= \text{finite}, \quad t > 0, \\ \Phi(b, t) &= 0, \quad t > 0, \\ \Phi(r, 0) &= 0, \quad 0 \leq r \leq b. \end{aligned} \quad (2.5)$$

Since the partial differential equation for the auxiliary problem is not homogeneous, a solution of the form is proposed.

$$\Phi(r, t) = Y(r, t) + Z(r). \quad (2.6)$$

This solution is then substituted in the differential equation of the auxiliary problem to give

$$\frac{1}{\alpha_T} \frac{\partial Y}{\partial t} = \frac{1}{r} \frac{\partial Y}{\partial r} + \frac{\partial^2 Y}{\partial r^2} + \frac{1}{r} \frac{dZ}{dr} + \frac{d^2 Z}{dr^2} + 1. \quad (2.7)$$

Let,

$$\frac{1}{r} \frac{dZ}{dr} + \frac{d^2 Z}{dr^2} + 1 = 0, \quad (2.8)$$

so that the differential equation for $Y(r, t)$ becomes a homogeneous partial differential equation (PDE). The boundary and initial conditions should also be organized.

By using the first boundary condition, we can write

$$\Phi(0, t) = Y(0, t) + Z(0) = \text{finite}. \quad (2.9)$$

If we let

$$Z(0) = \text{finite}, \quad (2.10)$$

then

$$Y(0, t) = \text{finite}. \quad (2.11)$$

From the second boundary condition

$$\Phi(b, t) = Y(b, t) + Z(b) = 0, \quad (2.12)$$

letting

$$Z(b) = 0, \quad (2.13)$$

one obtains

$$Y(b, t) = 0. \quad (2.14)$$

And finally, from the initial condition

$$\Phi(r, 0) = Y(r, 0) + Z(r) = 0, \quad (2.15)$$

it follows that

$$Y(r, 0) = -Z(r). \quad (2.16)$$

With these manipulations, the differential equation $\Phi(r, t)$ is divided into two differential equations. The first one is an ordinary differential equation (ODE) in $Z(r)$ and second one is a partial differential equation (PDE) in $Y(r, t)$.

The ODE part with conditions are as the following

$$\frac{1}{r} \frac{dZ}{dr} + \frac{d^2 Z}{dr^2} + 1 = 0, \quad (2.17)$$

with the boundary conditions

$$Z(0) = \text{finite}, \quad (2.18)$$

and

$$Z(b) = 0. \quad (2.19)$$

The solution of $Z(r)$ is

$$Z(r) = C_1 \ln r + C_2 - \frac{r^2}{4}. \quad (2.20)$$

Application of the boundary conditions reveals

$$C_1 = 0, \quad (2.21)$$

and

$$C_2 = \frac{b^2}{4}. \quad (2.22)$$

As a result the complete solution of $Z(r)$ takes the form

$$Z(r) = \frac{b^2 - r^2}{4}. \quad (2.23)$$

The PDE for $Y(r, t)$

$$\frac{1}{\alpha_T} \frac{\partial Y}{\partial t} = \frac{1}{r} \frac{\partial Y}{\partial r} + \frac{\partial^2 Y}{\partial r^2}, \quad (2.24)$$

subject to

$$Y(0, t) = \text{finite.}$$

$$Y(b, t) = 0. \quad (2.25)$$

$$Y(r, 0) = -Z(r).$$

is solved by the standard separation of variables method. A solution of the form is suggested

$$Y(r, t) = R(r)\theta(t). \quad (2.26)$$

Differentiating and substituting into Eqn. (2.24) we obtain

$$\frac{1}{\alpha_T} \frac{1}{\theta} \frac{d\theta}{dt} = \frac{1}{R} \left(\frac{1}{r} \frac{dR}{dr} + \frac{d^2 R}{dr^2} \right). \quad (2.27)$$

The left hand side of this equation depends only on t and the right hand side of this equation depends only on r . This is possible if both sides of this equation is equal to a same constant say $-\lambda^2$. The result is

$$\frac{1}{\alpha_T} \frac{1}{\theta} \frac{d\theta}{dt} = \frac{1}{R} \left(\frac{1}{r} \frac{dR}{dr} + \frac{d^2 R}{dr^2} \right) = -\lambda^2. \quad (2.28)$$

Separating the equations we get

$$\frac{1}{r} \frac{dR}{dr} + \frac{d^2 R}{dr^2} + \lambda^2 R = 0, \quad (2.29)$$

and

$$\frac{d\theta}{dt} + \alpha_T \lambda^2 \theta = 0. \quad (2.30)$$

The boundary conditions for $R(r)$ are obtained from the boundary conditions of $Y(r, t)$. They are

$$R(b) = 0. \quad (2.31)$$

and

$$R(0) = \text{finite}. \quad (2.32)$$

The solutions for $R(r)$ and $\theta(t)$ take, respectively, the forms

$$R(r) = C_1 J_0(\lambda r) + C_2 Y_0(\lambda r), \quad (2.33)$$

$$\theta(t) = C_3 e^{-\alpha_T \lambda^2 t}. \quad (2.34)$$

where J_0 and Y_0 are the first and second kind Bessel functions. The condition $R(0) = \text{finite}$ implies $C_2 = 0$ since $Y_0(0) \rightarrow -\infty$ and the one $R(b) = 0$ leads to

$$J_0(\lambda b) = 0. \quad (2.35)$$

Positive roots λ_n , for $n = 1, 2, \dots, \infty$, of this last equation gives the eigenvalues of the problem.

Hence, one solution is

$$Y_n(r, t) = A_n e^{-\alpha_T \lambda_n^2 t} J_0(\lambda_n r), \quad (2.36)$$

and by superposition

$$Y(r, t) = \sum_{n=1}^{\infty} A_n e^{-\alpha_T \lambda_n^2 t} J_0(\lambda_n r), \quad (2.37)$$

is also a solution. To determine A_n we use the initial condition $Y(r, 0) = -Z(r)$ which reads

$$\frac{r^2 - b^2}{4} = \sum_{n=1}^{\infty} A_n J_0(\lambda_n r). \quad (2.38)$$

Multiplying both sides by $r J_0(\lambda_m r)$ and integrating from 0 to b we get the equation

$$\int_0^b \left(\frac{r^2 - b^2}{4} \right) r J_0(\lambda_m r) dr = \sum_{n=1}^{\infty} A_n \int_0^b r J_0(\lambda_n r) J_0(\lambda_m r) dr. \quad (2.39)$$

Note that

$$\int_0^b r J_0(\lambda_n r) J_0(\lambda_m r) dr = \begin{cases} 0 & \text{if } m \neq n \\ \int_0^b r [J_0(\lambda_n r)]^2 dr & \text{if } m = n \end{cases}, \quad (2.40)$$

therefrom

$$A_n = \frac{\int_0^b \left(\frac{r^2 - b^2}{4} \right) r J_0(\lambda_n r) dr}{\int_0^b r [J_0(\lambda_n r)]^2 dr}, \quad (2.41)$$

and performing the integrations we obtain

$$A_n = -\frac{J_2(\lambda_n b)}{\lambda_n^2 [J_1(\lambda_n b)]^2} = -\frac{2}{\lambda_n^3 b J_1(\lambda_n b)}, \quad (2.42)$$

where the recurrence

$$J_1(\lambda_n b) = \frac{\lambda_n b}{2} [J_2(\lambda_n b) + J_0(\lambda_n b)] = \frac{\lambda_n b}{2} [J_2(\lambda_n b) + 0] = \frac{\lambda_n b}{2} [J_2(\lambda_n b)], \quad (2.43)$$

and the eigenvalue equation $J_0(\lambda_n b) = 0$ have been utilized. Hence, the solution for $Y(r, t)$ takes the form

$$Y(r, t) = -\frac{2}{b} \sum_{n=1}^{\infty} e^{-\alpha_T \lambda_n^2 t} \frac{J_0(\lambda_n r)}{\lambda_n^3 J_1(\lambda_n b)}. \quad (2.44)$$

Knowing the solution for $Z(r)$ and $Y(r, t)$, the solution for the auxiliary equation is written as

$$\Phi(r, t) = \frac{b^2 - r^2}{4} - \frac{2}{b} \sum_{n=1}^{\infty} e^{-\alpha_T \lambda_n^2 t} \frac{J_0(\lambda_n r)}{\lambda_n^3 J_1(\lambda_n b)}, \quad (2.45)$$

then by Duhamel's theorem given by Eqn. (2.3) the temperature distribution becomes

$$T(r, t) = \int_0^t Q(\beta) \frac{\partial}{\partial t} \Phi \left(\frac{b^2 - r^2}{4} - \frac{2}{b} \sum_{n=1}^{\infty} e^{-\alpha_T \lambda_n^2 (t-\beta)} \frac{J_0(\lambda_n r)}{\lambda_n^3 J_1(\lambda_n b)} \right) d\beta, \quad (2.46)$$

$$= \frac{2\alpha_T}{b} \sum_{n=1}^{\infty} \frac{J_0(\lambda_n r)}{\lambda_n J_1(\lambda_n b)} \int_0^t Q(\beta) e^{-\alpha_T \lambda_n^2 (t-\beta)} d\beta, \quad (2.47)$$

For the first case

$$Q(t) = A \sin(t) \quad (2.48)$$

so $Q(\beta) = A \sin(\beta)$. Hence the temperature distribution equation becomes

$$T(r, t) = \frac{2A\alpha_T}{b} \sum_{n=1}^{\infty} \frac{J_0(\lambda_n r)}{\lambda_n J_1(\lambda_n b)} \frac{e^{-\alpha_T \lambda_n^2 t} - \cos(t) + \alpha_T \lambda_n^2 \sin(t)}{(1 + \alpha_T^2 \lambda_n^4)}. \quad (2.49)$$

For the second case

$$Q(t) = At \cos(t), \quad (2.50)$$

so $Q(\beta) = A\beta \cos(\beta)$. If we use this condition and follow the same steps as above, $T(r, t)$ takes the form

$$T(r, t) = \frac{2A\alpha_T}{b} \sum_{n=1}^{\infty} \frac{J_0(\lambda_n r)}{\lambda_n J_1(\lambda_n b)} \Psi(\lambda_n, \alpha_T, t), \quad (2.51)$$

where

$$\Psi(\lambda_n, \alpha_T, t) = \frac{e^{-\alpha_T \lambda_n^2 t} (-1 + \alpha_T^2 \lambda_n^4) + \cos(t) - \alpha_T^2 \lambda_n^4 \cos(t) - 2\alpha_T \lambda_n^2 \sin(t) + t(1 + \alpha_T^2 \lambda_n^4)(\alpha_T \lambda_n^2 \cos(t) + \sin(t))}{(1 + \alpha_T^2 \lambda_n^4)^2}. \quad (2.52)$$

If we take the derivatives of $T(r, t)$ with respect to r according to the first and second cases, the temperature gradients are obtained respectively as;

$$\frac{\partial(T(r, t))}{\partial r} = -\frac{2A\alpha_T}{b} \sum_{n=1}^{\infty} \frac{J_1(\lambda_n r)}{J_1(\lambda_n b)} \frac{e^{-\alpha_T \lambda_n^2 t} - \cos(t) + \alpha_T \lambda_n^2 \sin(t)}{(1 + \alpha_T^2 \lambda_n^4)}, \quad (2.53)$$

and

$$\frac{\partial(T(r, t))}{\partial r} = -\frac{2A\alpha_T}{b} \sum_{n=1}^{\infty} \frac{J_1(\lambda_n r)}{J_1(\lambda_n b)} \Psi(\lambda_n, \alpha_T, t). \quad (2.54)$$

The verifications of the step by step solutions described above have been performed using finite element program [15]. With the help of this computer programme, verifications could be compared via making the programme be able to solve the periodic boundary condition problem and the graphs of the solutions are presented in Figures (2.2)-(2.5). The dots on the graphs indicate the results of the finite element program, whereas the lines denote the results of this work. These verifications have been performed for both cases, *Asint* and *Atcost*. In these solutions, A , which is the arbitrary constant, has been taken as 2, and α_T , which is thermal diffusivity, has been taken as 1 in order to make a nondimensional solution. Structural steel has been used as the material for the verifications. The mechanical properties of the material can be found in Append B.

The temperature distribution throughout the radial coordinate of the solid cylinder at different times is shown in Fig.(2.2) and Fig. (2.4). Figures (2.2) and (2.4) have been plotted for the cases *Asint* and *Atcost*, respectively. As can be seen in these figures,

as time increases in a certain radial coordinate, so does the temperature distribution. For example, in the center of the cylinder, $r = 0$ and time interval $0 - 1$, temperature distribution reaches its maximum value. However, closer to the surface of the cylinder, $r = 1$, the temperature distribution value decreases and is 0 on the surface. This indicates that the maximum temperature of the object is in the center, but the object gets cooler towards the surface, and reaches 0 degrees on the surface. This provides the boundary condition of our problem.

The evolution of the temperature gradient with radial coordinate of the solid cylinder at different times is illustrated in Figures (2.3) and (2.5). Figures (2.3) and (2.5) are plotted for $Asint$ and $Atcost$, respectively. In both graphs, in the center of the cylinder, $r = 0$, the temperature gradient is 0 and in time, as it got closer to the surface, this value decreased, reaching minus values. For example, in Fig. (2.3), $t = 1$ and $r = 1$, in other words on the surface, by reaching -0.8 in time interval $0 - 1$, temperature gradient value of the cylinder has reached its lowest value. This indicates that cooling increases towards the surface. From this we understand that as time passes and as it gets closer to the surface of the cylinder, the temperature gradient value starts decreasing in inverse proportion to this increase and takes its lowest value at the surface.

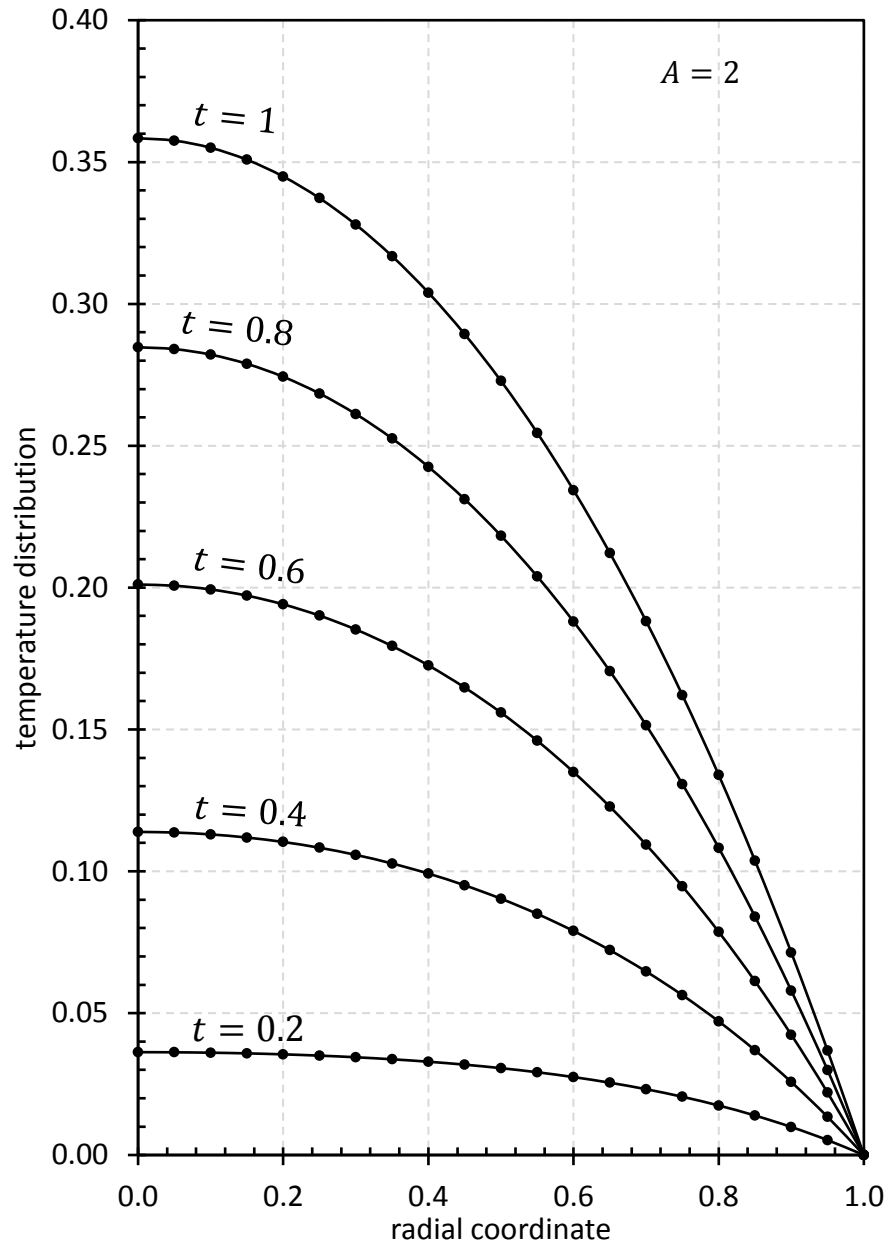


Figure 2.2: Temperature distribution verification of structural steel for Asint case.

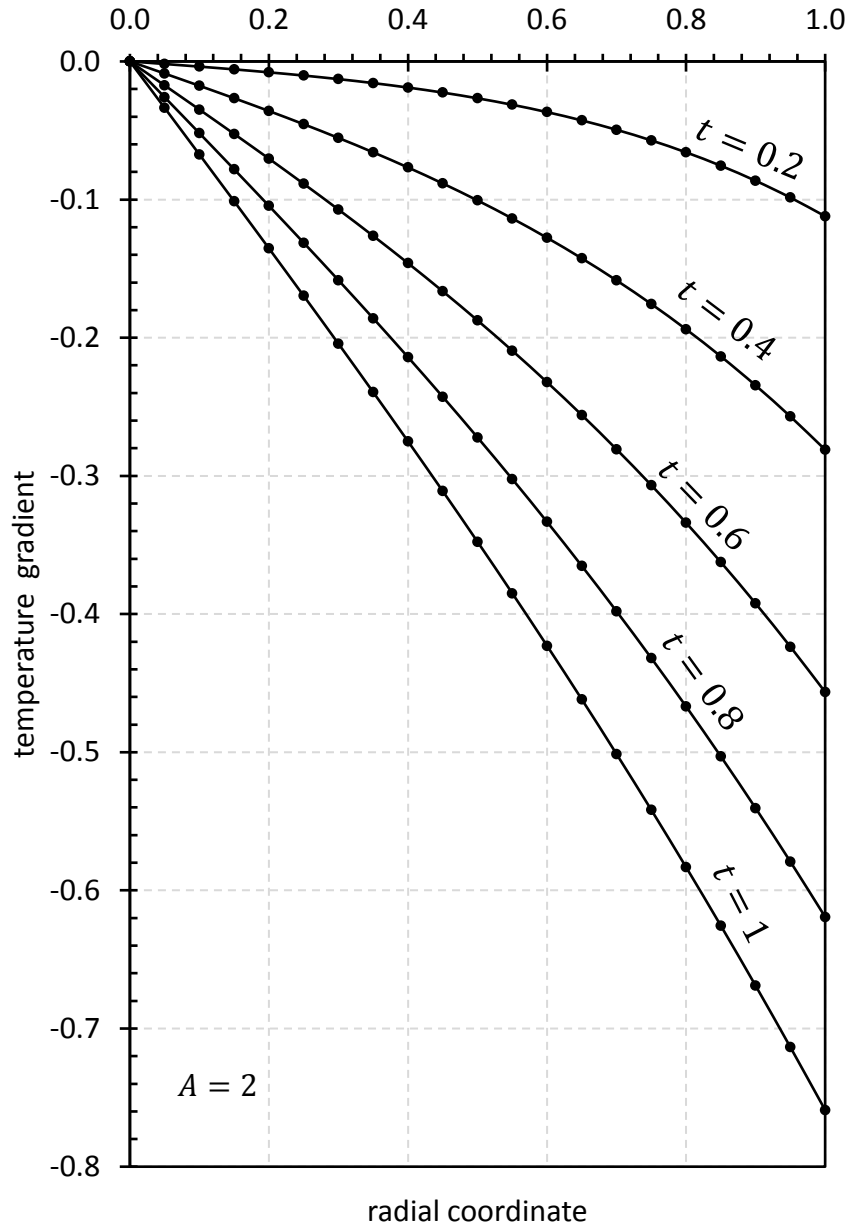


Figure 2.3: Temperature gradient verification of structural steel for Asint case.

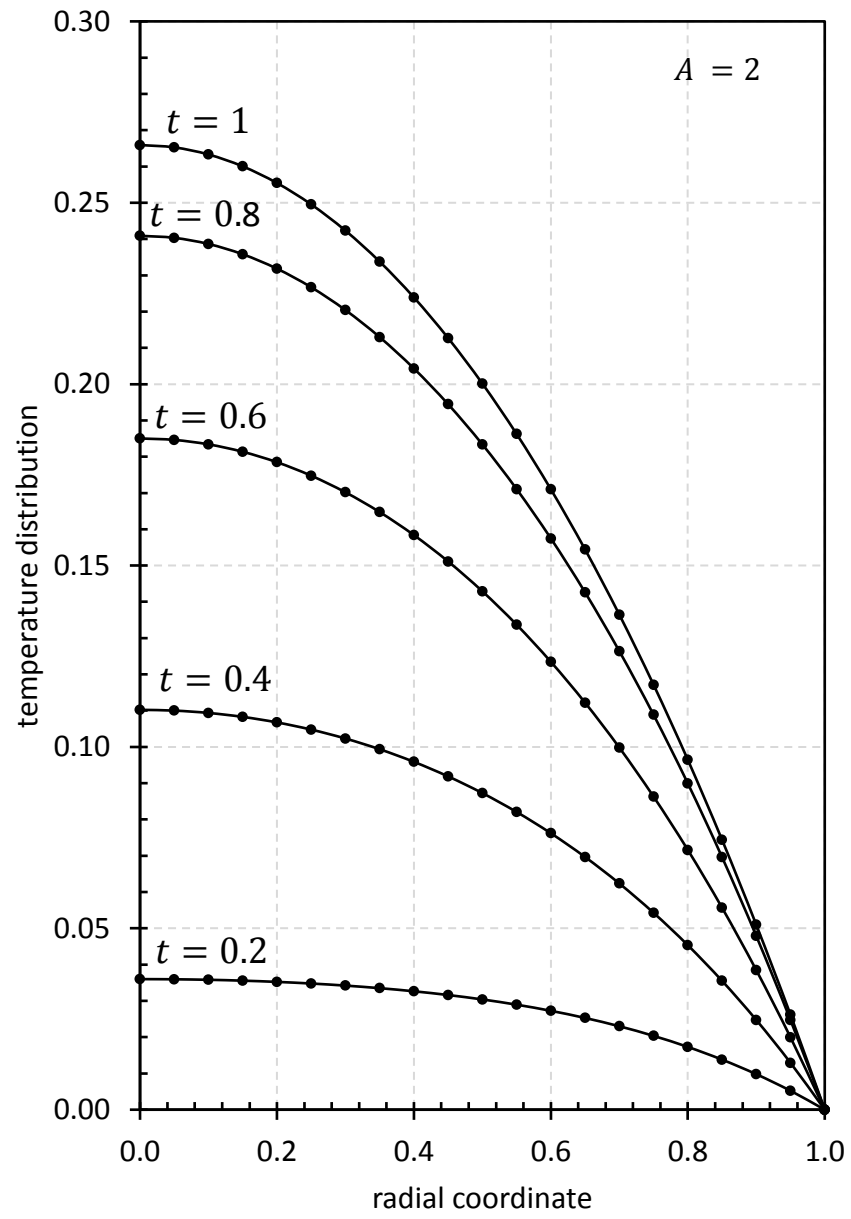


Figure 2.4: Temperature distribution verification of structural steel for Atcost case.

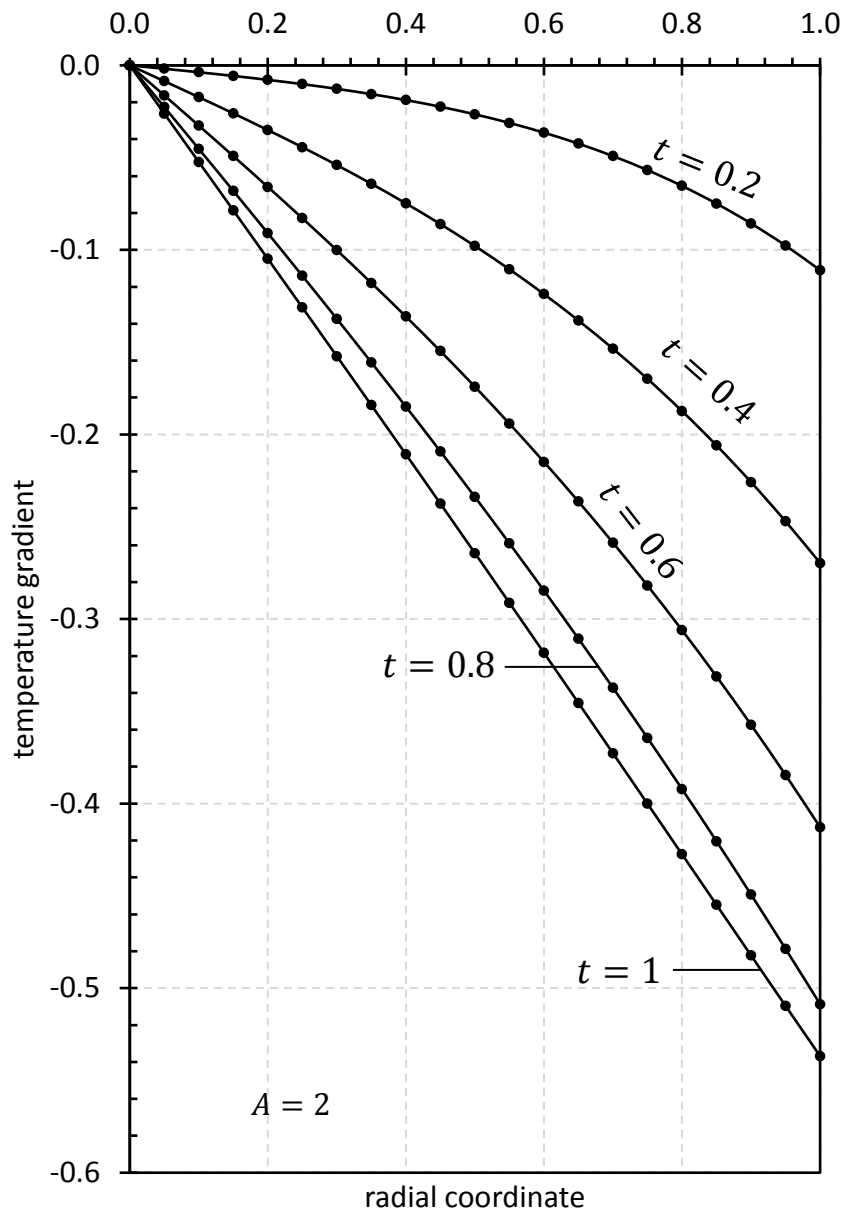


Figure 2.5: Temperature gradient verification of structural steel for Atcost case.

2.2 Elastic Solution

In this part, basic equations written using Timoshenko and Goodier notation [25], are defined. In these equations σ_j represents the stress component, ϵ_j the normal strain component and u the radial displacement. The governing equation examining the thermoelastic responses of the solid cylinder is derived and required stress, strain and radial displacement are achieved by the solution of this equation.

The equation of equilibrium and strain displacement relations are

$$\frac{d\sigma_r}{dr} + \frac{\sigma_r - \sigma_\theta}{r} = 0, \quad (2.55)$$

$$\epsilon_\theta = \frac{u}{r} ; \quad \epsilon_r = \frac{du}{dr} = u'. \quad (2.56)$$

Last equation is generalized Hooke's law

$$\begin{aligned} \epsilon_r &= \frac{1}{E} [\sigma_r - \nu (\sigma_\theta + \sigma_z)], \\ \epsilon_\theta &= \frac{1}{E} [\sigma_\theta - \nu (\sigma_r + \sigma_z)], \\ \epsilon_z &= \frac{1}{E} [\sigma_z - \nu (\sigma_r + \sigma_\theta)]. \end{aligned} \quad (2.57)$$

These equations are the elastic strains and in these equations E denotes the modulus of elasticity, ν the Poissons' ratio, α the coefficient of thermal expansion. When thermal part, which is $\alpha\Delta T$, is added to Eqns. (2.57), total strains are handled and these are;

$$\epsilon_r = \frac{1}{E} [\sigma_r - \nu (\sigma_\theta + \sigma_z)] + \alpha\Delta T, \quad (2.58)$$

$$\epsilon_\theta = \frac{1}{E} [\sigma_\theta - \nu (\sigma_r + \sigma_z)] + \alpha\Delta T, \quad (2.59)$$

$$\epsilon_z = \frac{1}{E} [\sigma_z - \nu (\sigma_r + \sigma_\theta)] + \alpha\Delta T. \quad (2.60)$$

$\Delta T = T(r, t) - T_{ref}$ is the temperature gradient at any radial coordinate r and T_{ref} is the reference temperature at time t in the cylinder. In case of the generalized plane strain, the axial strain, $\epsilon_z = \epsilon_0 = \text{constant}$, hence from Eqn. (2.60) the axial stress (σ_z) is determined in terms of radial (σ_r) and circumferential (σ_θ) stresses as

$$\sigma_z = E\epsilon_0 - \alpha ET + \nu (\sigma_r + \sigma_\theta). \quad (2.61)$$

The axial stress is eliminated in total strain expressions and the results are combined with strain-displacement relations to give:

$$\sigma_r = \frac{E\epsilon_0\nu}{(1+\nu)(1-2\nu)} + \frac{E}{(1+\nu)(1-2\nu)} \left[\nu \frac{u}{r} + (1-\nu)u' \right] - \frac{E\alpha T}{(1-2\nu)}, \quad (2.62)$$

$$\sigma_\theta = \frac{E\epsilon_0\nu}{(1+\nu)(1-2\nu)} + \frac{E}{(1+\nu)(1-2\nu)} \left[(1-\nu)\frac{u}{r} + \nu u' \right] - \frac{E\alpha T}{(1-2\nu)}. \quad (2.63)$$

Inserting these stresses into the equation of equilibrium, Eqn. (2.55), leads to the elastic equation in terms of the radial displacement as

$$r^2 \frac{d^2 u}{dr^2} + r \frac{du}{dr} - u = \frac{\alpha(1+\nu)}{(1-\nu)} r^2 \frac{dT}{dr}. \quad (2.64)$$

This is a Cauchy-Euler nonhomogeneous differential equation. After some algebra the general solution of this equation is put into the form :

$$u(r) = C_1^* r + \frac{1}{r} C_2^* + \frac{\alpha(1+\nu)}{(1-\nu)} \frac{1}{r} \int_0^r \eta T(\eta) d\eta, \quad (2.65)$$

where C_1^* and C_2^* are integration constants. Since u and the stresses must be finite at the center, i.e. at $r = 0$, so we require that $C_2^* = 0$. Therefore,

$$u(r) = C_1^* r + \frac{\alpha(1+\nu)}{(1-\nu)} \frac{1}{r} \int_0^r \eta T(\eta) d\eta. \quad (2.66)$$

Note that

$$\frac{1}{r} \int_0^r \eta T(\eta, t) d\eta, \quad (2.67)$$

is an indeterminate expression so its actual value is determined by using L'Hospital rule:

$$\lim_{r \rightarrow 0} \frac{\int_0^r \eta T(\eta, t) d\eta}{r} = \lim_{r \rightarrow 0} \frac{\frac{d}{dr} \int_0^r \eta T(\eta, t) d\eta}{\frac{d}{dr}(r)} = \lim_{r \rightarrow 0} r T(r) = 0. \quad (2.68)$$

If we substitute the displacement into the radial and circumferential stresses, we obtain :

$$\sigma_r = \frac{E}{(1+\nu)(1-2\nu)} (\epsilon_0\nu + C_1^*) - \frac{E\alpha}{(1-\nu)} \frac{1}{r^2} \int_0^r \eta T(\eta, t) d\eta, \quad (2.69)$$

and

$$\sigma_\theta = \frac{E(\epsilon_0\nu + C_1^*)}{(1+\nu)(1-2\nu)} + \frac{E\alpha}{(1-\nu)} \frac{1}{r^2} \int_0^r \eta T(\eta, t) d\eta - \frac{E\alpha T}{(1-\nu)}. \quad (2.70)$$

Note that, $\frac{\int_0^r \eta T(\eta, t) d\eta}{r^2}$ is also an indeterminate expression like above, so its numerical solution is handled by using L'Hospital rule again like

$$\lim_{r \rightarrow 0} \frac{\int_0^r \eta T(\eta, t) d\eta}{r^2} = \lim_{r \rightarrow 0} \frac{\frac{d}{dr} \int_0^r \eta T(\eta, t) d\eta}{\frac{d}{dr}(r^2)} = \frac{T(0, t)}{2}. \quad (2.71)$$

If σ_r and σ_θ are substituted into the σ_z which is Eqn. (2.61), the axial stress becomes as

$$\sigma_z = \frac{E}{(1+\nu)(1-2\nu)} [\epsilon_0(1-\nu) + 2\nu C_1^*] - \frac{E\alpha T}{(1-\nu)}. \quad (2.72)$$

At $r = 0$ radial and circumferential stresses become as

$$\sigma_r(0) = \sigma_\theta(0) = \frac{E}{(1-2\nu)(1+\nu)} (\epsilon_0\nu + C_1^*) - \frac{E\alpha T(0)}{2(1-\nu)}, \quad (2.73)$$

and the displacement is

$$u(0) = 0. \quad (2.74)$$

In these equations ϵ_0 and C_1^* are the unknown constants which should be determined. In order to find these constants we use two boundary conditions and they are

$$\sigma_r(b) = 0, \quad (2.75)$$

and $F_z = \sigma_z dA = 0$. In these equations F_z denotes the axial force and this boundary condition implies that the solid cylinder can expand and contract freely in axial direction at any temperature. Because of axial symmetry the axial force can be written as

$$F_z = \int \sigma_z dA = 2\pi \int_0^b r \sigma_z dr = \int_0^b r \sigma_z dr = 0. \quad (2.76)$$

By using these boundary conditions ϵ_0 and C_1^* constants are determined for the first case, which is given Eqn. (2.48), as

$$\epsilon_0 = \frac{2\alpha}{b^2} \int_0^b r T(r) dr, \quad (2.77)$$

$$= \frac{2\alpha}{b^2} \frac{2A\alpha_T}{b} \sum_{n=1}^{\infty} \frac{e^{-\alpha_T \lambda_n^2 t} - \cos(t) + \alpha_T \lambda_n^2 \sin(t)}{(1 + \alpha_T^2 \lambda_n^4)} \int_0^b r \frac{J_0(\lambda_n r)}{\lambda_n J_1(\lambda_n b)} dr, \quad (2.78)$$

$$= \frac{2\alpha}{b^2} \frac{2A\alpha_T}{b} \sum_{n=1}^{\infty} \frac{e^{-\alpha_T \lambda_n^2 t} - \cos(t) + \alpha_T \lambda_n^2 \sin(t)}{(1 + \alpha_T^2 \lambda_n^4)} \frac{b J_1(\lambda_n b)}{\lambda_n^2 J_1(\lambda_n b)}, \quad (2.79)$$

or

$$\epsilon_0 = \frac{4\lambda_n^2 A \alpha_T}{b^2} \sum_{n=1}^{\infty} \frac{1}{\lambda_n^2} \frac{e^{-\alpha_T \lambda_n^2 t} - \cos(t) + \alpha_T \lambda_n^2 \sin(t)}{(1 + \alpha_T^2 \lambda_n^4)}. \quad (2.80)$$

and

$$C_1^* = \frac{\alpha(1-3\nu)}{b^2(1-\nu)} \int_0^b r T(r) dr, \quad (2.81)$$

$$= \frac{\alpha(1-3\nu)}{b^2(1-\nu)} \frac{2A\alpha_T}{b} \sum_{n=1}^{\infty} \frac{e^{-\alpha_T \lambda_n^2 t} - \cos(t) + \alpha_T \lambda_n^2 \sin(t)}{(1 + \alpha_T^2 \lambda_n^4)} \frac{b}{\lambda_n^2}, \quad (2.82)$$

or

$$C_1^* = \frac{\alpha(1-3\nu)}{b^2(1-\nu)} 2A\alpha_T \sum_{n=1}^{\infty} \frac{1}{\lambda_n^2} \frac{e^{-\alpha_T \lambda_n^2 t} - \cos(t) + \alpha_T \lambda_n^2 \sin(t)}{(1 + \alpha_T^2 \lambda_n^4)}. \quad (2.83)$$

For the second case, which is given Eqn. (2.50), same steps are followed as above to achieve the constants ϵ_0 and C_1^* ,

$$\epsilon_0 = \frac{4\lambda_n^2 A\alpha_T}{b^2} \sum_{n=1}^{\infty} \frac{1}{\lambda_n^2} \Psi(\lambda_n, \alpha_T, t), \quad (2.84)$$

and

$$C_1^* = \frac{\alpha(1-3\nu)}{b^2(1-\nu)} 2A\alpha_T \sum_{n=1}^{\infty} \frac{1}{\lambda_n^2} \Psi(\lambda_n, \alpha_T, t). \quad (2.85)$$

Integrals which are used above equations are performed as;

$$\int_0^r \eta T(\eta) d\eta = \frac{2A\alpha_T}{b} \sum_{n=1}^{\infty} \frac{e^{-\alpha_T \lambda_n^2 t} - \cos(t) + \alpha_T \lambda_n^2 \sin(t)}{(1 + \alpha_T^2 \lambda_n^4)} \frac{r J_1(\lambda_n r)}{\lambda_n^2 J_1(\lambda_n b)} \quad (2.86)$$

$$= \frac{2A\alpha_T}{b} \sum_{n=1}^{\infty} \frac{r J_1(\lambda_n r)}{\lambda_n^2 J_1(\lambda_n b)} \frac{e^{-\alpha_T \lambda_n^2 t} - \cos(t) + \alpha_T \lambda_n^2 \sin(t)}{(1 + \alpha_T^2 \lambda_n^4)} \quad (2.87)$$

and

$$\int_0^b r T(r) dr = \frac{2A\alpha_T}{b} \sum_{n=1}^{\infty} \frac{e^{-\alpha_T \lambda_n^2 t} - \cos(t) + \alpha_T \lambda_n^2 \sin(t)}{(1 + \alpha_T^2 \lambda_n^4)} \frac{b}{\lambda_n^2}, \quad (2.88)$$

$$= 2A\alpha_T \sum_{n=1}^{\infty} \frac{1}{\lambda_n^2} \frac{e^{-\alpha_T \lambda_n^2 t} - \cos(t) + \alpha_T \lambda_n^2 \sin(t)}{(1 + \alpha_T^2 \lambda_n^4)}. \quad (2.89)$$

In the elastic verification graphics, our A value, the arbitrary constant, is 2 and our α_T value, the thermal diffusivity, is 1 because of the nondimensional solution and the material is structural steel. The dots indicate the solutions of the finite element program, whereas the lines indicate the results of this work. These graphs have been plotted at time, t , equals 0.5. The elastic solution verification has been done for both cases. The evolution of stresses and displacement with radial coordinate for the described time which is equal to 0.5 seconds, is shown in Figures (2.6) and (2.7). In Fig.(2.6), the heat generation rate, $Q(t)$, is equal to $Asint$ and for the second figure, Fig(2.7), heat generation rate is equal to $Atcost$.

In these graphs, at $r = 0$, the variation along the radial direction is 0, and the radial stress at $r = 1$ position is 0. The circumferential and axial stress values increase

towards the surface of the solid cylinder, and these two stress values coincide at some point. The fact that the dots and lines overlap proves that the problem we have solved is correct.

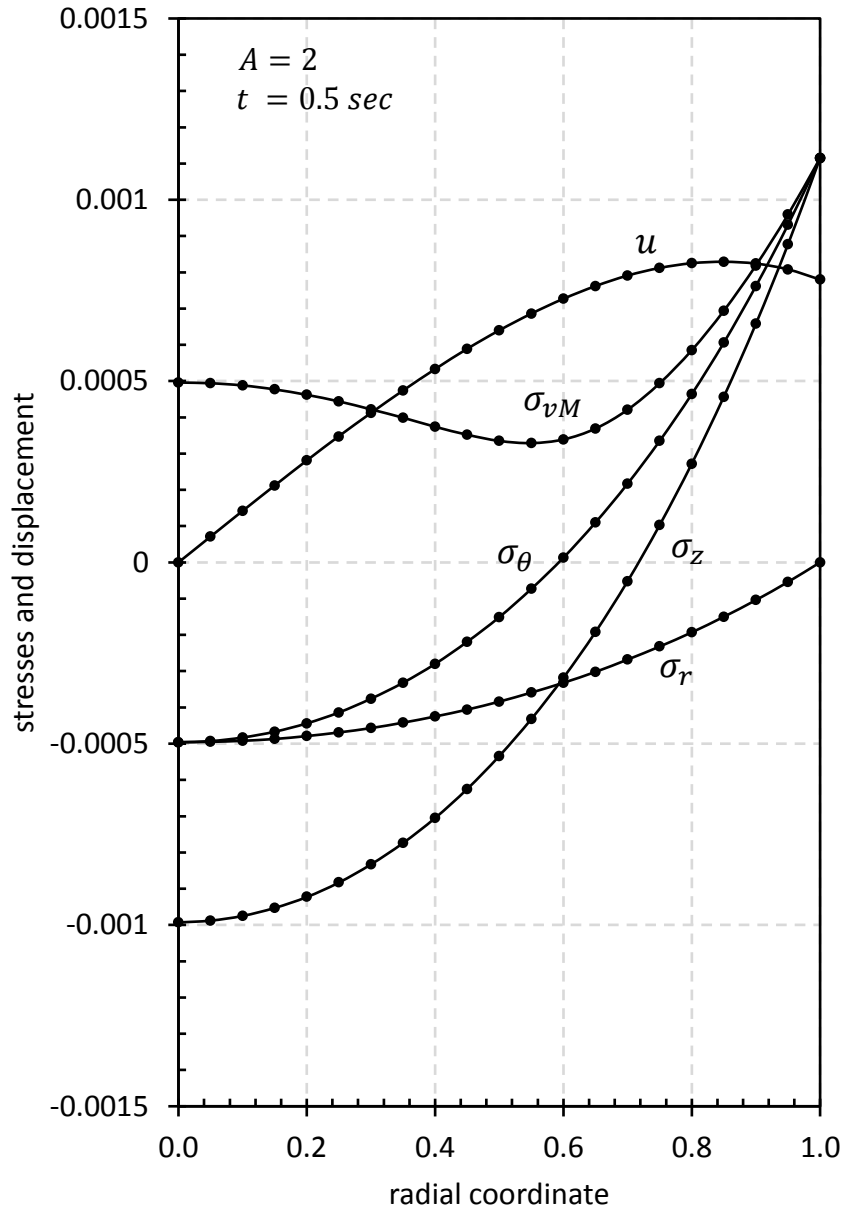


Figure 2.6: Elastic solution verification of structural steel for Asint case.

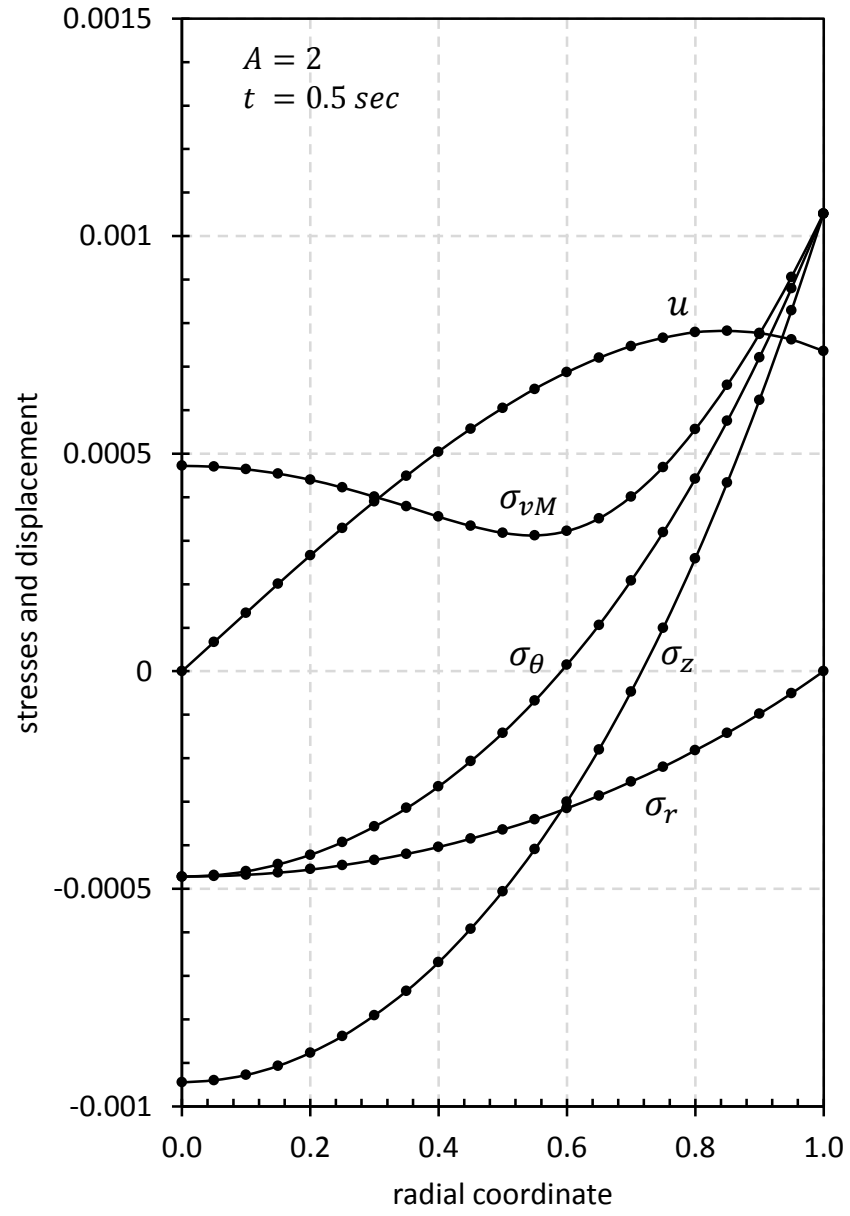


Figure 2.7: Elastic solution verification of structural steel for Atcost case.

CHAPTER 3

RESULTS AND DISCUSSION

In this study, two different heat generation rates, $Q(t)$, are used in the computations. For the first case, $Q(t) = Asint$ and for the second case $Q(t) = Atcost$ in which A is an amplitude of the function. These rates represent the periodic time dependent heat generation rate. In the calculations, Poisson's ratio, ν , is selected as 0.3 and while the unit for the α_T value is $m^2/second$ in the verifications, in the dimensional solutions, it is multiplied by 3600 and calculated as $m^2/hour$. Calculations are performed by using the Fortran programs. Program codes are presented in Append A. The nondimensional verifications of the temperature distribution, temperature gradient and elastic solution were presented in Chapter 2; the problem definition and solution. Being certain that the solutions and codes are correct, we are continuing our dimensionally solved work.

The problem is solved for each case by using two different materials, namely steel and brass and the mechanical properties of these materials can be found in Append A. The figures will be explained in four parts. The material in the first part is steel and $Q(t) = Asint$. In the second part, the material is steel again, but $Q(t) = Atcost$. In parts three and four, yellow brass is used as the material. For the third part $Q(t) = Asint$, whereas for the fourth part $Q(t) = Atcost$. In this study our solutions made dimensional except verifications which is performed in Chapter 2, but in this chapter figures are presented in nondimensional form. Figures (3.1) and (3.2) show the evolution of Sine and Cosine functions with time and we understood that our solutions are correct by controlling with these graphs.

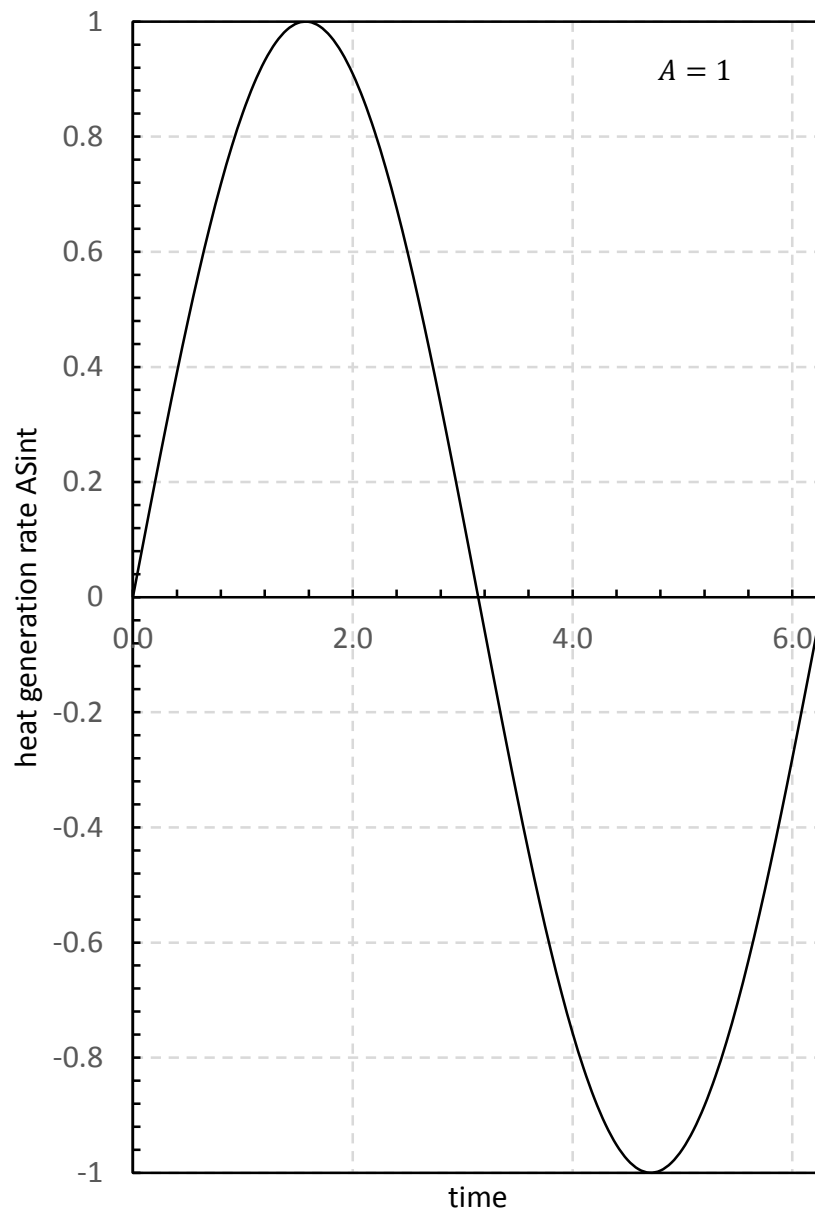


Figure 3.1: The variation of heat generation rate AS_{int} with time for $A=1$.

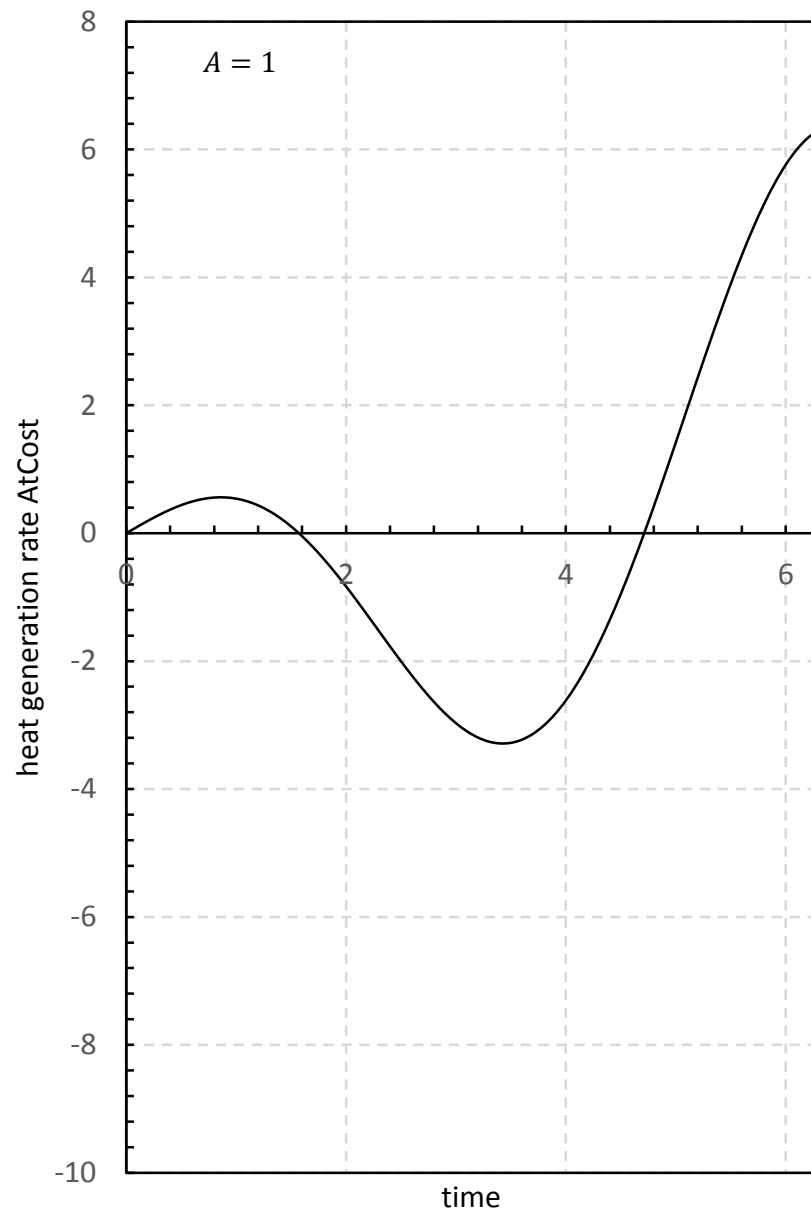


Figure 3.2: The variation of heat generation rate $AtCost$ with time for $A=1$.

Figures (3.3)-(3.11) show the dimensional solutions for the steel material under $Asint$ condition. In this condition, the value of α_T is $0.04807 \text{ m}^2/\text{hour}$, t is between 0 and 5 hours, and A is taken as 1525. The reason the A value is taken as 1525 is that according to the von Mises criteria, for σ_{vM} to reach its maximum value before moving on to the plastic area, the value of A is found to be 1525, and the solutions are obtained accordingly.

Fig.(3.3) is the graph for radial coordinate versus temperature distribution. In this graph, at $t = 0.01h$, the temperature distribution is almost 0, and this provides the initial condition of our problem. When time is between 0 – 5, $r = 1$, the temperature distribution equals 0, and this provides the boundary condition of our problem. When time is between 0.01 and 3 at the center of the cylinder, the temperature distribution also increases with time, and reaches its highest value at $t = 3h$. Later on, at $t = 4h$ and $t = 5h$ the temperature distribution value decreases and reaches its minimum value at $t = 5h$. The path time is in the shape of a \sin function and this once more indicates that our solution is correct. Fig.(3.4) is the temperature gradient and radial coordinate graph. In this graph, at $0.01h$ and $0 < r < 1$ interval the temperature gradient value is almost 0, and with time, from 1 to 2 hours the temperature gradient value decreased even more, and reached its minimum value at $t = 2h$ at the surface of the cylinder. Afterwards, the temperature gradient value started to increase, and at $t = 5$, $r = 1$ it reached its maximum value.

In the temperature gradient graph, the temperature gradient value is 0 at $r = 0$ this is proof that our problem is correct because our boundary condition which is, $T(0, t) = \text{finite}$, so dT/dr is also becomes 0 at $r = 0$. The radial stress and radial coordinate graph is shown in Fig. (3.5). At $r = 1$ the solid cylinder is free of radial stress. This means that there is no stress in the radial direction at the surface of the cylinder. The lowest radial stress, compressive stress, is -0.40 at $t = 3$ and $r = 0$. This shows us that, at the radial direction, there is a compression in the center of the cylinder in the third hour. Fig.(3.6) and Fig.(3.7) represent the evolution of circumferential and axial stresses with radial coordinate respectively. In both graphs in the $0 < r < 1$ interval, the similar activities are observed at the same time. At $t = 3$ axial and circumferential stresses reach their maximum value, but they stop before moving on to the plastic region. This is because of the A value mentioned above. Again at

$t = 0.01$ the stress values for both axial and circumferential stresses are 0. At $r = 0$, which is the center of the cylinder, the axial and circumferential stresses reach their minimum values, which are -0.8 and -0.4 respectively, at $t = 3$. The fact that these values are negative, show that there is a compression at that specific time at the cylinder center.

The change in von Mises stress throughout the radial coordinate is presented in Fig. (3.8). At $t = 0.01$, the von Mises stress in the cylinder is 0. Again with the A value provided at the surface of the cylinder at $t = 3$, it reaches its maximum value of $\sigma_{vM} = 0.98$ at $r = 1$. The displacement of the cylinder at the time interval determined throughout the radial coordinate can clearly be seen in Fig. (3.9). At $r = 0$ no displacement is observed at all times, but as we move away from the center of the cylinder towards the surface, displacement increases and at $r = 1$ and $t = 3$, approximately 0.7 meter displacement is observed. We can see the harmony between the displacement graph and the temperature distribution graph, which is Fig. (3.3).

All changes in stress and displacements throughout the radial coordinate can be seen in one graph, Fig. (3.10). This graph is drawn for $t = 2.65h$ because at this time the von Mises stress reaches its maximum value. Here we understand that the difference between the principal stresses is always on the surface of the cylinder. Our last graph for this condition is Fig. (3.11) in which the change of the axial strain with time is seen. At $t = 3$ the strain in the axial direction reaches its maximum value at 0.0009. As in the other graphs, this graph also acts like a *sine* function.

As mentioned before, in the second part, the steel material is examined for the case of $Atcost$ and the results are presented in Figures (3.12) -(3.20). Because α_T , thermal diffusivity, is a material property, it is the same as in part 1, $0.04807 \text{ m}^2/\text{hour}$. However, the A value for $Atcost$ is found to be 498. Temperature distribution throughout the radial coordinate of the solid cylinder at different times is shown in Fig.(3.12). At $t = 0.01h$ all throughout the radial coordinate, the temperature distribution is 0. At $r = 1$, on the surface of the cylinder, for all times the temperature distribution equals 0 because according to our boundary condition, at the surface, the temperature distribution of the cylinder is 0. At $t = 4$ and $r = 0$ the cylinder reaches its minimum temperature distribution value of -120 , and this indicates that the most cooling at that

time and condition.

At $0 < r < 0.2$ interval, at times $t = 1$ and $t = 2$, the temperature distribution of the cylinder reaches its maximum value. In other words, it starts heating because it is positive, and at this radial coordinate interval, the temperature at the 1st and 2nd hours are equal to each other. The temperature gradient and radial coordinate graphs are seen in Fig. (3.13). The temperature gradient at the center of the cylinder is 0. In time, as the r value increases and moves away from the center of the cylinder, the temperature gradient value starts gaining values other than 0 and at $t = 4$, $r = 1$, it reaches its maximum value. In Fig.(3.14), the change in the radial direction stress throughout the radial coordinate is shown. As in the *Asint* graph, there is no radial direction stress on the surface of the cylinder, and σ_r reaches its maximum value at $t = 5h$ at the center of the cylinder. In other words, as we move away from the center of the cylinder, the radial stress decreases and becomes 0 at the surface. Figures (3.15) and (3.16) respectively indicate the circumferential and axial stresses. These two stresses, both show the same fluctuation throughout the radial coordinate. As can be understood from both graphs, at $r = 0$ and $t = 5$, both reach their highest value in the positive direction, and at $r = 1$ and $t = 4$ they both reach their highest value in the " – " direction, and the highest compression is observed here. Based on these graphs, this cylinder compresses as it moves towards the surface in axial and circumferential directions, at $t = 3, 4$, and 5th hours. The von Mises stress and radial coordinate change figure is Fig.(3.15). At $t = 0.001h$ the von Mises stress is almost 0. At the surface of the cylinder, at $t = 4$, it reaches the maximum value in elastic region. The displacement change throughout the radial coordinate can be seen in Fig.(3.18). Here, as in Fig. (3.9) no change occurs at the center of the cylinder. The reason for this is that the changes in the solid cylinder at the center make the cylinder a tube as the middle starts puncturing. For this reason, at $r = 0$, time has no displacement effect. In Fig. (3.18), at $t = 4$ and $r = 1$, it has the highest compression with $u = 0.7$. $t = 4.35^{th}$ hour is the time when the solid cylinder in the elastic region is about to move on to the plastic. The changes in all stresses and displacement throughout the radial coordinate are seen in Fig. (3.19). As can be understood from this graph, the maximum difference between the minimum and maximum principal stresses is on the surface of the cylinder. The change in the axial strain is presented in Fig. (3.20).

Time is taken between the interval 0 and 6. It is seen that it reaches its maximum compression value in the fourth hour. However, we observe that as time increases the *cos* fluctuation continues and increases and decreases at certain periods.

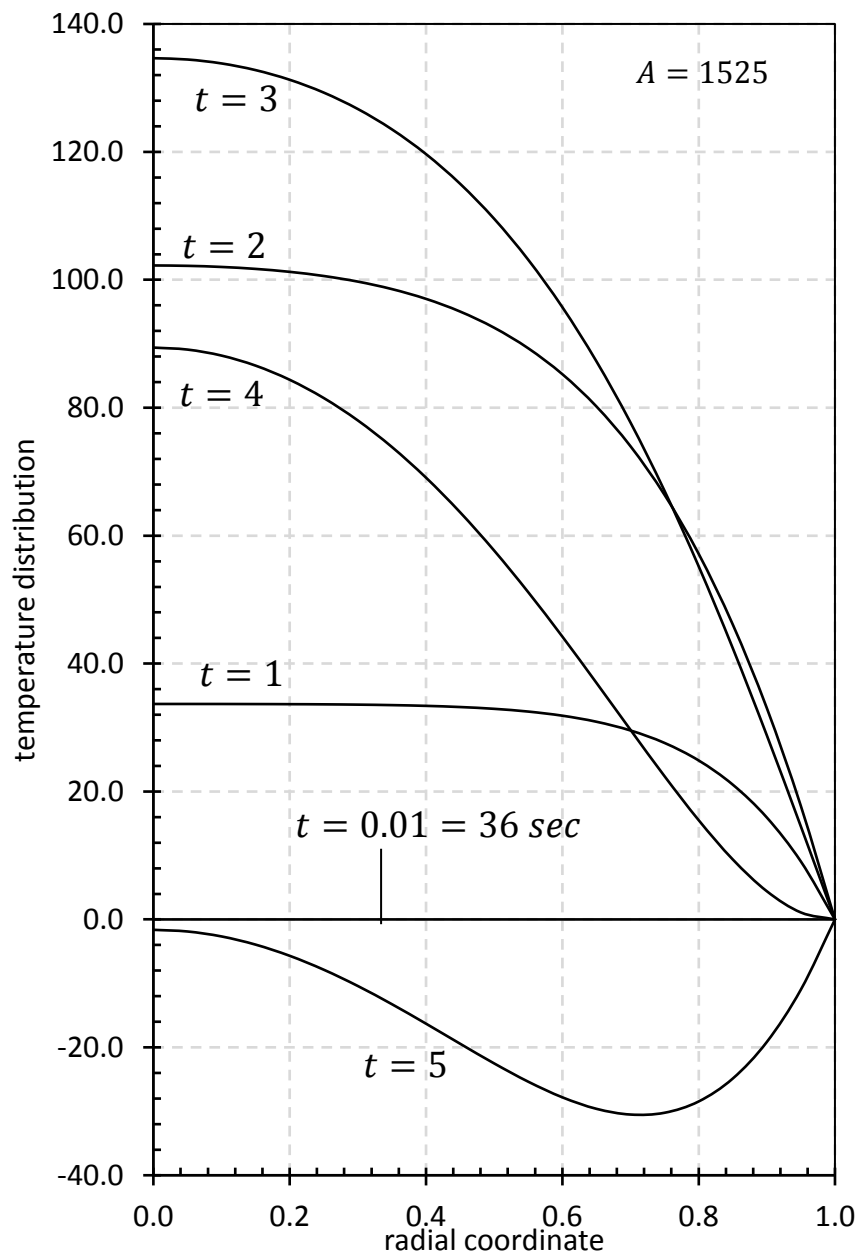


Figure 3.3: The temperature distribution in the steel cylinder at different times for the heat generation rate $ASint$.

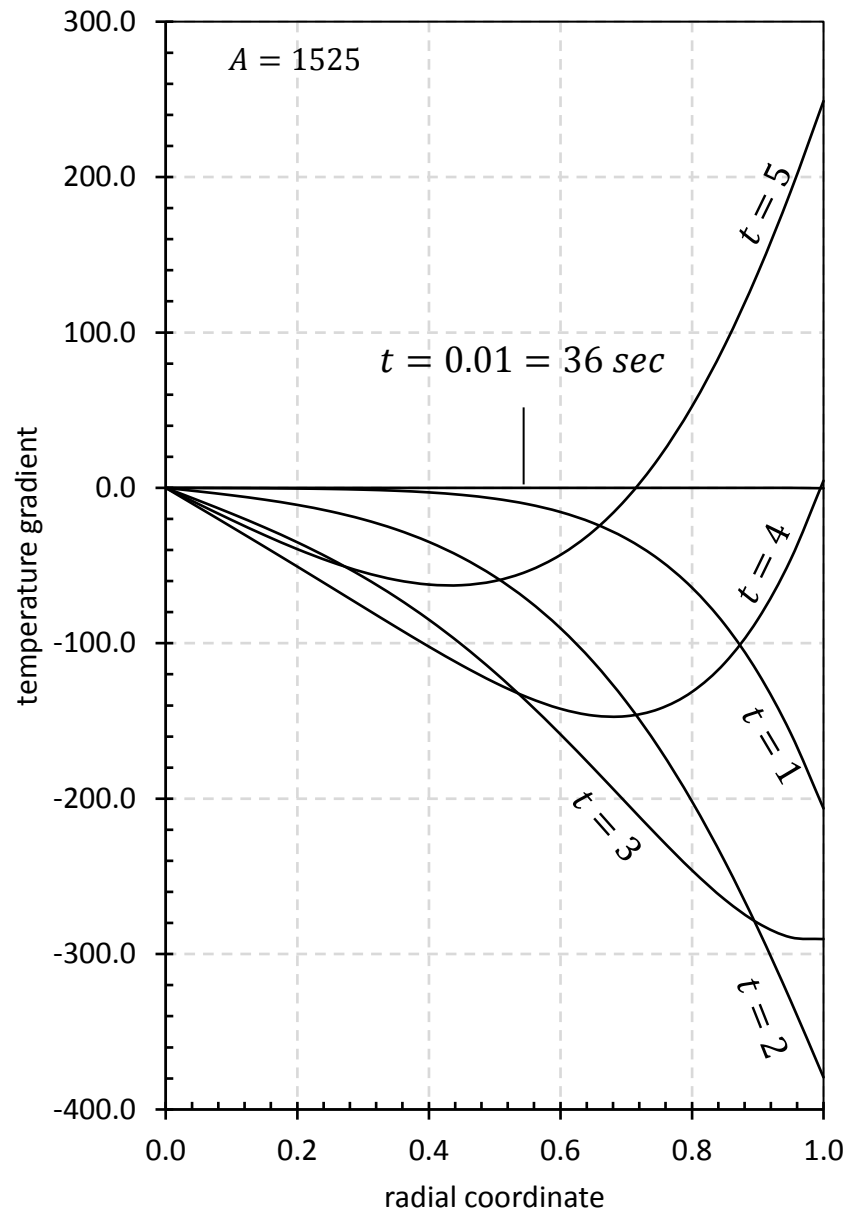


Figure 3.4: The temperature gradient in the steel cylinder at different times for the heat generation rate A_{Sint} .

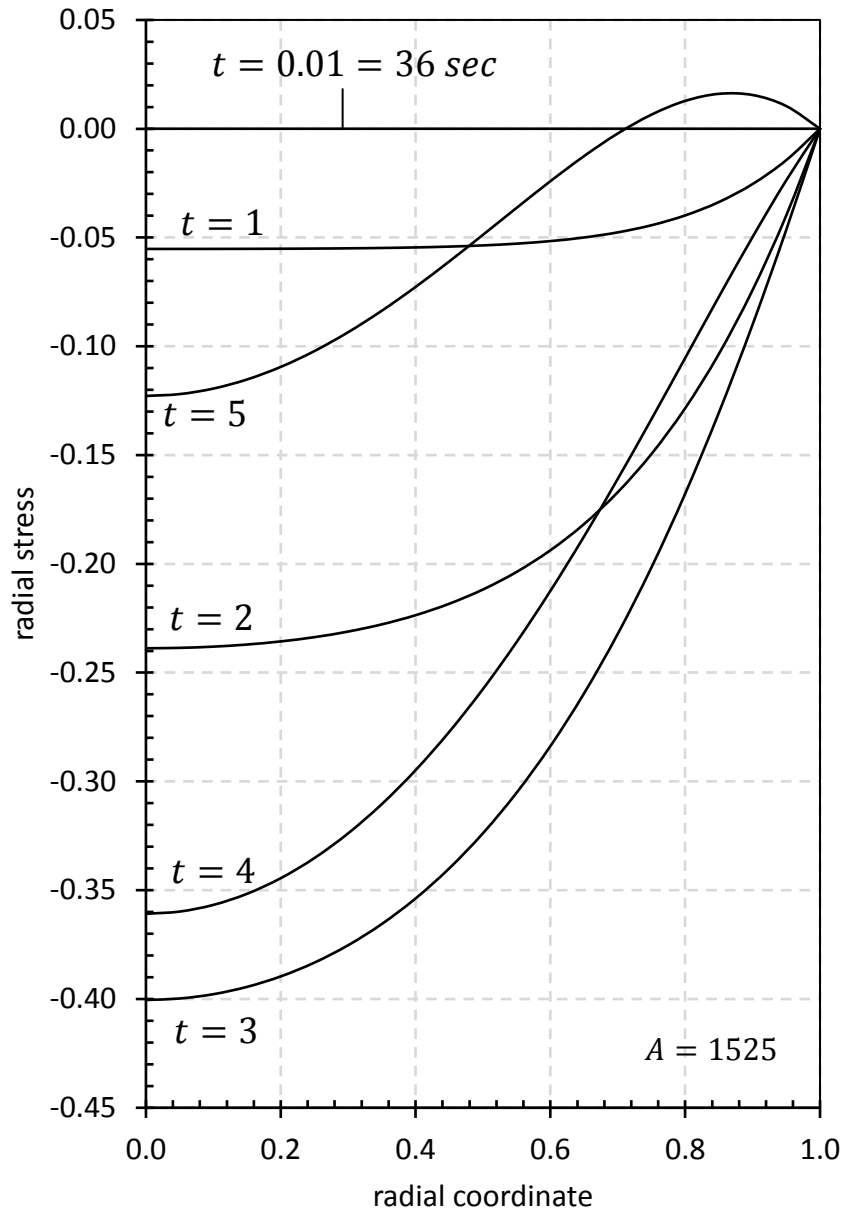


Figure 3.5: The radial stress in the steel cylinder at different times for the heat generation rate $A \sin t$.

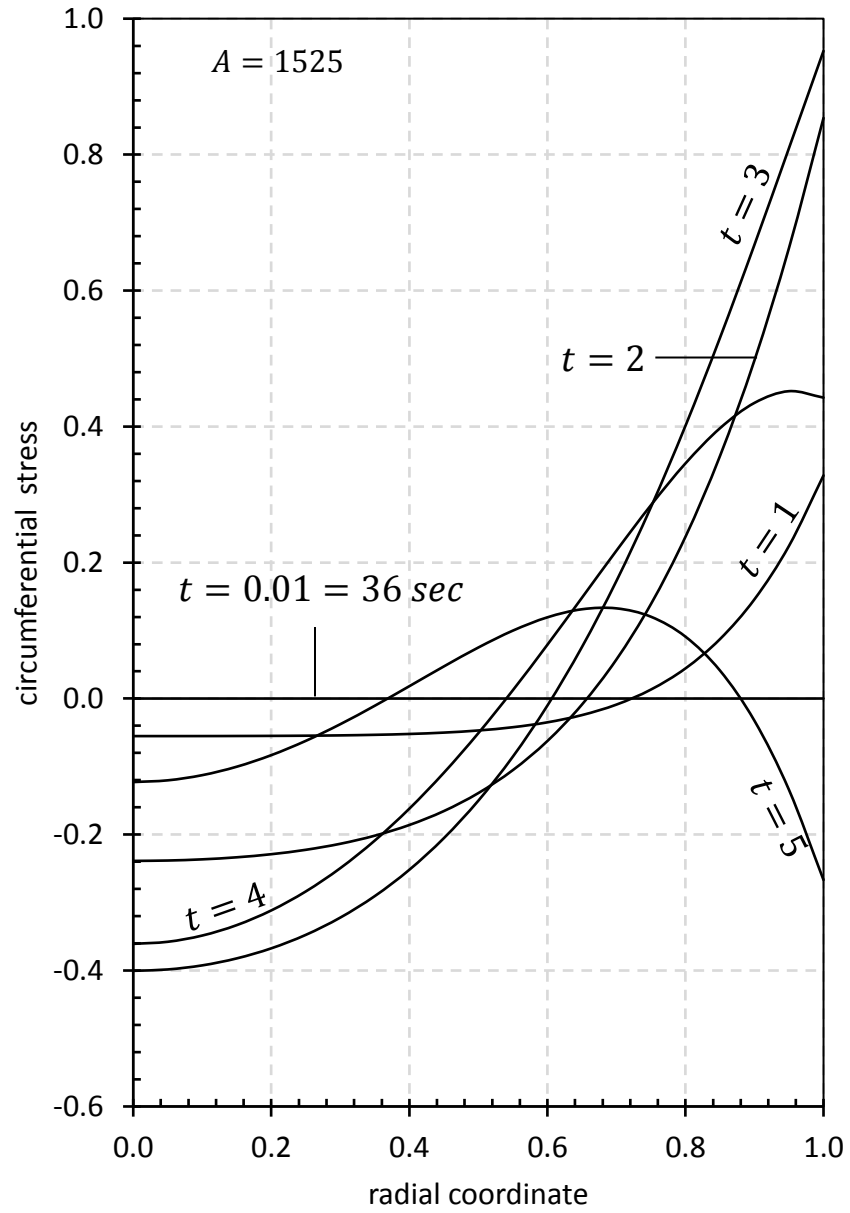


Figure 3.6: The circumferential stress in the steel cylinder at different times for the heat generation rate AS_{int} .

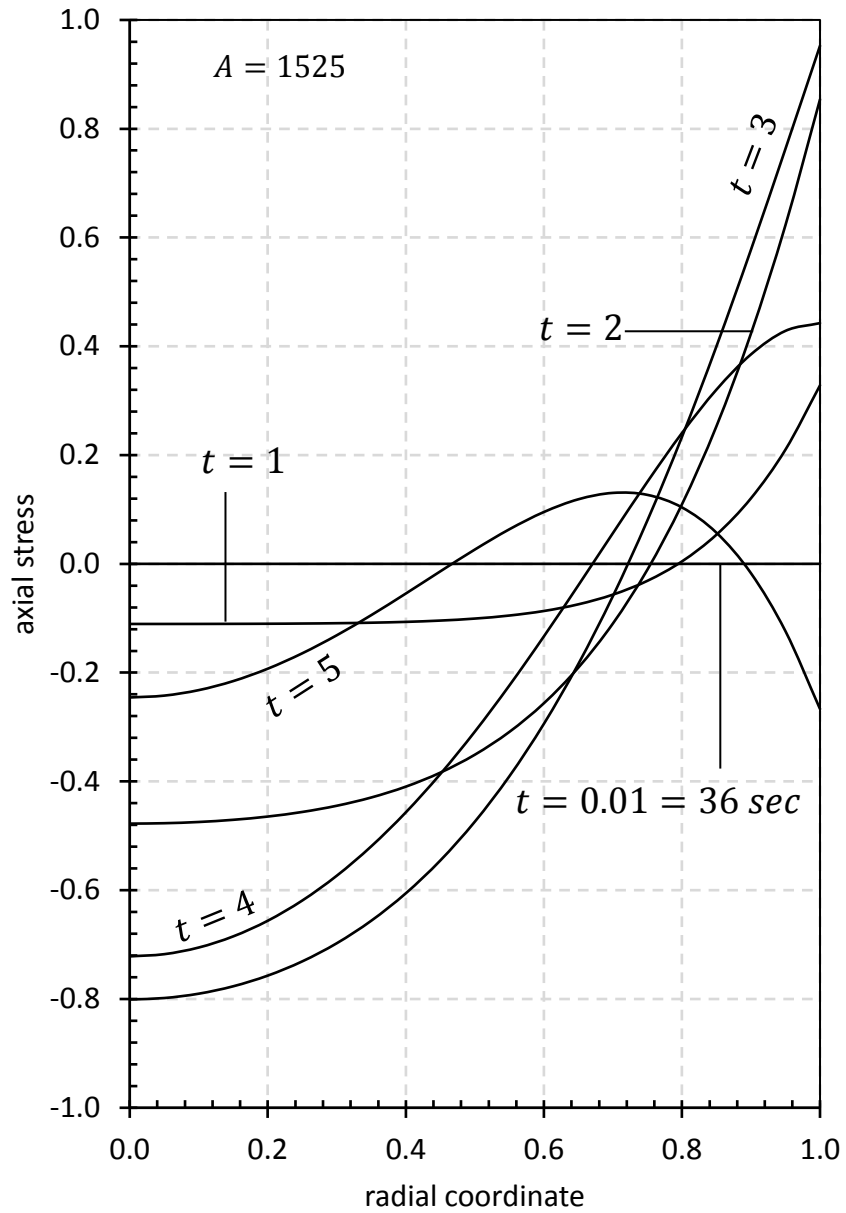


Figure 3.7: The axial stress in the steel cylinder at different times for the heat generation rate $A \sin t$.

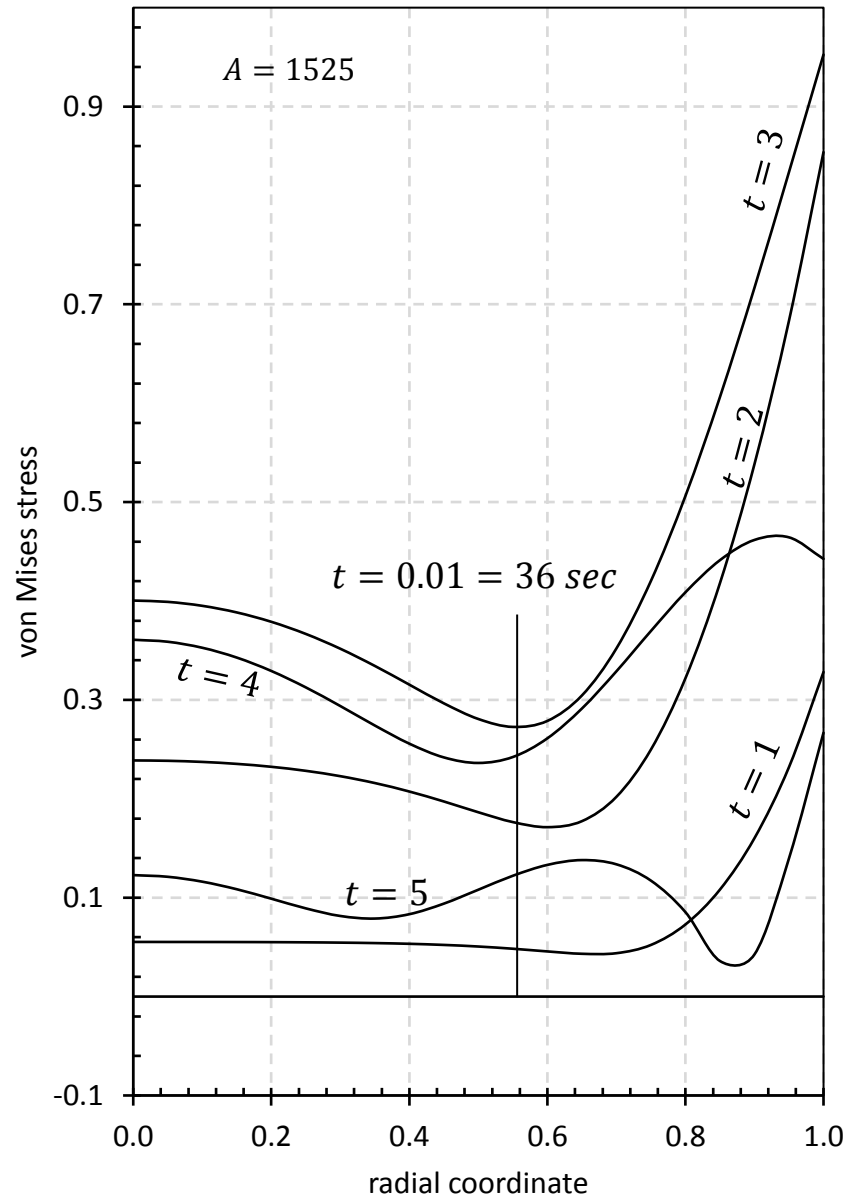


Figure 3.8: The von Mises stress in the steel cylinder at different times for the heat generation rate A_{Sint} .

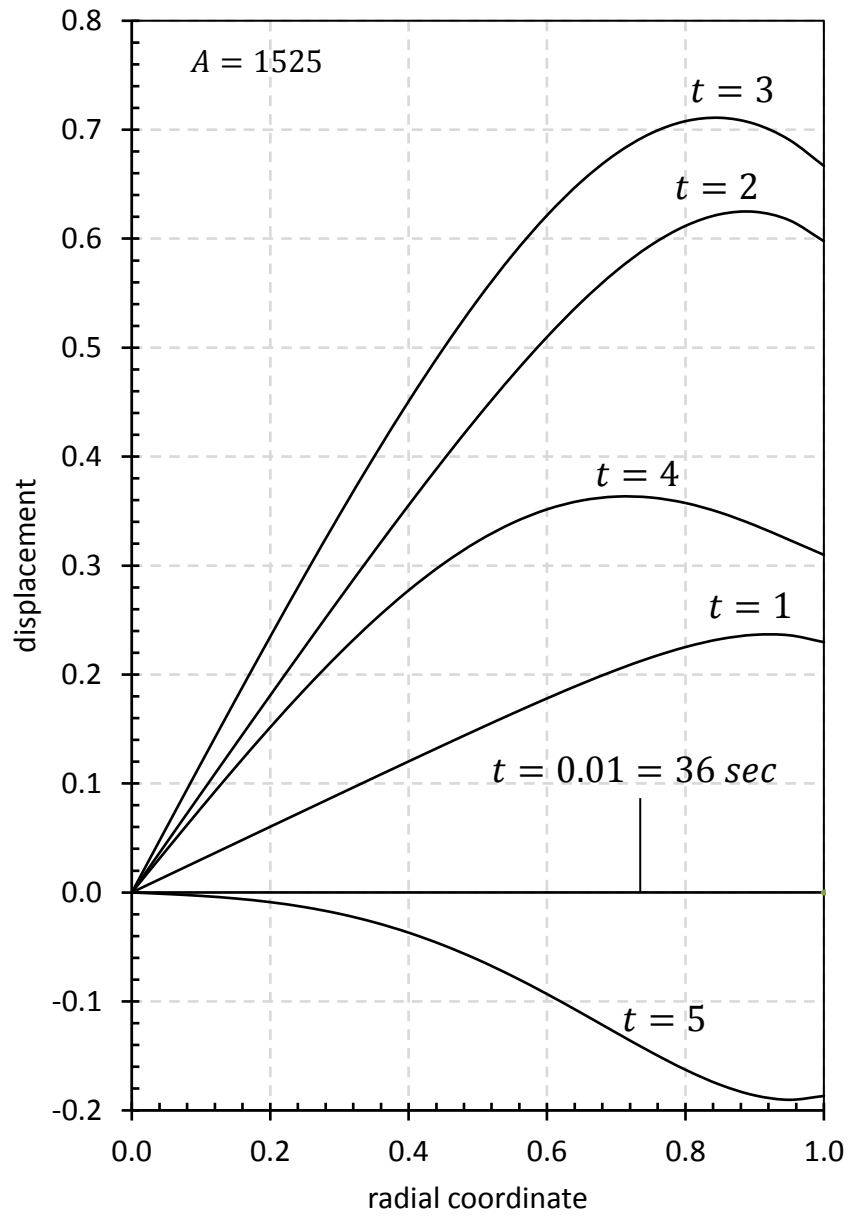


Figure 3.9: The evolution of displacement of the steel cylinder at different times for the heat generation rate $A \text{ Sint}$.

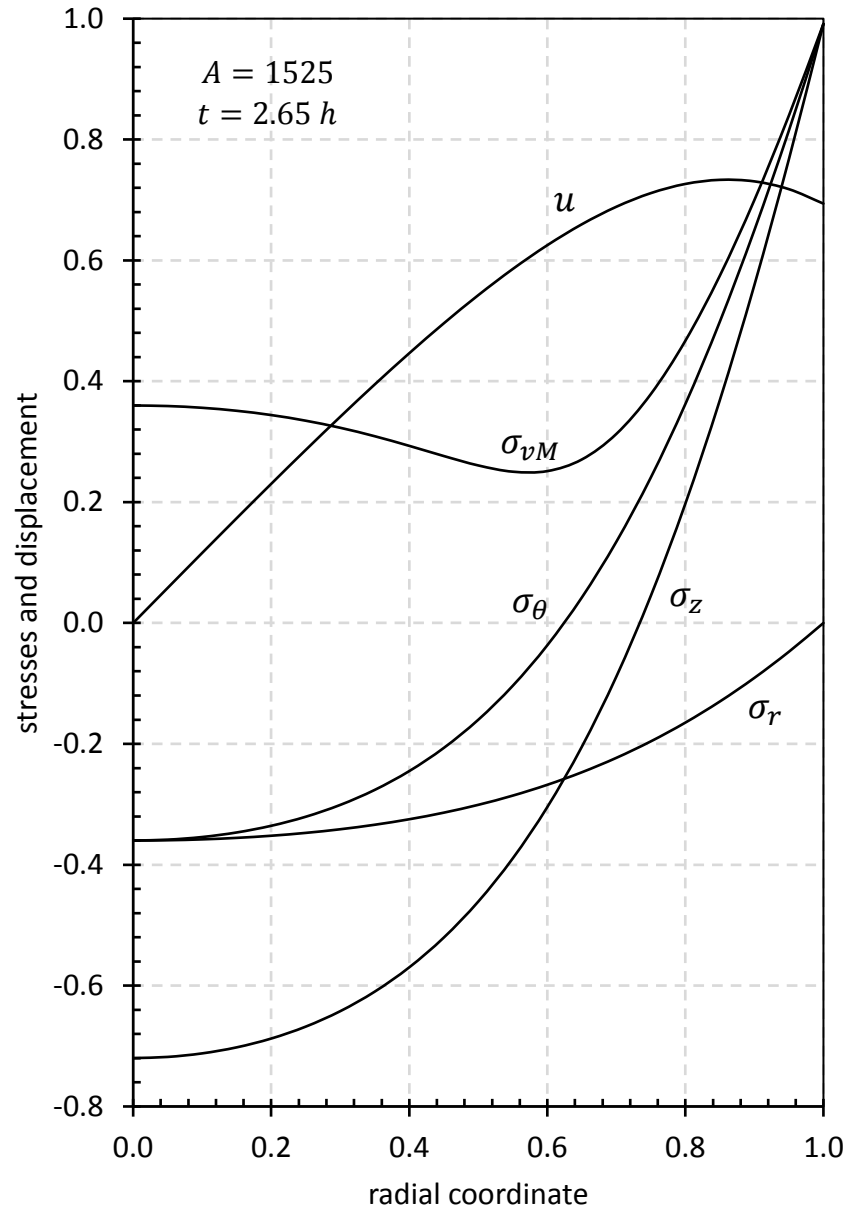


Figure 3.10: The evolution of stresses and displacement of the steel cylinder at $t=2.65$ hour for the heat generation rate A_{Sint} .

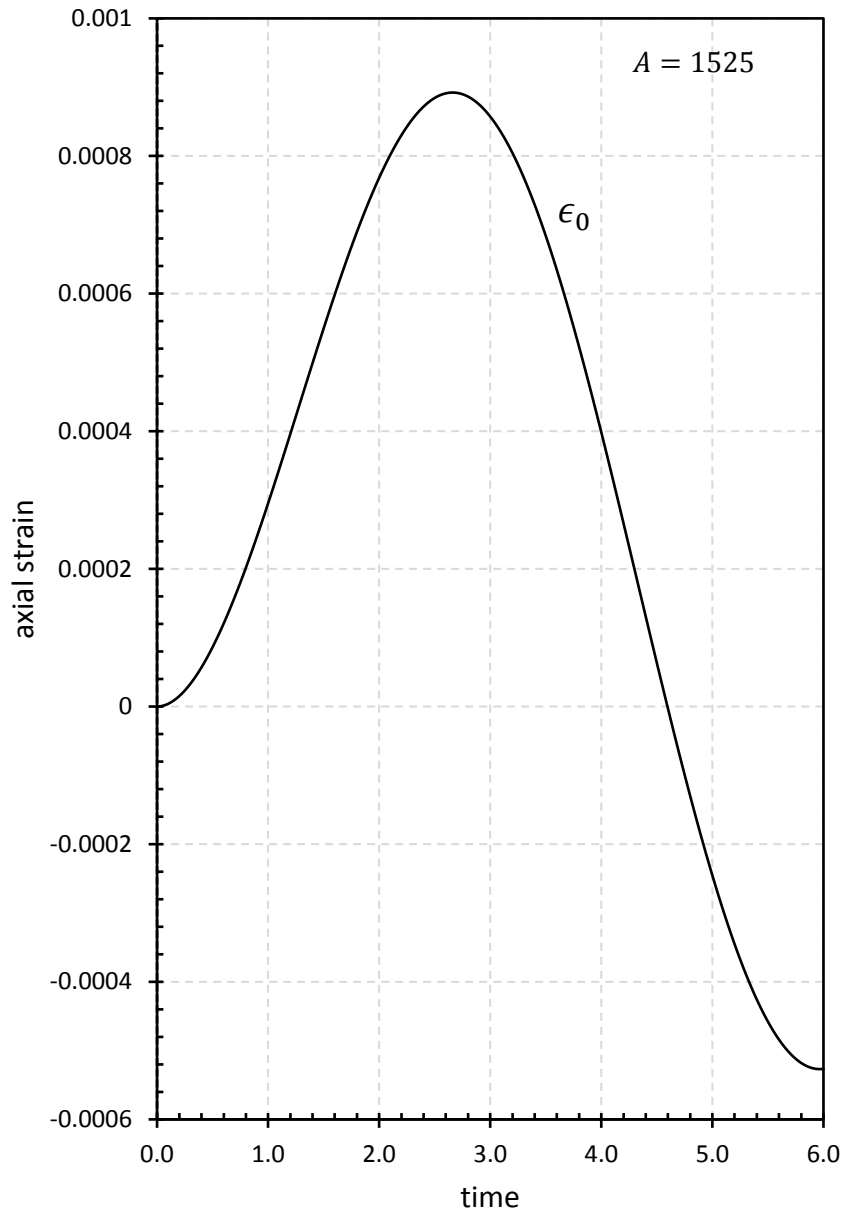


Figure 3.11: The evolution of axial strain of the steel cylinder at different times for the heat generation rate AS_{int} .

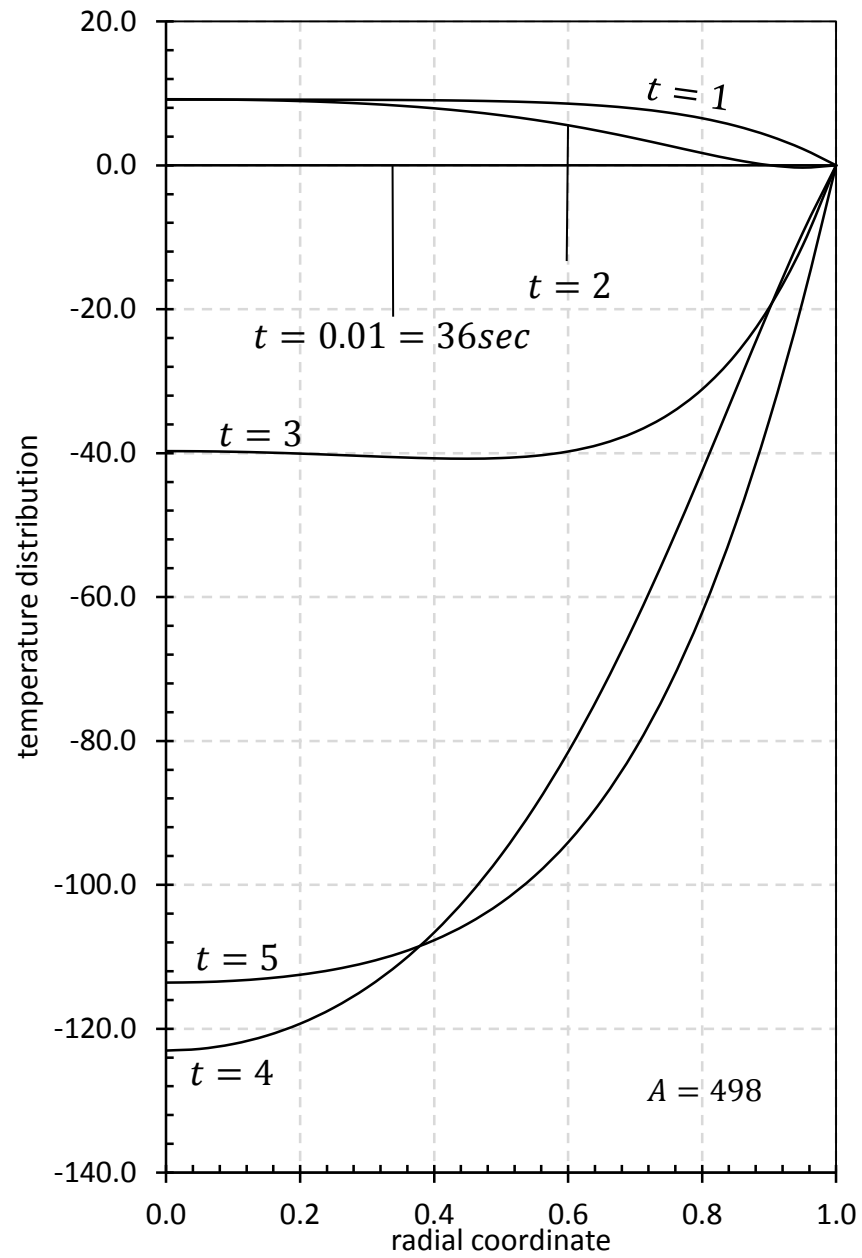


Figure 3.12: The temperature distribution in the steel cylinder at different times for the heat generation rate $A t \text{Cost}$.

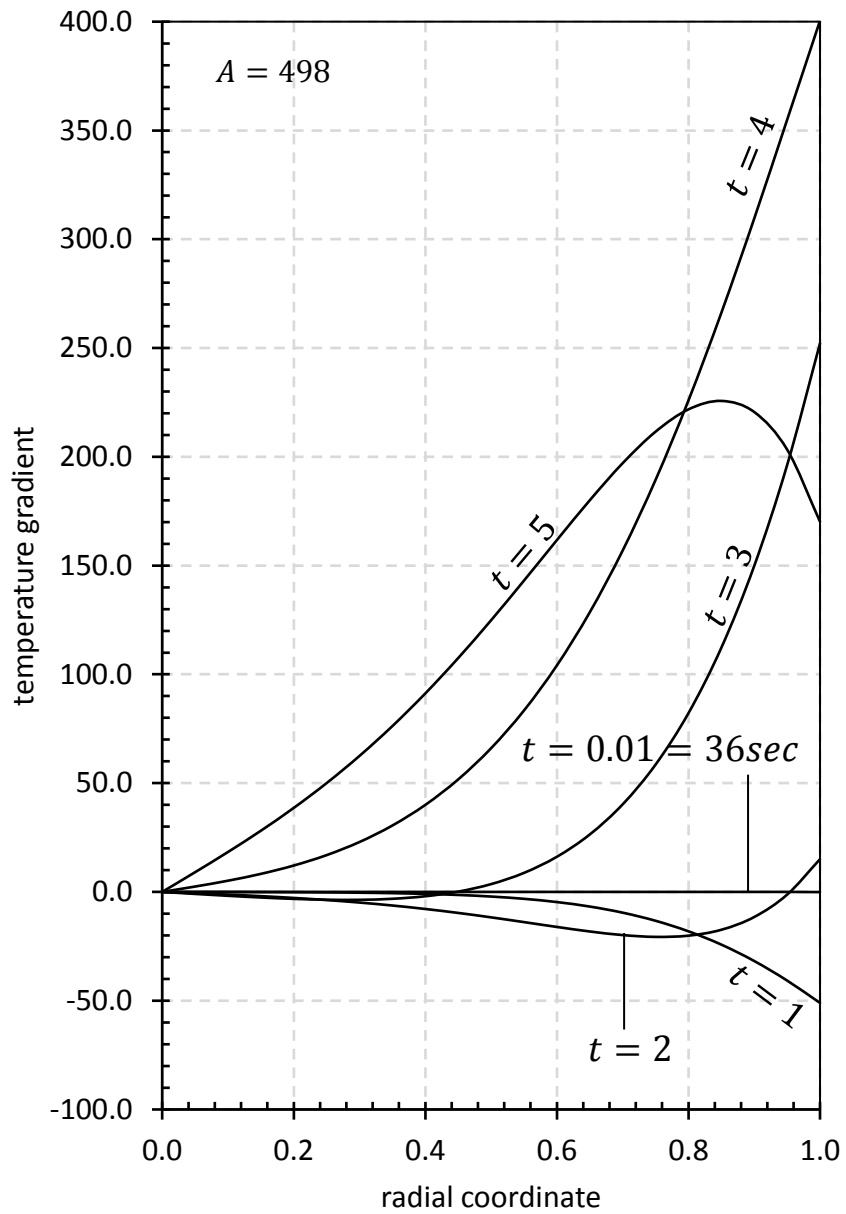


Figure 3.13: The temperature gradient in the steel cylinder at different times for the heat generation rate $A t \text{Cost}$.

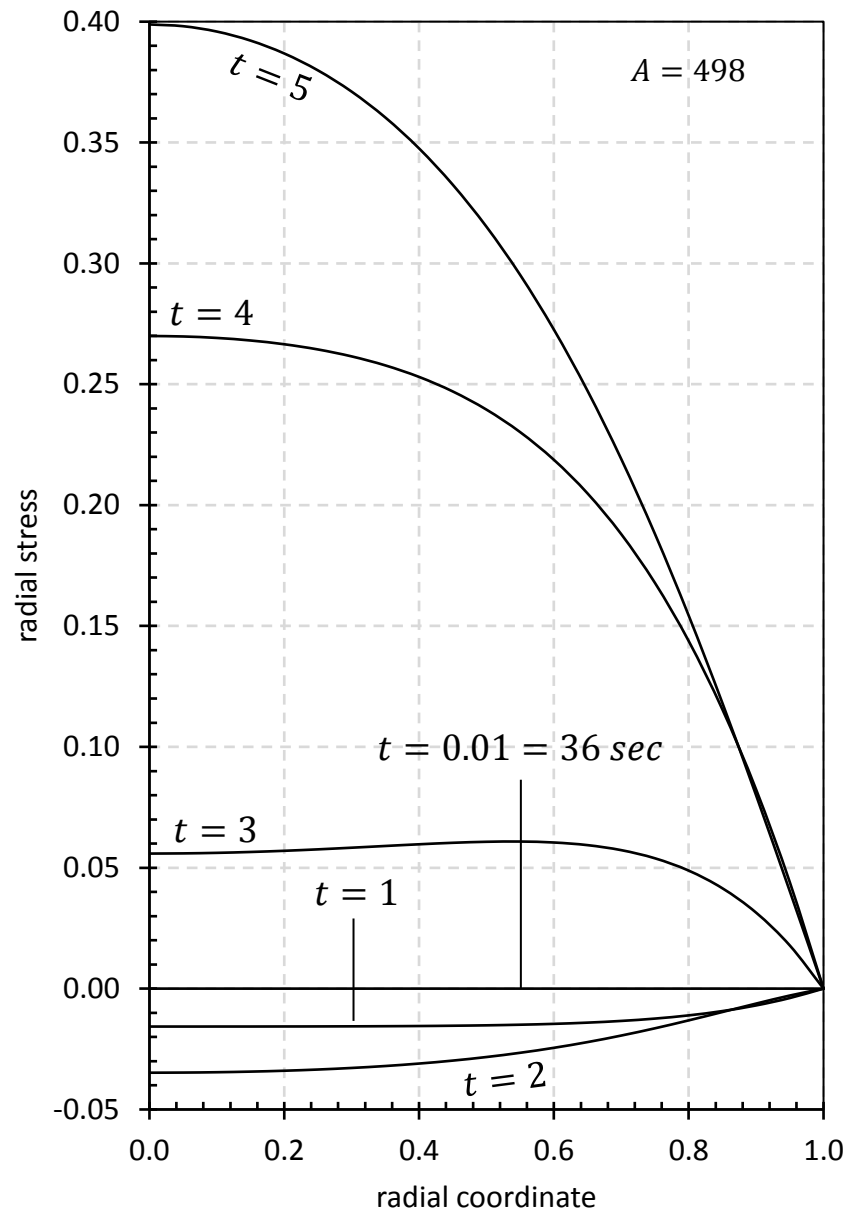


Figure 3.14: The radial stress in the steel cylinder at different times for the heat generation rate $A t \text{Cost}$.

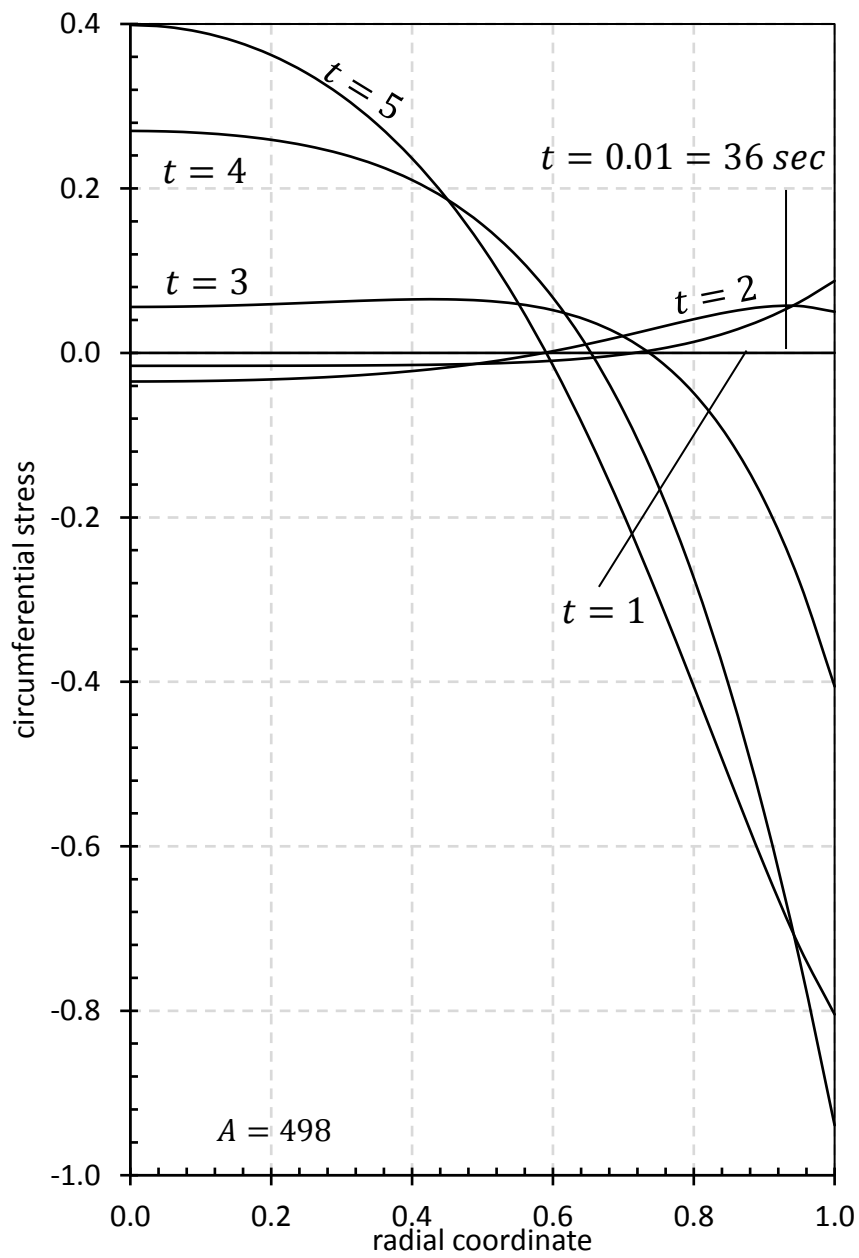


Figure 3.15: The circumferential stress in the steel cylinder at different times for the heat generation rate $A t \cos t$.

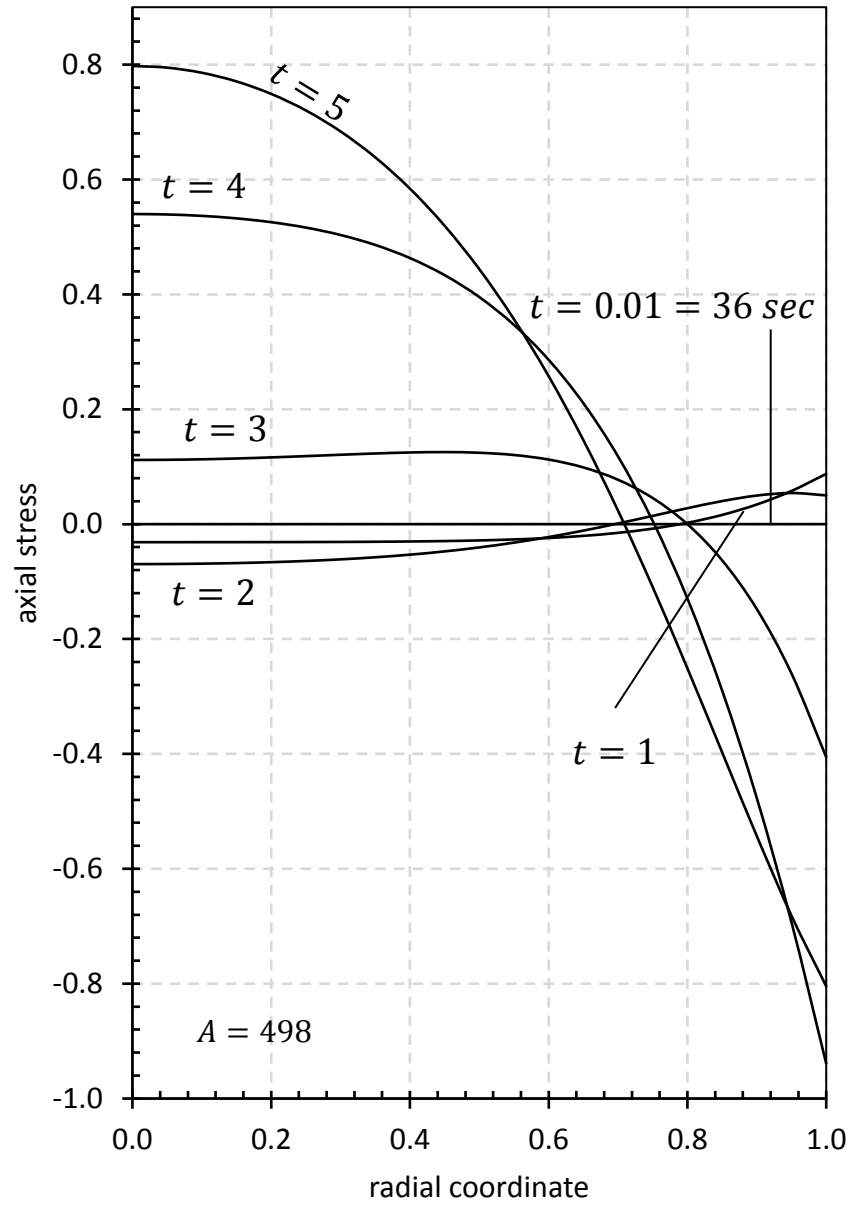


Figure 3.16: The axial stress in the steel cylinder at different times for the heat generation rate $A t \text{Cost}$.

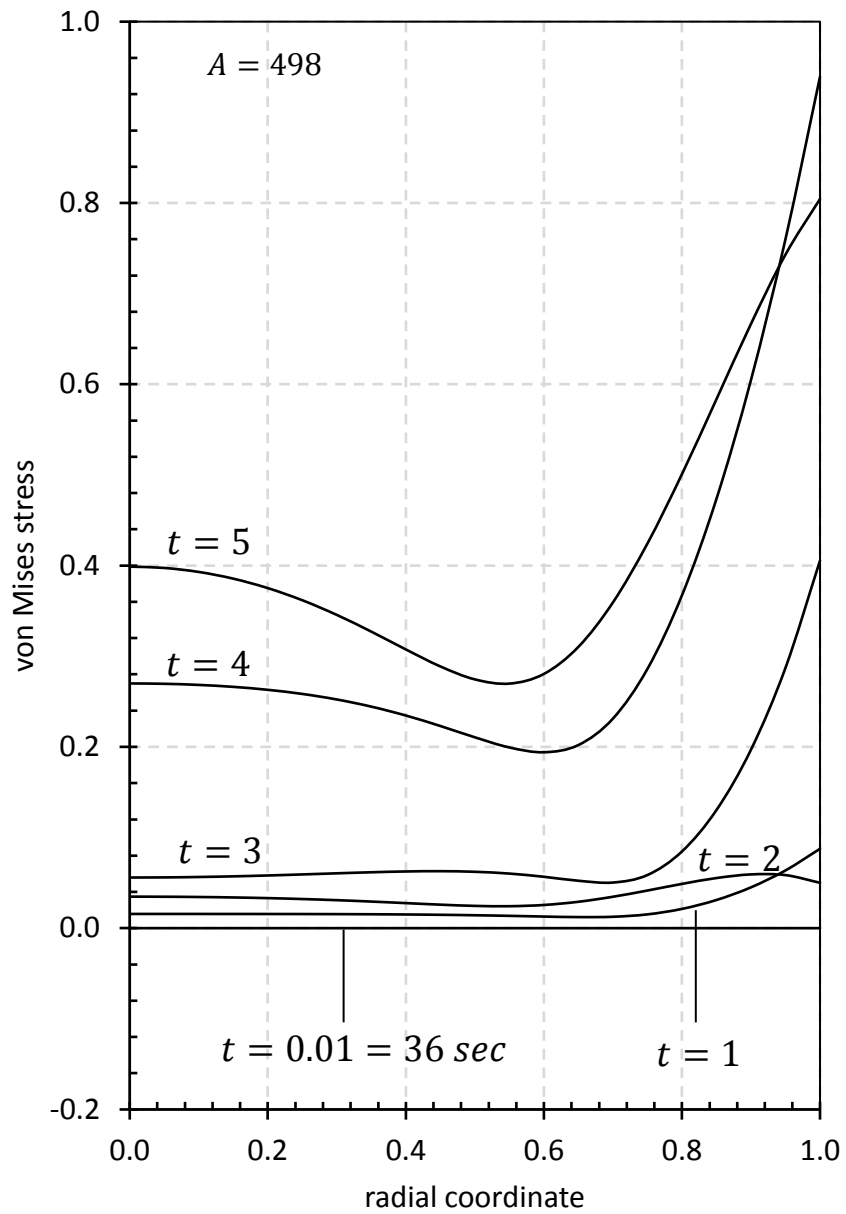


Figure 3.17: The von Mises stress in the steel cylinder at different times for the heat generation rate $A t \cos t$.

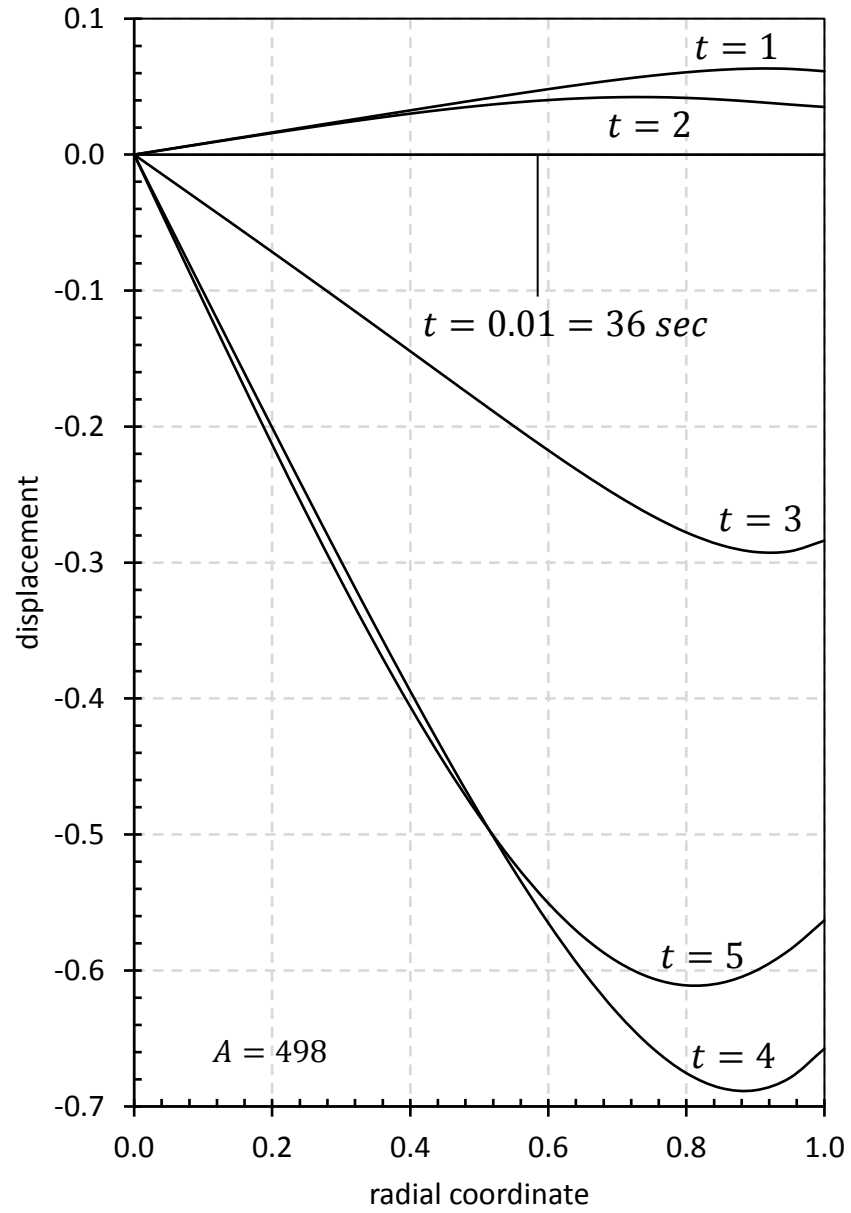


Figure 3.18: The evolution of displacement of the steel cylinder at different times for the heat generation rate $A t \cos t$.

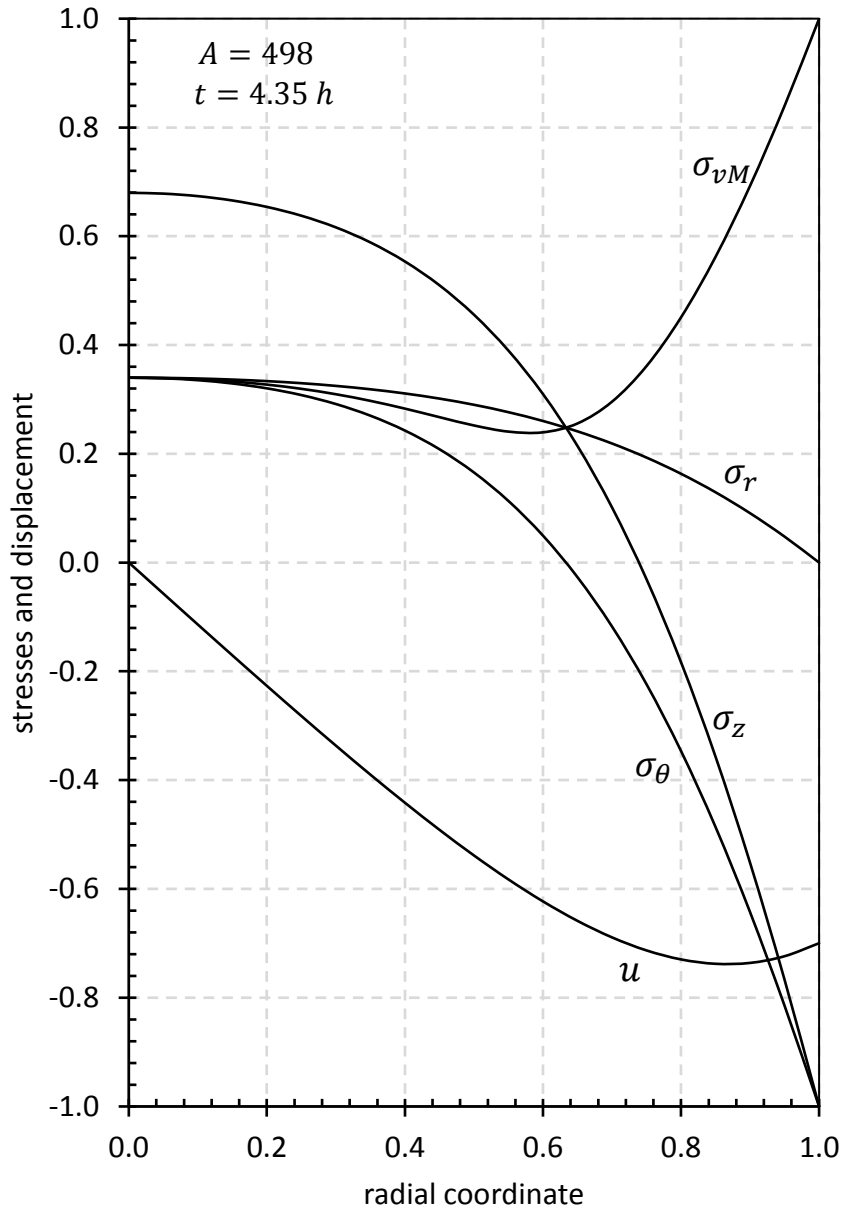


Figure 3.19: The evolution of stresses and displacement of the steel cylinder at $t=4.35$ hour for the heat generation rate $A t C o s t$.

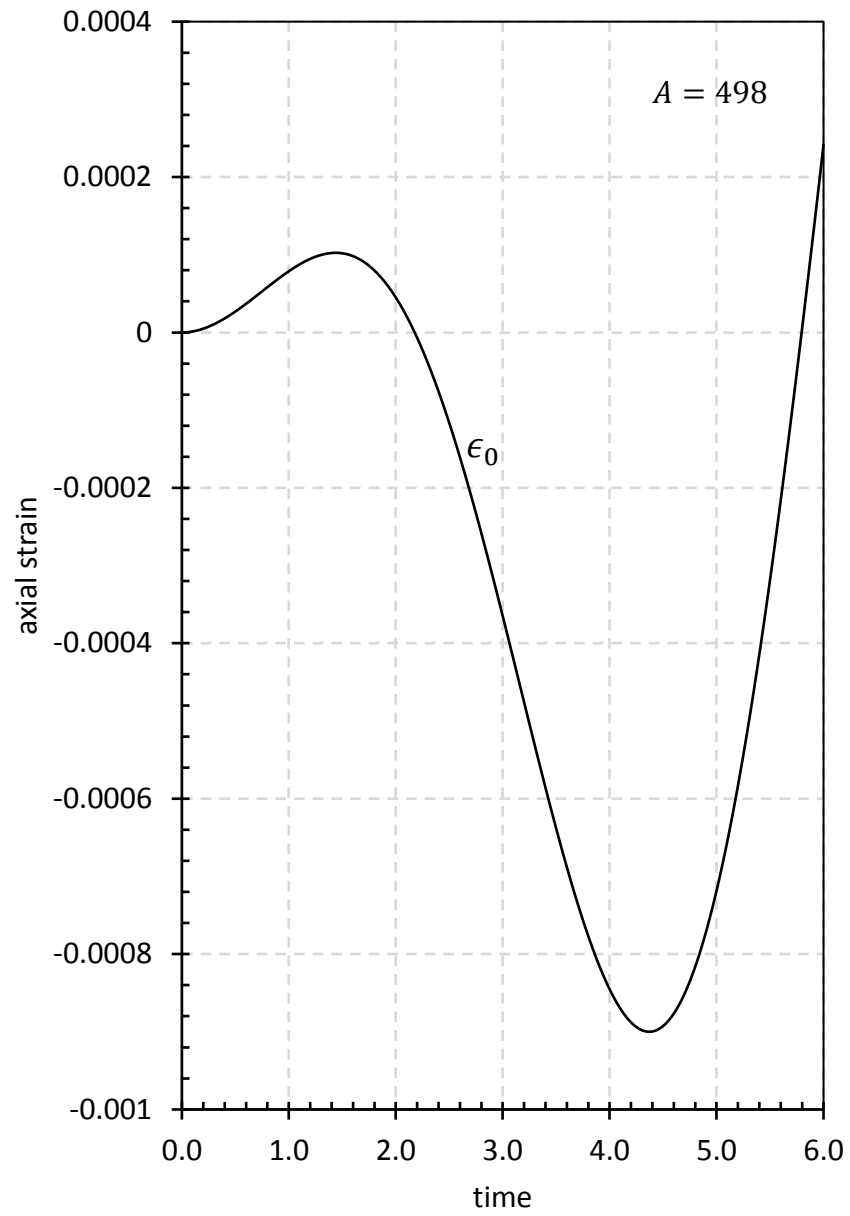


Figure 3.20: The evolution of axial strain of the steel cylinder at different times for the heat generation rate A_{tCost} .

The figures in the third and fourth parts are done for brass. α_T is calculated as $0.13171133 \text{ m}^2/\text{hour}$ because of the material properties of the brass. Figures between (3.21) and (3.24) are figures for the *Asint* condition of the brass material. In this part, A value is calculated as 595, and the solutions are done accordingly. Figures between (3.25) ve (3.28) are for the *Atcost* condition of the brass material. A value for this condition is calculated as 185. We can see the changes in stresses and displacement throughout the radial coordinate for the brass material in Fig.(3.21) and Fig.(3.25). For Fig.(3.21) this graph is plotted at $t = 2.35h$, whereas for Fig.(3.25) it is plotted at $t = 4.11h$. As can be understood from these two graphs, at $r = 0$ displacement is 0, and at $t = 1$ radial stress is 0. Because Fig. (3.21) is plotted for the *Asint* condition, axial and circumferential stresses move from negative values to positive at the $0 - 5$ time interval. At $r = 1$, in other words at the surface, they reach their maximum value. In Fig. (3.25), plotted according to the *Atcost* condition, axial and circumferential stresses are at the start, $r = 0$ position, at their maximum values and as they move away from the center, they take negative values and compress. The highest compression is seen at $r = 1$.

The change in axial strain with time is seen in Fig.(3.22) and Fig.(3.26). In Fig.(3.22), at approximately $t = 2.3$ the axial strain reaches its maximum value and, because this graph is drawn according to the *Asint* case, *sin* function is seen. On the other hand, in Fig (3.26), at $t = 4$ the axial strain compresses taking its maximum negative value, and since the *Atcost* condition is used, the graph moves as *cos* function.

Figures (3.23) and (3.27) are temperature distribution graphs throughout the radial coordinate. In these two graphs at $r = 1$ temperature distribution is 0. In Fig. (3.23), the temperature distribution at $r = 0$ reaches its maximum value at $t = 2$. In Fig. (3.27), at $r = 0$ and $t = 4$, the time causing maximum stress in the negative direction causes the temperature distribution in the center of the cylinder to cool down to -90 degree. Lastly, if we look at the temperature gradient graphs, Fig (3.24) is a temperature gradient graph for the *Asint* condition, whereas Fig. (3.28) is the one for the *Atcost* condition. In this work, as all temperature gradient graphs, these graphs are 0 degrees at the center of the cylinder and reach their maximum values at the surface. The solid cylinder in Fig. (3.24) reaches its maximum value at $r = 1$ and $t = 5$, but at $r = 1$ and $t = 2$ it takes a value of -220 reaching its maximum value at this position.

In Fig. (3.28), at $r = 1$ and $t = 4$, it reaches its maximum temperature gradient value.

Figures (3.29) and (3.30) are the verification graphs between steel and brass materials under the heat generation rate $Asint$. In this figures solid lines represent the structural steel and dash lines denotes the yellow brass.

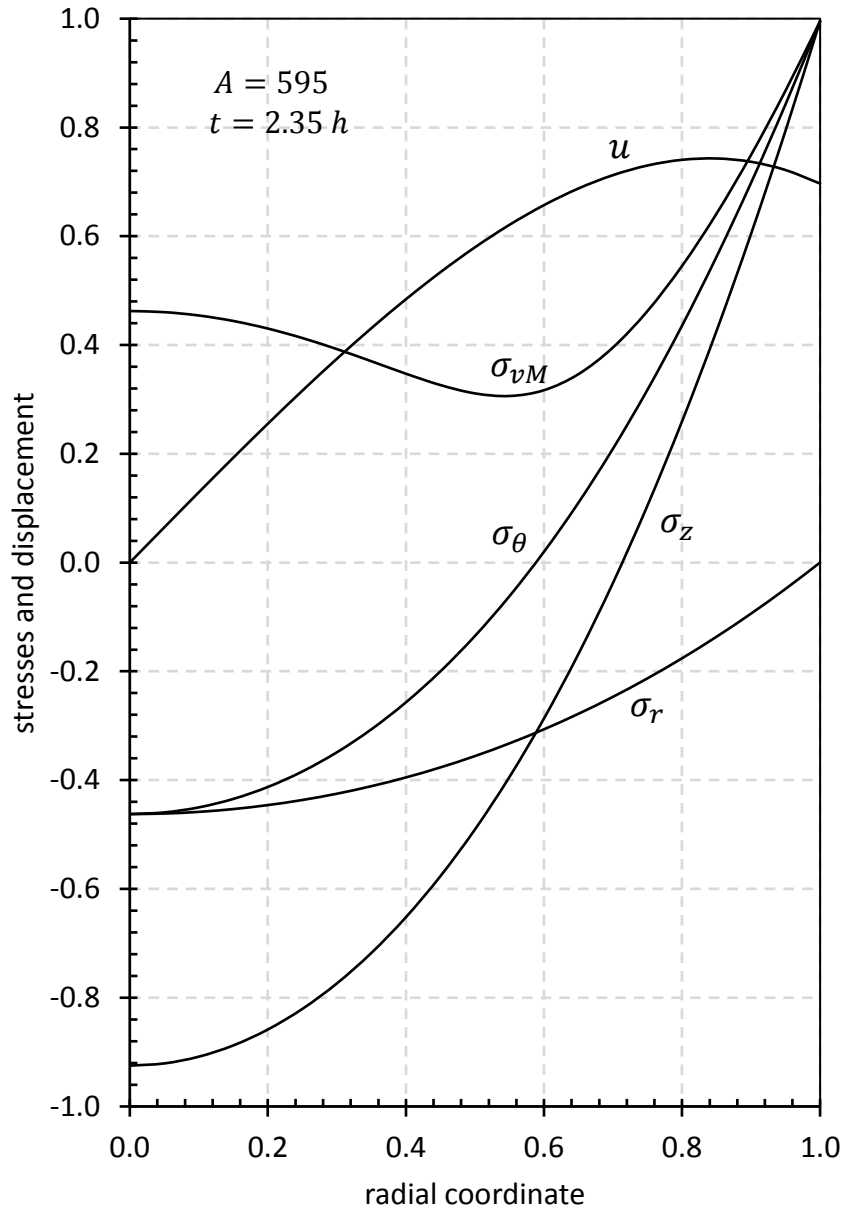


Figure 3.21: The evolution of stresses and displacement of the brass cylinder at $t=2.35$ hour for the heat generation rate AS_{int} .

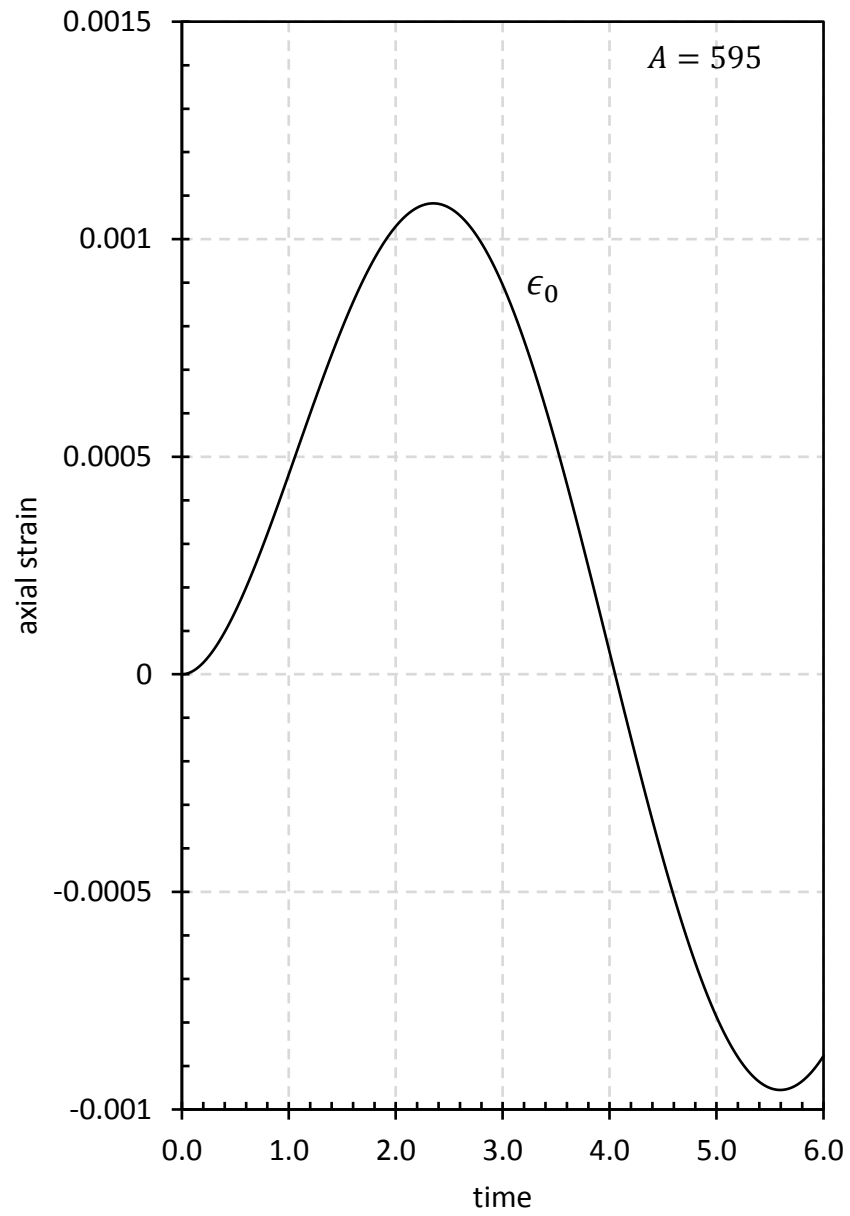


Figure 3.22: The evolution of axial strain of the brass cylinder at different times for the heat generation rate AS_{int} .

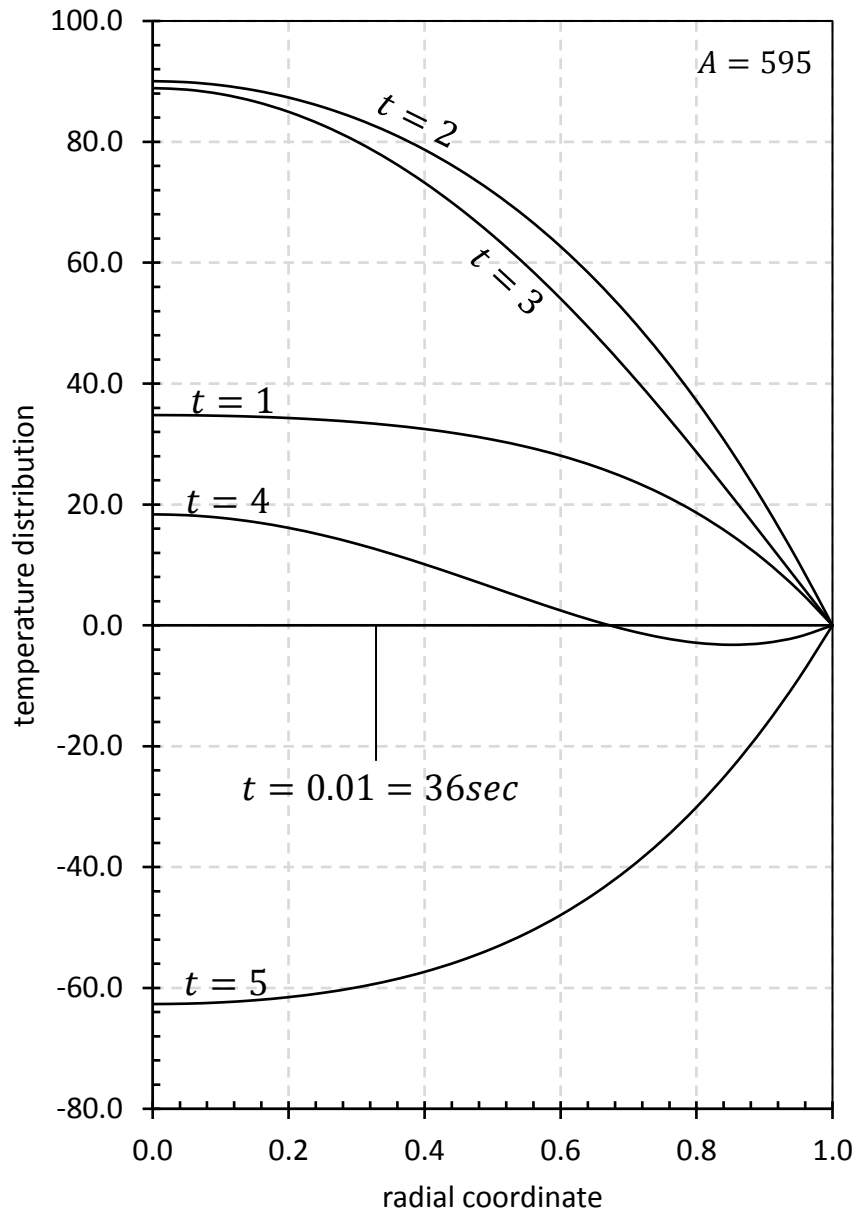


Figure 3.23: The temperature distribution in the brass cylinder at different times for the heat generation rate $A \sin t$.

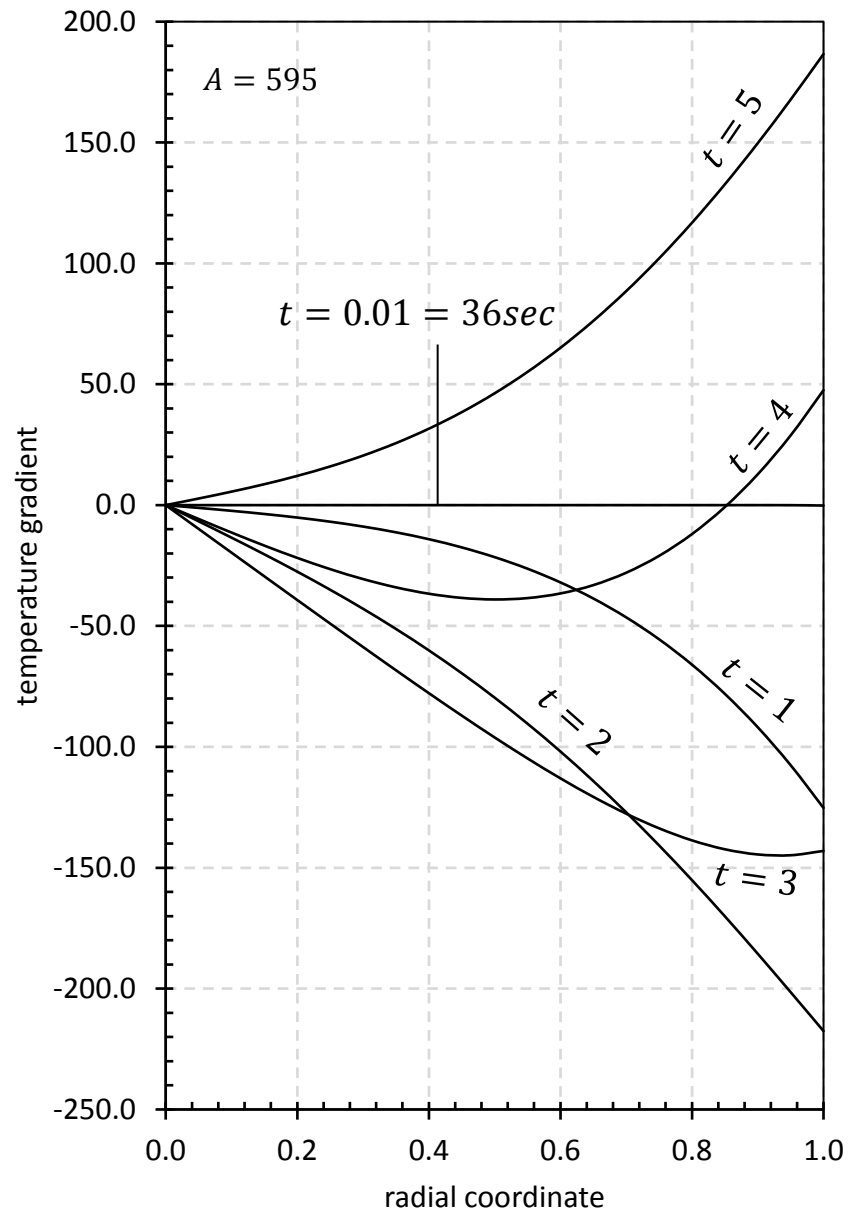


Figure 3.24: The temperature gradient in the brass cylinder at different times for the heat generation rate AS_{int} .

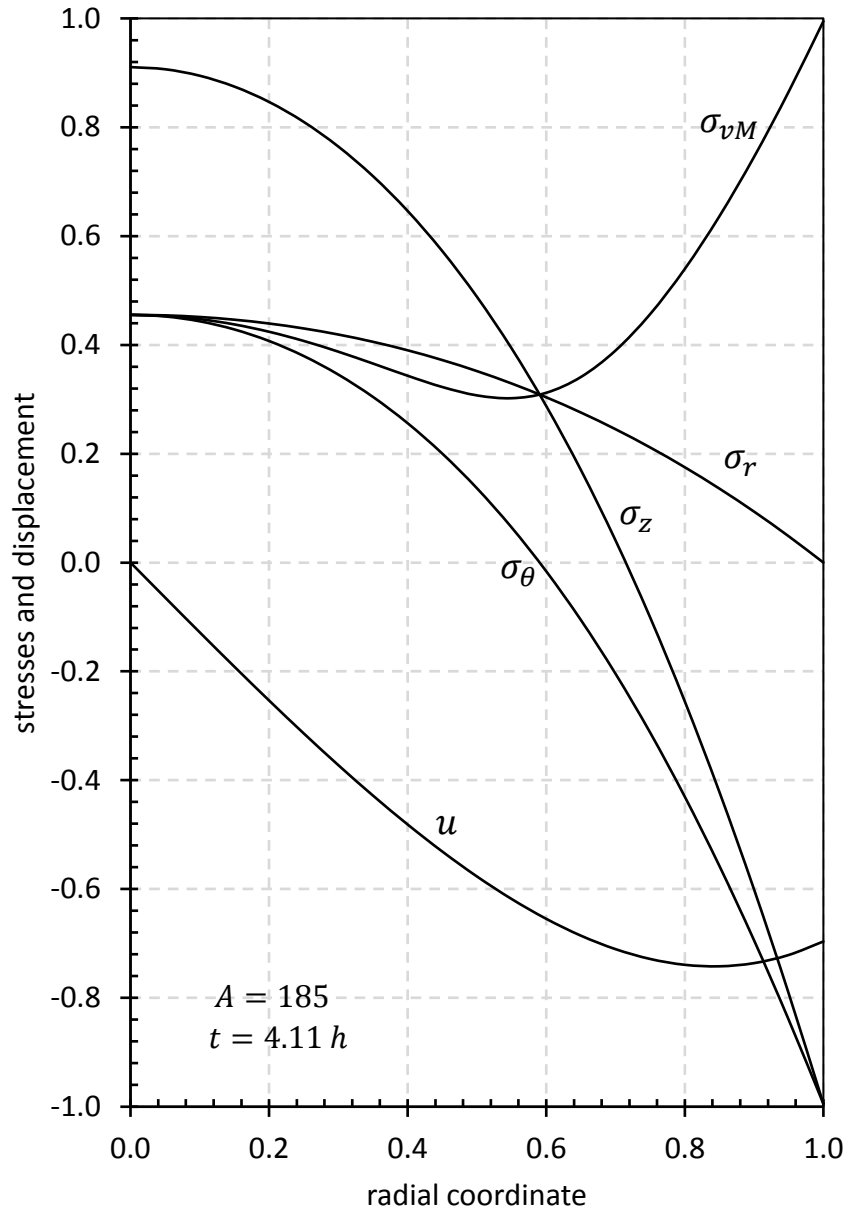


Figure 3.25: The evolution of stresses and displacement of the brass cylinder at $t=4.11$ hour for the heat generation rate $A t C o s t$.

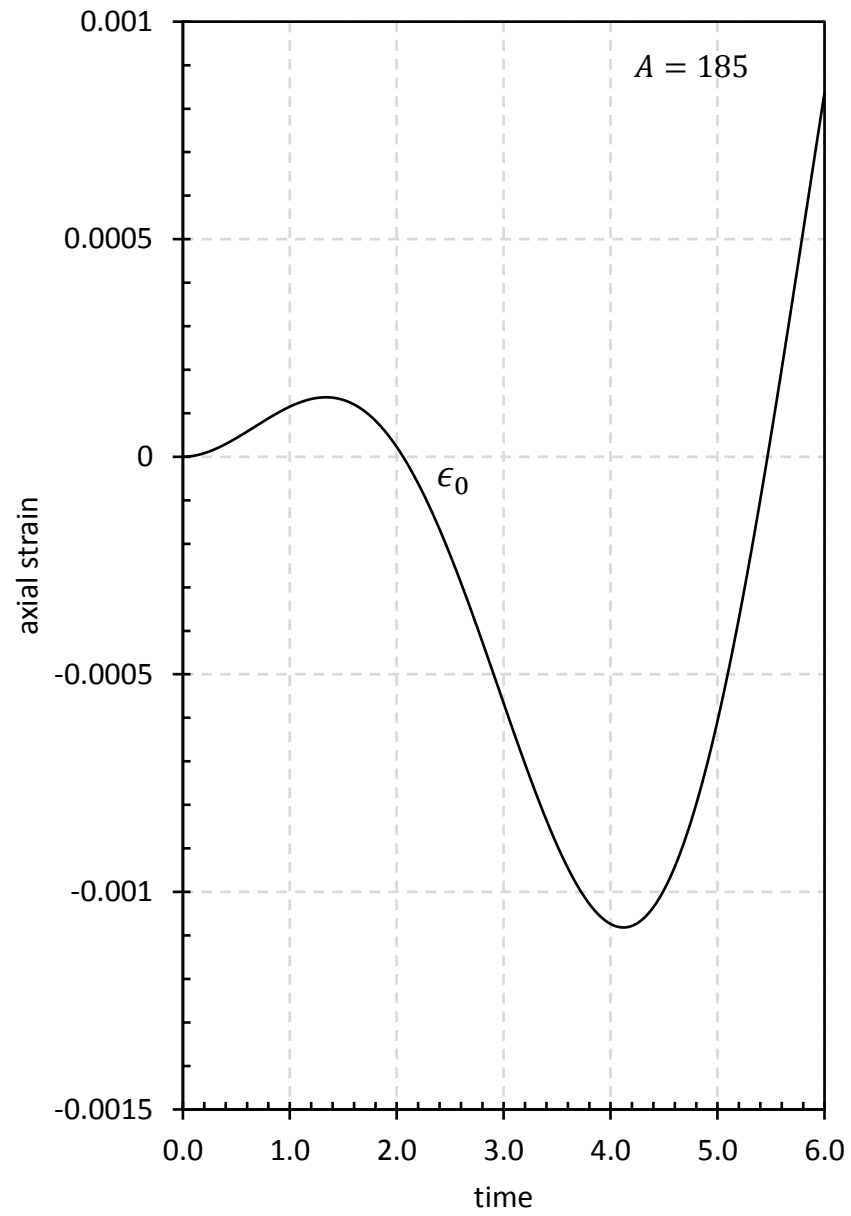


Figure 3.26: The evolution of axial strain of the brass cylinder at different times for the heat generation rate $AtCost$.

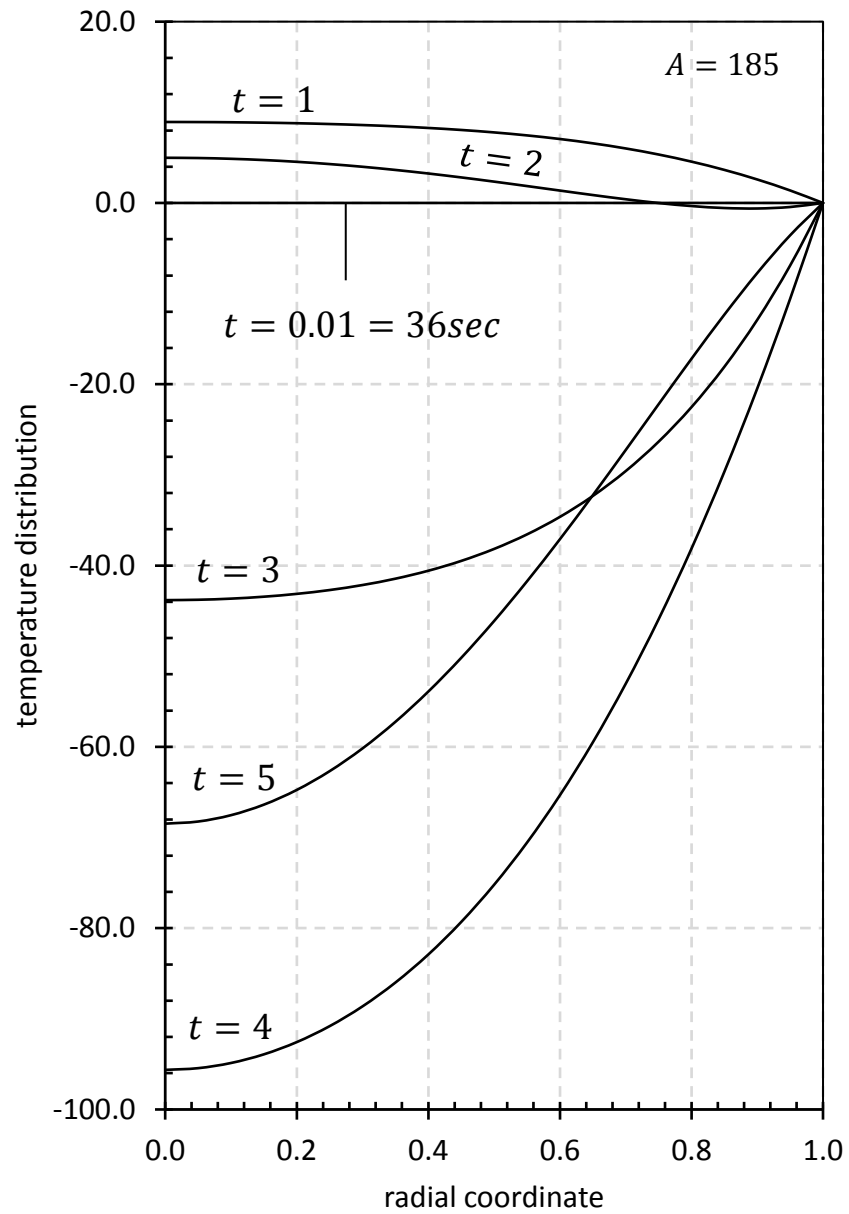


Figure 3.27: The temperature distribution in the brass cylinder at different times for the heat generation rate A at cost.

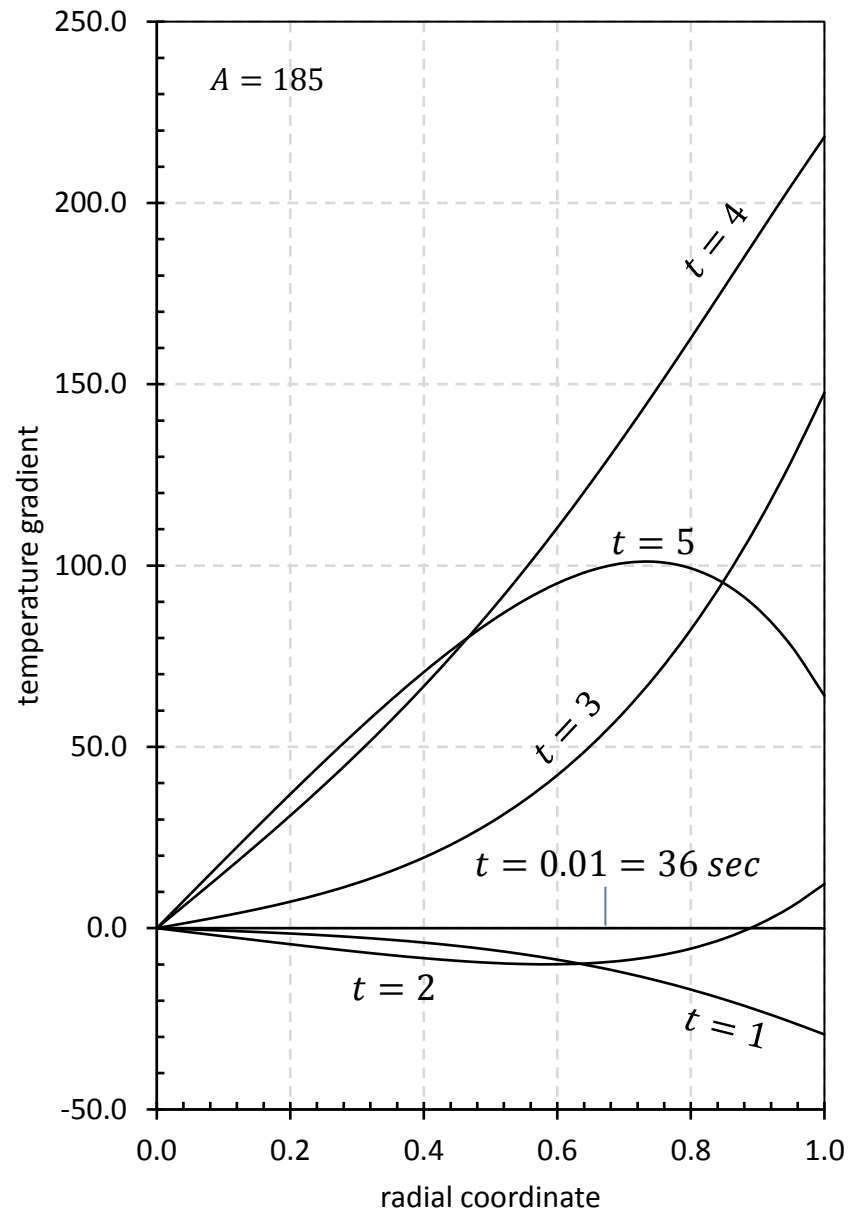


Figure 3.28: The temperature gradient in the brass cylinder at different times for the heat generation rate $A t \cos t$.

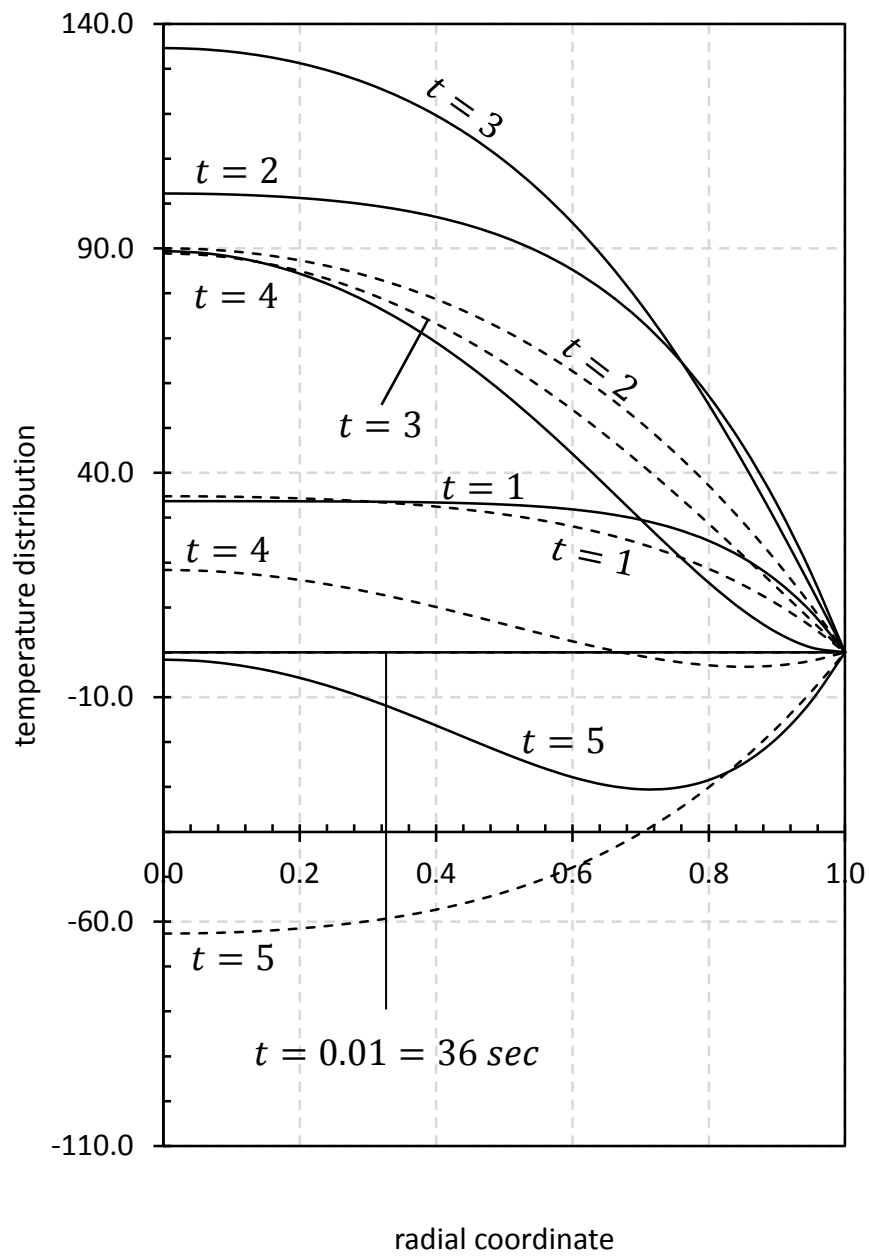


Figure 3.29: The verification of the temperature distribution between the materials steel and brass at different times for the heat generation rate AS_{int} .

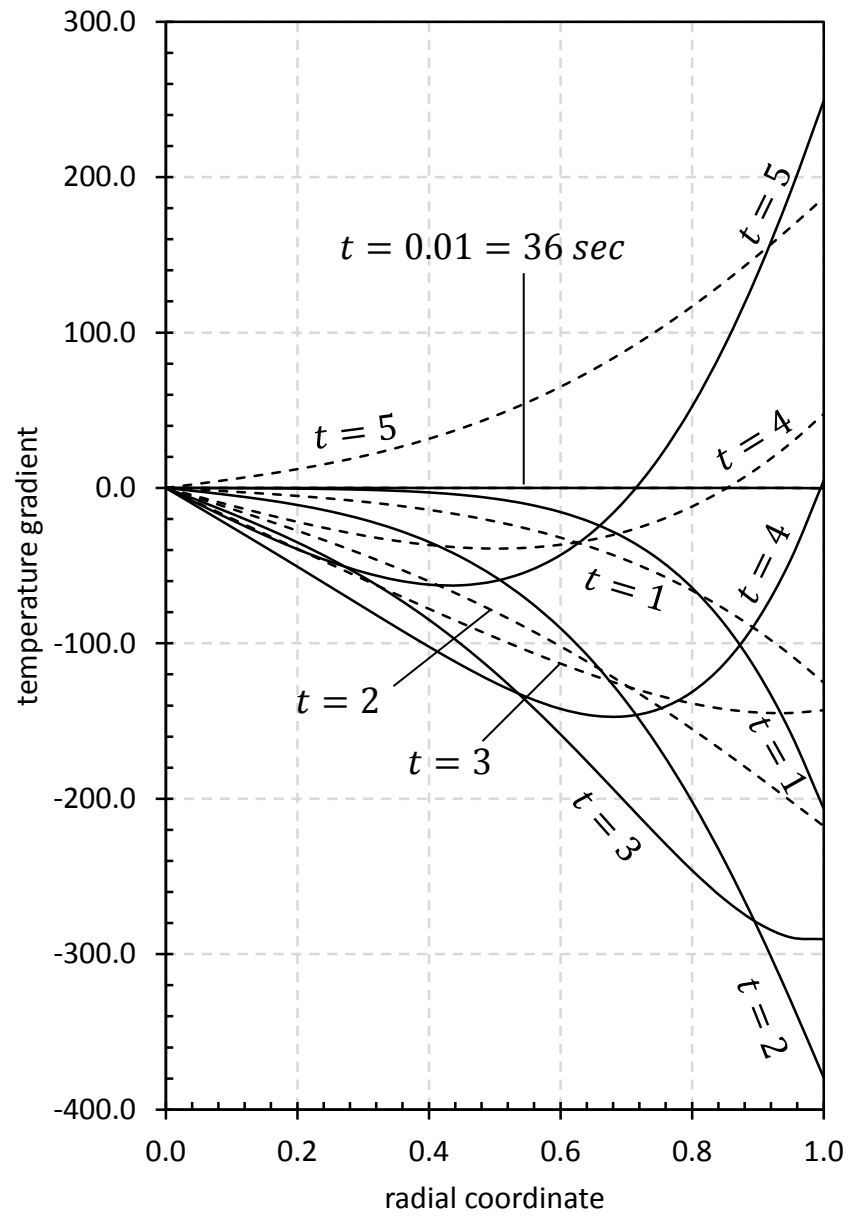


Figure 3.30: The verification of the temperature gradient between the materials steel and brass at different times for the heat generation rate AS_{int} .

CHAPTER 4

CONCLUSION

In this study, thermoelastic stress behavior of a periodic heat generating solid cylinder is investigated. The cylinder is regarded to have general plane strain condition. Two different time dependent periodic heat generation rates are used : ASint and AtCost. The temperature distribution in the solid cylinder is obtained by using Duhamel's theorem. Two periodic heat generating functions that are used in this study are applied to structural steel and yellow brass; and their time-dependent temperature distribution and thermoelastic solutions are obtained. These solutions are conducted in a dimensional manner and their comparisons with non-dimensional conjugates are given in Chapter 2 to prove their accuracy. The reason for this phenomenon is the formation of a tube from the cylinder as a result of the displacement of the center of the cylinder. The driving force in this study is temperature gradient in which stresses are generated. The graphs represented in the results and discussion part are correlated with the temperature gradient figures.

At the center of the cylinder, different temperature profiles are obtained for six different times; however, at the surface of the cylinder, temperature distribution is zero for all times which is consistent with the boundary condition $T(b, t) = 0$ of the problem. Temperature gradient results are inverse of the temperature distribution results. At $r = 0$, temperature gradient is zero at all times, while it gains minimum and maximum values for different times as the radial coordinates moves away from the center and approaches the surface. The highest temperature gradients are observed at the surface of the cylinder, i.e that is $r = b$. In those four different cases, one of the most important results of this research is that, when stress distributions are observed,

it is seen that the difference between minimum and maximum values of the principle stresses are always obtained when $r = b$. Accordingly, yielding commences at the surface of the solid cylinder if the thermal loads are further increased.

This study enlightens the path of further works related with it such as elastic solutions for internal heat generation among other basic structures and plastic solutions under higher loads applied.

REFERENCES

- [1] E. Arslan and A. N. Eraslan. Analytical solution to the bending of a nonlinearly hardening wide curved bar. *Acta Mechanica*, 210(1-2):71–84, 2010.
- [2] E. Arslan and W. Mack. Elastic-plastic states of a radially heated thick-walled cylindrically curved panel. *Forschung im Ingenieurwesen*, 78(1-2):1–11, 2014.
- [3] E. Arslan, W. Mack, and U. Gamer. Elastic limits of a radially heated thick-walled cylindrically curved panel. *Forschung im Ingenieurwesen*, 77(1-2):13–23, 2013.
- [4] M. A. Biot. Thermoelasticity and irreversible thermodynamics. *Journal of Applied Physics*, 27(3):240–253, 1956.
- [5] B. Boley and J. Weiner. Theory of thermal stress, 1960.
- [6] B. A. Boley. Thermal stress in curved beams. 2012.
- [7] A. N. Eraslan. On the linearly hardening rotating solid shaft. *European Journal of Mechanics-A/Solids*, 22(2):295–307, 2003.
- [8] A. N. Eraslan. Thermally induced deformations of composite tubes subjected to a nonuniform heat source. *Journal of thermal stresses*, 26(2):167–193, 2003.
- [9] A. N. Eraslan. A class of nonisothermal variable thickness rotating disk problems solved by hypergeometric functions. *Turkish Journal of Engineering and Environmental Sciences*, 29(4):241–269, 2005.
- [10] A. N. Eraslan. Stresses in fgm pressure tubes under non-uniform temperature distribution. *Structural Engineering and Mechanics*, 26(4):393–408, 2007.
- [11] A. N. Eraslan and T. Akis. On the elastic–plastic deformation of a rotating disk subjected to a radial temperature gradient. *Mechanics based design of structures and machines*, 31(4):529–561, 2003.
- [12] A. N. Eraslan and H. Argeso. Computer solutions of plane strain axisymmetric thermomechanical problems. *Turkish Journal of Engineering and Environmental Sciences*, 29(6):369–381, 2005.
- [13] A. N. Eraslan and H. Argeso. On the application of von mises’ yield criterion to a class of plane strain thermal stress problems. *Turkish J. Eng. Env. Sci*, 29:113–128, 2005.

- [14] A. N. Eraslan and M. E. Kartal. Stress distributions in cooling fins of variable thickness with and without rotation. *Journal of Thermal Stresses*, 28(8):861–883, 2005.
- [15] A. N. Eraslan and E. Varlı. Elastic response of heat generating rod at a variable generating rate. In *Proceedings of the International Conference on Numerical Analysis and Applied Mathematics 2014 (ICNAAM-2014)*, volume 1648, page 850085. AIP Publishing, 2015.
- [16] A. Galka. Singular solutions of thermoelasticity(singular solutions of concentrated force and concentrated heat source thermoelasticity). *Academie Polonaise Des Sciences, Bulletin, Serie Des Sciences Techniques*, 13(10):887–893, 1965.
- [17] M. Gulgeç, Y. Orcan. Influence of the temperature dependence of the yield stress on the stress distribution in a heat-generating tube with free ends. *Journal of thermal stresses*, 23(6):529–547, 2000.
- [18] G. Herrmann. *On variational principles in thermoelasticity and heat conduction*. Columbia University, Department of Civil Engineering and Engineering Mechanics, Institute of Flight Structures, 1960.
- [19] Y. Kaya and A. N. Eraslan. Thermoelastic response of a long tube subjected to periodic heating. *Mathematical Sciences and Applications E-Notes*, 2(1), 2014.
- [20] F. Lockett and I. Sneddon. Propagation of thermal stresses in an infinite medium. *Proceedings of the Edinburgh Mathematical Society (Series 2)*, 11(04):237–244, 1959.
- [21] E. Melan and H. Parkus. *Wärmespannungen: Infolge Stationärer Temperaturfelder*. Springer-Verlag, 2013.
- [22] W. Nowacki. *Thermoelasticity*. Elsevier, 2013.
- [23] Y. Orcan. Thermal stresses in a heat generating elastic-plastic cylinder with free ends. *International journal of engineering science*, 32(6):883–898, 1994.
- [24] Y. Orcan and A. Eraslan. Thermal stresses in elastic-plastic tubes with temperature-dependent mechanical and thermal properties. *Journal of thermal stresses*, 24(11):1097–1113, 2001.
- [25] S. Timoshenko and J. Goodier. *Theory of elasticity*. 1951. New York, 412:108.

APPENDIX A

FORTRAN CODES

A.1 MAIN PROGRAMS OF ASINT CASE

```
PROGRAM ELASTIC SOLUTION
C  -----
C  PURPOSE
C  -----
C  THIS PROGRAM CALCULATES THE ELASTIC SOLUTION OF
C  THE PROBLEM FOR THE FIRST CASE "Q(T)=ASINT".
C  ALL CALCULATIONS ARE DONE FOR DIMENSIONAL
C  PARAMETERS.INPUT AND OUTPUT PARAMETERS ARE
C  PRESCRIBED BELOW.RESULTS ARE PRINTED TO THE
C  OUTPUT FILE WHICH IS TITLED "A-ELAST.DAT".
C  -----
C
C  CONNECTED CODES
C  1) BLOCK DATA (LI)
C  2) BSSLY0Y1J0J1 (Y0, Y1, J0, J1)
C
C  -----
C  CONNECTED SUBROUTINES
C  1) ELAST(R,T,C1,EPS0,SIGR,SIGT,SIGZ,U,SIGVM)
C
```

```

C -----
C DESCRIPTION OF PARAMETERS
C -----
C INPUT :
C -----
C ND          : NUMBER OF CORRECT DIGITS
C ALPHA       : THERMAL EXPANSION COEFFICIENT
C ALPHAT      : THERMAL DIFFUSIVITY
C B           : BOUNDARY SURFACE
C A           : NON-ZERO INPUT PARAMETER
C NU          : POISSON'S RATIO
C E           : MODULUS OF ELASTICITY
C SIGY        : YIELD STRESS
C T           : TIME
C R           : RADIAL COORDINATE WHICH IS  $0 < R < B$ 
C -----
C OUTPUT :
C -----
C EPS0        : AXIAL STRAIN
C SIGR        : RADIAL STRESS COMPONENT
C SIGT        : CIRCUMFERENTIAL STRESS COMPONENT
C SIGZ        : AXIAL STRESS COMPONENT
C U           : RADIAL DISPLACEMENT COMPONENT
C C1          : NON-ZERO INTEGRATION CONSTANT
C -----
C
C IMPLICIT NONE
C INTEGER ND
C DOUBLE PRECISION ALPHA,ALPHAT,B,SIGR,SIGT,SIGZ,
1      NU,E,R,T,T1,INTG,C1,EPS0 U,
2      SIGY,SIGVM,AD,A,DHM
C COMMON /CONVER/ ND
C COMMON /PROPS/ ALPHA,ALPHAT,B,E,NU,SIGY,A

```

```

OPEN(6, FILE='A-ELAST.DAT')
C
ND      = 8
ALPHA   = 21.2D-06
ALPHAT  = 0.13171133D0
A       = 595.0D0
B       = 1.0D0
NU      = 0.3D0
E       = 103.0D09
SIGY    = 160.0D06
C
WRITE(6,*) ' ND      = ', ND
WRITE(6,*) ' ALPHA   = ', ALPHA
WRITE(6,*) ' ALPHAT  = ', ALPHAT
WRITE(6,*) ' A       = ', A
WRITE(6,*) ' B       = ', B
WRITE(6,*) ' NU      = ', NU
WRITE(6,*) ' E       = ', E
WRITE(6,*) ' SIGY    = ', SIGY
C
DO 40 T = 0.00D0, 5.0D0, 0.01D0
T1      = INTG (B, T)
C1      = ALPHA*(1.0D0 - 3.0*NU)
        / (B**2*(1.0D0 - NU))*T1
EPS0    = 2.0*ALPHA/B**2 * T1
WRITE(6,*)
WRITE(6,*) ' TIME = ', T
WRITE(6,*)
WRITE(6,*) ' EPS0 = ', EPS0
WRITE(6,*)
C
DO 30 R = 0.0D0, 1.0D0, 0.05D0
C ALL ELAST (R,T,C1,EPS0,SIGR,SIGT,SIGZ,U,SIGVM)

```

```

      SIGVM= SQRT(0.5*((SIGR-SIGT)**2+
                  (SIGR-SIGZ)**2+(SIGT-SIGZ)**2))
      WRITE(6,100) R , SIGR, SIGT, SIGZ, SIGVM, U
C
30  CONTINUE
40  CONTINUE
    PAUSE
    STOP
100  FORMAT(2X,F5.2,4(3X,F18.6))
    END
C
C -----
SUBROUTINE ELAST(R,T,C1,EPS0,SIGR,SIGT,SIGZ,U,SIGVM)
C -----
C
    IMPLICIT NONE
    DOUBLE PRECISION ALPHA,B,E,NU,SIGY,R,T,SIGR,SIGT,
1      SIGZ,U,T1,T2,T3,EPS0,C1,TEMP,INTG,
2      T4,A,SIGVM,T5,AD
C
    COMMON /PROPS/ ALPHA,AD,B,E,NU,SIGY,A
C
    T1  = 1.0D0 - NU
    T2  = 1.0D0 + NU
    T3  = 1.0D0 - 2.0*NU
C
    IF (R .EQ. 0.0D0) THEN
    T4  = TEMP (R, T)
    SIGR = E*(EPS0*NU + C1)/(T3*T2) - E*ALPHA*T4/(2.0*T1)
    SIGT = SIGR
    SIGZ = E*EPS0 - ALPHA*E*T4 + NU*(SIGR + SIGT)
    U = 0.0D0
    ELSE

```

```

T4    = TEMP (R, T)
T5    = INTG (R, T)
SIGR  = E*(EPS0*NU + C1)/(T3*T2)
      - E*ALPHA*T5/(R**2*T1)
SIGT  = E*(EPS0*NU + C1)/(T3*T2)
      + E*ALPHA*T5/(R**2*T1)
1      - E*ALPHA*T4/T1
SIGZ  = E*EPS0 - ALPHA*E*T4
      + NU*(SIGR + SIGT)
U      = C1*R + ALPHA*T2/(T1*R)*T5
ENDIF

SIGR = SIGR / SIGY
SIGT = SIGT / SIGY
SIGZ = SIGZ / SIGY
U     = U*E / (SIGY*B)
RETURN
END

C
C      -----
C      DOUBLE PRECISION FUNCTION TEMP (R, T)
C      -----

IMPLICIT NONE
INTEGER ND, NPTS, I
DOUBLE PRECISION ES, SOLD, SUM, EA, T1T2, T3, T, R,
1          B, DBJ0, DBJ1, L, ARG, LI, ALPHA,
2          E, NU, A, SIGY, AD, DHM

DIMENSION L(2500)
COMMON /EIG/L
COMMON /CONVER/ ND
COMMON /PROPS/ AD, ALPHA, B, E, NU, SIGY, A
C
NPTS  = 2500
ES    = 0.5D0*10.0D0**(2 - ND)

```

```

C
SUM    = 0.0D0
SOLD   = SUM
DO 10 I = 1, NPTS
LI = L(I)
T1 = DBJ0(LI*R) / (LI* DBJ1(LI*B))
C
SUM = SUM + T1 * DHM(ALPHA, LI, T)
EA  = (SUM - SOLD)/SUM * 100.0
SOLD = SUM
IF (DABS(EA).LT. ES) GO TO 20
10  CONTINUE
20  CONTINUE
TEMP = 2*A*ALPHA/B * SUM
RETURN
END
C
C -----
DOUBLE PRECISION FUNCTION INTG (R, T)
C -----
IMPLICIT NONE
INTEGER ND, NPTS, I
DOUBLE PRECISION ES, SOLD, SUM, EA, T1,T2,T3,
1          B, DBJ1, L,ARG,LI, ALPHA, SIGY,
2          T, R, E, NU,AD, A, DHM
DIMENSION L(2500)
COMMON /EIG/L
COMMON /CONVER/ ND
COMMON /PROPS/ AD, ALPHA, B, E, NU, SIGY, A
C
NPTS  = 2500
ES    = 0.5D0*10.0D0**(2 - ND)
C

```

```

SUM      = 0.0D0
SOLD     = SUM
DO 10 I = 1, NPTS
LI = L(I)
T1 = R*DBJ1(LI*R) / (LI**2*DBJ1(LI*B))
SUM = SUM + T1 * DHM(ALPHA, LI, T)
EA  = (SUM - SOLD)/SUM * 100.0
SOLD = SUM
IF (DABS(EA).LT. ES) GO TO 20
10 CONTINUE
20 CONTINUE
INTG = 2*A*ALPHA/B * SUM
RETURN
END
C -----
DOUBLE PRECISION FUNCTION DHM( ALF, L, T )
C -----
IMPLICIT NONE
DOUBLE PRECISION ALF, L, T, ARG, T1
C
ARG = -ALF*L**2*T
IF (DABS(ARG) .GT. 250.0D0) THEN
T1 = 0.0D0
ELSE
T1 = DEXP(ARG)
ENDIF
DHM = (T1-DCOS(T)+ALF*L**2*DSIN(T))
2      / (1.0D0 + (ALF**2 * L**4))
RETURN
END

```

PROGRAM TEMPERATURE DISTRIBUTION FOR CASE ASINT

```

C  -----
C  A SOLID CYLINDER INITIALLY AT ZERO TEMPERATURE;
C  FOR TIMES>0 THE TEMPERATURE OF THE BOUNDARY
C  SURFACE AT R=B IS ZERO AND THE TEMPERATURE OF
C  THE MIDDLE SURFACE AT R=0 IS FINITE
C  -----
C  CONNECTED CODES
C  1) BLOCK DATA (LI)
C  2) BSSLY0Y1J0J1 (Y0, Y1, J0, J1)
C  -----
C  DESCRIPTION OF PARAMETERS
C  -----
C  INPUT :
C  -----
C  ND          : NUMBER OF CORRECT DIGITS
C  ALPHA       : THERMAL DIFFUSIVITY
C  B           : BOUNDARY SURFACE
C  A           : NON-ZERO INPUT PARAMETER
C  DR          : INCREMENT OF THE RADIAL COORDINATE
C  TIME        : TIME
C  -----
C  OUTPUT :
C  -----
C  T           : TEMPERATURE DISTRIBUTION
C  -----
IMPLICIT NONE
INTEGER ND, NPTS, I, J
PARAMETER ( NPTS = 2500 )
DOUBLE PRECISION ES, SOLD, SUM, EA, T1, TIME, R, DHM,
1          A, B, T, DBJ0, DBJ1, L, LI, ALPHA, DR
DIMENSION L(NPTS)

```

```

COMMON /EIG/L
OPEN(6,FILE='A-OUT.DAT')
C
ND      = 8
ALPHA = 0.13171133D0
B       = 1.0D0
A       = 595.0D0
DR      = B / 20.0D0
C
ES      = 0.5D0*10.0D0**(2 - ND)
C
DO 40 TIME = 0.0D0, 5.0D0, 0.01D0
WRITE(6,*)
WRITE(6,*) '   TIME = ',TIME
WRITE(6,*)
R = 0.0D0
DO 30 J = 1, 21
SUM  = 0.0D0
SOLD = SUM
DO 10 I = 1, NPTS
LI = L(I)
T1 = DBJ0(LI*R) / (LI*DBJ1(LI*B))
SUM = SUM+T1*DHM(ALPHA, LI, TIME)
EA  = (SUM-SOLD) / SUM*100.0
T   = 2*A*ALPHA/B * SUM
SOLD = SUM
IF (DABS(EA).LT. ES) GO TO 20
10  CONTINUE
20  CONTINUE
    WRITE(6,100) R , T, I
    R      = R + DR
30  CONTINUE
40  CONTINUE

```

```

        PAUSE
        STOP
100    FORMAT (5X,F5.2,5X,F15.8,5X,I5)
        END

C
C -----
      DOUBLE PRECISION FUNCTION DHM(ALF,L,TIME)
C -----
      IMPLICIT NONE
      DOUBLE PRECISION ALF, L, TIME, ARG, T1
C
      ARG = -ALF*L**2*TIME
      IF (DABS(ARG) .GT. 250.0D0) THEN
        T1 = 0.0D0
      ELSE
        T1 = DEXP(ARG)
      ENDIF
C
      DHM = (T1-DCOS(TIME)+ALF*L**2*DSIN(TIME))
2      / (1.0D0 + (ALF**2 * L**4))
C
      RETURN
END

```

```

PROGRAM TEMPERATURE GRADIENT FOR CASE ASINT
C  -----
C  CONNECTED CODES
C  1) BLOCK DATA (LI),
C  2) BSSLY0Y1J0J1 (Y0, Y1, J0, J1)
C  -----
C  DESCRIPTION OF PARAMETERS
C  -----
C  INPUT :
C  -----
C  ND              : NUMBER OF CORRECT DIGITS
C  ALPHA           : THERMAL DIFFUSIVITY
C  B               : BOUNDARY SURFACE
C  A               : NON-ZERO INPUT PARAMETER
C  DR              : INCREMENT OF THE RADIAL COORDINATE
C  TIME            : TIME
C  -----
C  OUTPUT :
C  -----
C  DT              : TEMPERATURE GRADIENT
C  -----
IMPLICIT NONE
INTEGER ND, NPTS, I, J
PARAMETER ( NPTS = 2500 )
DOUBLE PRECISION ES, SOLD, SUM, EA, T1, TIME, R, DHM,
1              A, B, DT, DBJ0, DBJ1, L, LI, ALPHA, DR
DIMENSION L(NPTS)
COMMON /EIG/L
OPEN(6, FILE='A-OUT.DAT')
C
ND      = 8
ALPHA = 0.13171133D0

```

```

B      = 1.0D0
A      = 595.0D0
DR     = B / 20.0D0
C
ES     = 0.5D0*10.0D0**(2 - ND)
C
DO 40 TIME = 0.0D0, 5.0D0, 0.01D0
WRITE(6,*)
WRITE(6,*) '   TIME = ',TIME
WRITE(6,*)
R = 0.0D0
DO 30 J = 1, 21
SUM    = 0.0D0
SOLD   = SUM
DO 10 I = 1, NPTS
LI = L(I)
T1 = DBJ1(LI*R) / DBJ1(LI*B)
SUM = SUM + T1 * DHM(ALPHA, LI, TIME)
EA  = (SUM - SOLD)/SUM * 100.0
DT   = -2*A*ALPHA/B * SUM
SOLD = SUM
IF (DABS(EA).LT. ES) GO TO 20
10  CONTINUE
20  CONTINUE
    WRITE(6,100) R , DT, I
    R      = R + DR
30  CONTINUE
40  CONTINUE
    PAUSE
STOP
100  FORMAT(5X,F5.2,5X,F15.8,5X,I5)
END

```

```

C
C -----
  DOUBLE PRECISION FUNCTION DHM(ALF,L,TIME)
C -----
  IMPLICIT NONE
  DOUBLE PRECISION ALF, L, TIME, ARG, T1
C
  ARG = -ALF*L**2*TIME
  IF (DABS(ARG) .GT. 250.0D0) THEN
    T1 = 0.0D0
  ELSE
    T1 = DEXP(ARG)
  ENDIF
C
    DHM = (T1-DCOS(TIME)+ALF*L**2*DSIN(TIME))
2      / (1.0D0 + (ALF**2 * L**4))
C
  RETURN
END

```

```

PROGRAM ROOT FINDING
-----
IMPLICIT NONE
INTEGER ITMAX, I, N, NJ, NC, NR
DOUBLE PRECISION A,B,DX,TOL,FUN,P,ADUM,BDUM,ROOT
PARAMETER ( NR = 2500 )
    DIMENSION ROOT(NR)
EXTERNAL FUN
C
    OPEN(6,FILE='A-ROOTS.DAT')
    N      = 10000
    A      = 0.0D0
    B      = 8000.0D0
    DX     = (B-A)/N
    NJ     = 0
    NC     = 10
ITMAX = 50
    DO 10 I = 1, N
        B      = A + DX
        P      = FUN(A) * FUN(B)
        IF (P .LT. 0.0D0) THEN
            IF ( NJ+1 .GT. NR) GO TO 20
            ADUM      = A
            BDUM      = B
            CALL RFALSI (FUN,ADUM,BDUM,NC,ITMAX)
            NJ        = NJ + 1
            ROOT(NJ) = ADUM
        END IF
        A = B
    10  CONTINUE
    20  CONTINUE
C

```

```

        WRITE(6,200) "DATA"
DO 40 I = 1, NR, 2
IF (I .EQ. NR) THEN
WRITE(6,100)  ROOT(I)
ELSE
        WRITE(6,100) I, ROOT(I), I+1, ROOT(I+1)
        ENDIF
        IF ((MOD((I+1),100).EQ.0) .
        AND.(I+1 .LT. NR-100)) THEN
        WRITE(6,200) "DATA"
        ENDIF
40    CONTINUE
        WRITE (6,200) "END"
        PAUSE
        STOP
100  FORMAT(5X,'*R(',I4,')/',F15.10,'D0 /
        2      ,',',R(',I4,') /'
        3      , F15.10,'D0 /')
200  FORMAT (8X, A)
END
C
C -----
        DOUBLE PRECISION FUNCTION FUN( LAMBDA )
C -----
IMPLICIT NONE
DOUBLE PRECISION LAMBDA, B, DBJ0, DBJ1
        B = 1.0D0
C
        FUN = DBJ0(LAMBDA * B)
C
        RETURN
END

```

```

C
C =====
C SUBROUTINE RFALSI (F, A, B, NC, ITMAX)
C =====
C IMPLICIT DOUBLE PRECISION (A-H , O-Z)
C INTEGER ITER, ITMAX, NC
C EXTERNAL F
C -----
C SUBROUTINE RFALSI COMPUTES THE ROOT
C OF A NONLINEAR EQUATION
C  $F(P) = 0$ 
C USING METHOD OF FALSE POSITIONS (REGULA FALSI).
C
C PARAMETER LIST :
C -----
C F:THE NAME OF THE EXTERNAL FUNCTION
C THAT DEFINES THE
C FORM OF THE EQUATION  $F(P) = 0$ .
C THIS FUNCTION SHOULD
C BE DECLARED EXTERNAL IN THE CALLING PROGRAM.
C A, B:END POINTS OF F SUCH THAT F(A) AND F(B) HAVE
C OPPOSITE SIGNS. IF F(A) AND F(B) HAVE THE SAME SIGN
C SUBROUTINE RETURNS TO THE CALLER PRINTING AN ERROR
C MESSAGE. ON OUTPUT, THE COMPUTED ROOT P IS ASSIGNED
C TO A.
C TOL:ERROR BOUND TO TERMINATE THE REGULA FALSI
C ITERATIONS. ITERATIONS ARE TERMINATED WHEN
C  $ABS(P - P0) .LT. TOL$ , WHERE P0 IS THE PREVIOUS
C ITERATION VALUE OF P.
C ITMAX : MAXIMUM NUMBER OF ITERATIONS ALLOWED.
C ON RETURN
C ITMAX IS SET EQUAL TO THE NUMBER OF ITERATIONS
C PERFORMED TO HIT THE GIVEN ERROR BOUND.

```

```

C
C AHMET N. ERASLAN
C 3 - 7 - 1993
C-----
C... INITIALIZE
      DATA P0 /0.0/
ES = 0.5D0*10.0**(2 - NC)
      FA = F(A)
      FB = F(B)
      IF ((FA * FB) .GT. 0.0) WRITE(6,200)
      IF ((FA * FB) .GT. 0.0) RETURN
C
C.ITERATION LOOP :
      DO 10 ITER = 1 , ITMAX
      FA = F(A)
      P  = A - FA * (B - A) / (F(B) - FA)
EA = DABS((P - P0) / P) * 100.0
      IF ( EA .LT. ES )   GOTO 20
      FP = F(P)
      IF ((FA * FP) .LT. 0.0)  A = P
      IF ((FA * FP) .GT. 0.0)  B = P
10    P0 = P
C
C.ITERATIONS CONVERGED;
C SET NUMBER OF ITERATIONS AND RETURN
20 ITMAX = ITER
      A      = P
      RETURN
200  FORMAT(///10X,'FROM SUBROUTINE RFALSI :'/
1      10X,'F(A) AND F(B) HAVE THE SAME SIGN,'
2      , ' METHOD IS NOT APPLICABLE...')
      END

```

A.2 MAIN PRAGRAMS OF ATCOST CASE

```
      PROGRAM ELASTIC SOLUTION
C  -----
C  PURPOSE
C  -----
C  THIS PROGRAM CALCULATES THE ELASTIC SOLUTION
C  OF THE PROBLEM FOR THE FIRST CASE
C  "Q(T)=ATCOST". ALL CALCULATIONS ARE DONE
C  FOR DIMENSIONAL PARAMETERS.INPUT AND OUTPUT
C  PARAMETERS ARE PRESCRIBED BELOW.RESULTS ARE
C  PRINTED TO THE OUTPUT FILE WHICH
C  IS TITLED "A-ELAST.DAT".
C  -----
C
C  CONNECTED CODES
C  1) BLOCK DATA (LI)
C  2) BSSLY0Y1J0J1 (Y0, Y1, J0, J1)
C
C  -----
C  CONNECTED SUBROUTINES
C  1) ELAST(R,T,C1,EPS0,SIGR,SIGT,SIGZ,U,SIGVM)
C
C  -----
C  DESCRIPTION OF PARAMETERS
C  -----
C  INPUT :
C  -----
C  ND           : NUMBER OF CORRECT DIGITS
C  ALPHA        : THERMAL EXPANSION COEFFICIENT
C  ALPHAT       : THERMAL DIFFUSIVITY
C  B            : BOUNDARY SURFACE
```

```

C      A              : NON-ZERO INPUT PARAMETER
C      NU             : POISSON'S RATIO
C      E              : MODULUS OF ELASTICITY
C      SIGY           : YIELD STRESS
C      T              : TIME
C      R              : RADIAL COORDINATE WHICH IS 0<R<B
C      -----
C      OUTPUT :
C      -----
C      EPS0           : AXIAL STRAIN
C      SIGR           : RADIAL STRESS COMPONENT
C      SIGT           : CIRCUMFERENTIAL STRESS COMPONENT
C      SIGZ           : AXIAL STRESS COMPONENT
C      U              : RADIAL DISPLACEMENT COMPONENT
C      C1             : NON-ZERO INTEGRATION CONSTANT
C      -----
C
      IMPLICIT NONE
      INTEGER ND
      DOUBLE PRECISION ALPHA, ALPHAT, B, SIGR, SIGT, SIGZ,
1          NU, E, R, T, T1, INTG, C1, EPS0,
2          SIGY, SIGVM, U, AD, A, DHM
      COMMON /CONVER/ ND
      COMMON /PROPS/ ALPHA, ALPHAT, B, E, NU, SIGY, A
      OPEN(6, FILE='A-ELAST.DAT')
C
      ND      = 8
      ALPHA   = 21.2D-06
      ALPHAT  = 0.13171133D0
      A       = 185.0D0
      B       = 1.0D0
      NU      = 0.3D0
      E       = 103.0D09

```

SIGY = 160.0D06

C

```
WRITE(6,*) ' ND      = ', ND
WRITE(6,*) ' ALPHA   = ', ALPHA
WRITE(6,*) ' ALPHAT  = ', ALPHAT
WRITE(6,*) ' A       = ', A
WRITE(6,*) ' B       = ', B
WRITE(6,*) ' NU      = ', NU
WRITE(6,*) ' E       = ', E
WRITE(6,*) ' SIGY    = ', SIGY
```

C

```
DO 40 T = 0.00D0, 5.0D0, 0.01D0
T1      = INTG (B, T)
C1      = ALPHA*(1.0D0 - 3.0*NU)
        / (B**2*(1.0D0 - NU)) * T1
EPS0    = 2.0*ALPHA/B**2 * T1
WRITE(6,*)
WRITE(6,*) ' TIME = ', T
WRITE(6,*)
WRITE(6,*) ' EPS0 = ', EPS0
WRITE(6,*)
```

C

```
DO 30 R = 0.0D0, 1.0D0, 0.05D0
CALL ELAST (R,T,C1,EPS0,SIGR,SIGT,SIGZ,U,SIGVM)
SIGVM= SQRT(0.5*((SIGR-SIGT)**2 +
              (SIGR-SIGZ)**2 + (SIGT-SIGZ)**2))
WRITE(6,100) R , SIGR, SIGT, SIGZ, SIGVM, U
```

C

```
30  CONTINUE
40  CONTINUE
    PAUSE
    STOP
100  FORMAT(2X,F5.2,4(3X,F18.6))
```

```

END
C
C -----
SUBROUTINE ELAST(R,T,C1,EPS0,SIGR,SIGT,SIGZ,U,SIGVM)
C -----
IMPLICIT NONE
DOUBLE PRECISION ALPHA,B,E,NU,SIGY,R,T,SIGR,SIGT,
1          SIGZ,U,T1,T2,T3,EPS0,C1,TEMP,
2          T4,A,SIGVM,INTG,T5,AD
C
COMMON /PROPS/ ALPHA, AD, B, E, NU, SIGY, A
C
T1  = 1.0D0 - NU
T2  = 1.0D0 + NU
T3  = 1.0D0 - 2.0*NU
C
IF (R .EQ. 0.0D0) THEN
T4  = TEMP (R, T)
SIGR = E*(EPS0*NU + C1)/(T3*T2)
      - E*ALPHA*T4/(2.0*T1)
SIGT = SIGR
SIGZ = E*EPS0 - ALPHA*E*T4
      + NU*(SIGR + SIGT)
U = 0.0D0
ELSE
T4  = TEMP (R, T)
T5  = INTG (R, T)
SIGR = E*(EPS0*NU + C1)/(T3*T2)
      - E*ALPHA*T5/(R**2*T1)
SIGT = E*(EPS0*NU + C1)/(T3*T2)
      + E*ALPHA*T5/(R**2*T1)
1    - E*ALPHA*T4/T1
SIGZ = E*EPS0 - ALPHA*E*T4

```

```

        + NU*(SIGR + SIGT)
U      = C1*R + ALPHA*T2/(T1*R)*T5
ENDIF
SIGR = SIGR / SIGY
SIGT = SIGT / SIGY
SIGZ = SIGZ / SIGY
U      = U*E / (SIGY*B)

RETURN
END
C      -----
      DOUBLE PRECISION FUNCTION TEMP (R, T)
C      -----
      IMPLICIT NONE
      INTEGER ND, NPTS, I
      DOUBLE PRECISION ES,SOLD,SUM,EA,T1,T2,T3,T,R,
1          B,DBJ0,DBJ1,L,ARG,LI,ALPHA,
2          E,NU,A,SIGY,AD,DHM
      DIMENSION L(2500)
      COMMON /EIG/L
      COMMON /CONVER/ ND
      COMMON /PROPS/ AD, ALPHA, B, E, NU, SIGY, A
C
      NPTS = 2500
      ES = 0.5D0*10.0D0**(2 - ND)
C
      SUM = 0.0D0
      SOLD = SUM
      DO 10 I = 1, NPTS
      LI = L(I)
      T1 = DBJ0(LI*R) / (LI* DBJ1(LI*B))
C
      SUM = SUM + T1 * DHM(ALPHA, LI, T)

```

```

EA  = (SUM - SOLD)/SUM * 100.0
SOLD = SUM
IF (DABS(EA).LT. ES) GO TO 20
10  CONTINUE
20  CONTINUE

TEMP = 2*A*ALPHA/B * SUM
RETURN
END

C      -----
      DOUBLE PRECISION FUNCTION INTG (R, T)
C      -----

IMPLICIT NONE
INTEGER ND, NPTS, I
DOUBLE PRECISION ES, SOLD, SUM, EA, T1, T2, T3, T,
1          B, DBJ1, L, ARG, LI, ALPHA,
2          R, E, NU, SIGY, AD, A, DHM
DIMENSION L(2500)
COMMON /EIG/L
COMMON /CONVER/ ND
COMMON /PROPS/ AD, ALPHA, B, E, NU, SIGY, A
C
NPTS  = 2500
ES    = 0.5D0*10.0D0**(2 - ND)
C
SUM    = 0.0D0
SOLD  = SUM
DO 10 I = 1, NPTS
LI    = L(I)
T1    = R*DBJ1(LI*R) / (LI**2*DBJ1(LI*B))
SUM  = SUM + T1 * DHM(ALPHA, LI, T)
EA    = (SUM - SOLD)/SUM * 100.0
SOLD = SUM
IF (DABS(EA).LT. ES) GO TO 20

```

```

10  CONTINUE
20  CONTINUE
    INTG = 2*A*ALPHA/B * SUM
    RETURN
    END
C  -----
    DOUBLE PRECISION FUNCTION DHM( ALF,L,TIME)
C  -----
    IMPLICIT NONE
    DOUBLE PRECISION ALF,L,TIME,ARG,T1,T2,T3,T4,T5
C
    ARG = -ALF*L**2*TIME
    IF (DABS(ARG) .GT. 250.0D0) THEN
        T1 = 0.0D0
    ELSE
        T1 = DEXP(ARG)
    ENDIF
    T2 = T1*(-1+ALF**2*L**4) + DCOS(TIME)
    T3 = - ALF**2*L**4*DCOS(TIME)
        -2*ALF*L**2*DSIN(TIME)
    T4 = TIME*(1+ALF**2*L**4)*
        (ALF*L**2*DCOS(TIME)+DSIN(TIME))
    T5 = (1.0D0 + (ALF**2 * L**4))**2
    DHM = (T2+T3+T4)/T5
    RETURN
    END

```

```

PROGRAM TEMPERATURE DISTRIBUTION FOR CASE ATCOST
C  -----
C  A SOLID CYLINDER INITIALLY AT ZERO TEMPERATURE;
C  FOR TIMES>0 THE TEMPERATURE OF THE BOUNDARY
C  SURFACE AT R=B IS ZERO AND THE TEMPERATURE OF
C  THE MIDDLE SURFACE AT R=0 IS FINITE
C  -----
C  CONNECTED CODES
C  1) BLOCK DATA (LI)
C  2) BSSLY0Y1J0J1 (Y0, Y1, J0, J1)
C  -----
C  DESCRIPTION OF PARAMETERS
C  -----
C  INPUT :
C  -----
C  ND          : NUMBER OF CORRECT DIGITS
C  ALPHA       : THERMAL DIFFUSIVITY
C  B           : BOUNDARY SURFACE
C  A           : NON-ZERO INPUT PARAMETER
C  DR          : INCREMENT OF THE RADIAL COORDINATE
C  TIME        : TIME
C  -----
C  OUTPUT :
C  -----
C  T           : TEMPERATURE DISTRIBUTION
C  -----
IMPLICIT NONE
INTEGER ND, NPTS, I, J
PARAMETER ( NPTS = 2500 )
DOUBLE PRECISION ES, SOLD, SUM, EA, T1, TIME, R, DHM,
1          A, B, T, DBJ0, DBJ1, L, LI, ALPHA, DR
DIMENSION L(NPTS)

```

```

COMMON /EIG/L
OPEN(6,FILE='A-OUT.DAT')
C
ND      = 8
ALPHA   = 0.13171D0
B        = 1.0D0
A        = 185.0D0
DR       = B / 20.0D0
C
ES       = 0.5D0*10.0D0**(2 - ND)
C
DO 40 TIME = 0.0D0, 5.0D0, 0.01D0
WRITE(6,*)
WRITE(6,*) '    TIME = ',TIME
WRITE(6,*)
R        = 0.0D0
DO 30 J = 1, 21
SUM       = 0.0D0
SOLD      = SUM
DO 10 I = 1, NPTS
LI        = L(I)
T1        = DBJ0(LI*R) / (LI* DBJ1(LI*B))
SUM       = SUM + T1 * DHM(ALPHA, LI, TIME)
EA        = (SUM - SOLD)/SUM * 100.0
T         = 2 * A * ALPHA /B * SUM
SOLD      = SUM
IF (DABS(EA).LT. ES) GO TO 20
10  CONTINUE
20  CONTINUE
WRITE(6,100) R , T, I
R         = R + DR
30  CONTINUE
40  CONTINUE

```

```

        PAUSE
STOP
100  FORMAT (5X,F5.2,5X,F15.8,5X,I5)
END

C
C -----
DOUBLE PRECISION FUNCTION DHM(ALF,L,TIME)
C -----
IMPLICIT NONE
DOUBLE PRECISION ALF,L,TIME,ARG,T1,T2,T3,T4,T5
C
ARG = -ALF*L**2*TIME
IF (DABS(ARG) .GT. 250.0D0) THEN
T1 = 0.0D0
ELSE
T1 = DEXP(ARG)
ENDIF
C
T2 = T1*(-1+ALF**2*L**4) + DCOS(TIME)
T3 = - ALF**2*L**4*DCOS(TIME)
      -2*ALF*L**2*DSIN(TIME)
T4 = TIME*(1+ALF**2*L**4)*
      (ALF*L**2*DCOS(TIME)+DSIN(TIME))
T5 = (1.0D0 + (ALF**2 * L**4))**2
DHM = (T2+T3+T4)/T5
C
RETURN
END

```

```

PROGRAM TEMPERATURE GRADIENT FOR CASE ATCOST
C  -----
C  CONNECTED CODES
C  1) BLOCK DATA (LI),
C  2) BSSLY0Y1J0J1 (Y0, Y1, J0, J1)
C  -----
C  DESCRIPTION OF PARAMETERS
C  -----
C  INPUT :
C  -----
C  ND          : NUMBER OF CORRECT DIGITS
C  ALPHA       : THERMAL DIFFUSIVITY
C  B           : BOUNDARY SURFACE
C  A           : NON-ZERO INPUT PARAMETER
C  DR          : INCREMENT OF THE RADIAL COORDINATE
C  TIME        : TIME
C  -----
C  OUTPUT :
C  -----
C  DT          : TEMPERATURE GRADIENT
C  -----
IMPLICIT NONE
INTEGER ND, NPTS, I, J
PARAMETER ( NPTS = 2500 )
DOUBLE PRECISION ES, SOLD, SUM, EA, T1, TIME, R, DHM,
1          A, B, DT, DBJ0, DBJ1, L, LI, ALPHA, DR
DIMENSION L(NPTS)
COMMON /EIG/L
OPEN(6, FILE='A-OUT.DAT')
C
ND      = 8
ALPHA = 0.13171133

```

```

B      = 1.0D0
A      = 185.0D0
DR     = B / 20.0D0
C
ES     = 0.5D0*10.0D0**(2 - ND)
C
DO 40 TIME = 0.0D0, 5.0D0, 0.01D0
WRITE(6,*)
WRITE(6,*) '   TIME = ',TIME
WRITE(6,*)
R = 0.0D0
DO 30 J = 1, 21
SUM    = 0.0D0
SOLD   = SUM
DO 10 I = 1, NPTS
LI = L(I)
T1 = DBJ1(LI*R) / DBJ1(LI*B)
SUM = SUM + T1 * DHM(ALPHA, LI, TIME)
EA  = (SUM - SOLD)/SUM * 100.0
DT  = -2*A*ALPHA/B * SUM
SOLD = SUM
IF (DABS(EA).LT. ES) GO TO 20
10  CONTINUE
20  CONTINUE
    WRITE(6,100) R , DT, I
    R      = R + DR
30  CONTINUE
40  CONTINUE
    PAUSE
STOP
100  FORMAT(5X,F5.2,5X,F15.8,5X,I5)
END

```

```

C
C -----
      DOUBLE PRECISION FUNCTION DHM(ALF,L,TIME)
C -----
      IMPLICIT NONE
      DOUBLE PRECISION ALF,L,TIME,ARG,T1,
1          T2,T3,T4,T5
C
      ARG = -ALF*L**2*TIME
      IF (DABS(ARG) .GT. 250.0D0) THEN
      T1 = 0.0D0
      ELSE
      T1 = DEXP(ARG)
      ENDIF
C
      T2 = T1*(-1+ALF**2*L**4) + DCOS(TIME)
      T3 = - ALF**2*L**4*DCOS(TIME)
           -2*ALF*L**2*DSIN(TIME)
      T4 = TIME*(1+ALF**2*L**4)*(ALF*L**2*
           DCOS(TIME)+DSIN(TIME))
      T5 = (1.0D0 + (ALF**2 * L**4))**2
      DHM = (T2+T3+T4)/T5
C
      RETURN
END

```

APPENDIX B

MATERIAL PROPERTIES

B.1 MATERIAL PROPERTIES OF STRUCTURAL STEEL

Mechanical Properties	
Mechanical Properties of Structural Steel	Metric
Poisson's Ratio	0.3
Thermal Expansion Coefficient	$11 \times 10^{-6} 1/K$
Elastic Modulus	210 GPa
Yield Strength	270 MPa
Tensile Strength	400-550 MPa
Specific Heat Capacity	480 J/kgK
Thermal Conductivity	50 W/mK
Density	$7.8 \times 10^3 kg/m^3$
Thermal Diffusivity	$0.04807 m^2/h$

B.2 MATERIAL PROPERTIES OF YELLOW BRASS

Mechanical Properties	
Mechanical Properties of Yellow Brass	Metric
Poisson's Ratio	0.3
Thermal Expansion Coefficient	$21.2 \times 10^{-6} 1/K$
Elastic Modulus	103 GPa
Yield Strength	160 MPa
Tensile Strength	414 MPa
Specific Heat Capacity	377 J/kgK
Thermal Conductivity	116 W/mK
Density	$8.41 \times 10^3 kg/m^3$
Thermal Diffusivity	$0.131711 m^2/h$